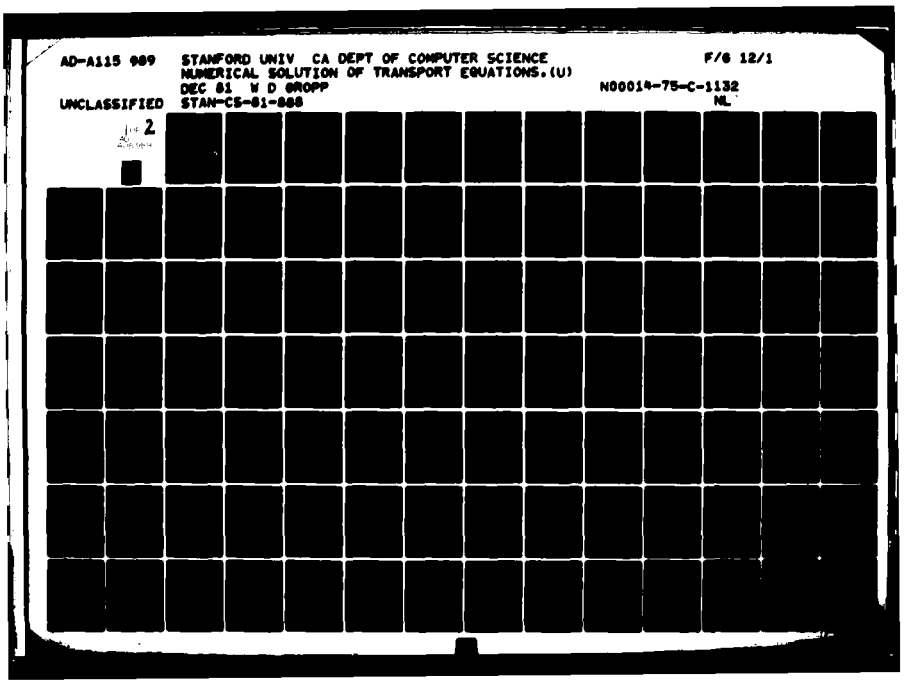
AD-A115 989
STANFORD UNIV CA DEPT OF COMPUTER SCIENCE
F/G 12/1
NUMERICAL SOLUTION OF TRANSPORT EQUATIONS.(U)
DEC 81 W D GROPP
N00014-75-C-1132
UNCLASSIFIED
STAN-CS-81-868
NL
2

1 OF 2

AD A115 989

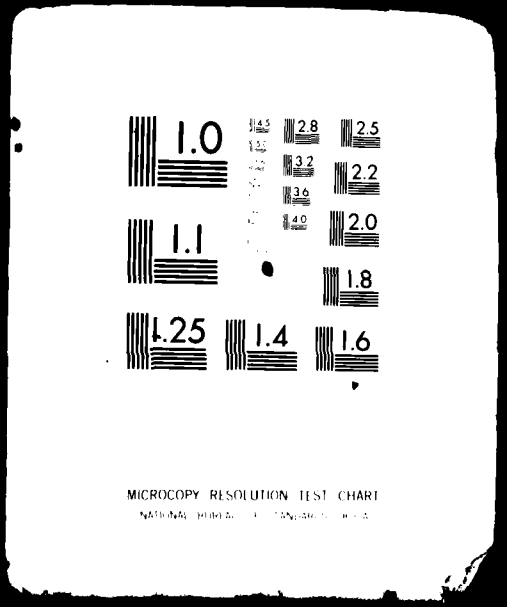

December 1981

Report. No. STAN-CS-81-888

(24)

Numerical Solution of Transport Equations

by

William D. Gropp

C-11

Department of Computer Science

Stanford University
Stanford, CA 94305

NUMERICAL SOLUTION OF TRANSPORT EQUATIONS

A DISSERTATION

SUBMITTED TO THE DEPARTMENT OF COMPUTER SCIENCE

AND THE COMMITTEE ON GRADUATE STUDIES

OF STANFORD UNIVERSITY

IN PARTIAL FULFILLMENT OF THE REQUIREMENTS

FOR THE DEGREE OF

DOCTOR OF PHILOSOPHY

by

William Douglas Gropp

December 1981

Numerical Solution of Transport Equations

William D. Gropp, Ph.D.
Stanford University, 1982

In this dissertation we discuss the numerical solution of systems of hyperbolic partial differential equations with lower order terms and step function initial data. These equations arise in modeling the propagation of a signal with loss, such as a signal in a resistive co-axial cable, or the flow of neutrons in a reactor. Majda and Osher have shown that dissipative finite difference approximations to such problems display a numerical artifact which is not encountered for scalar equations. Namely, noise from an initial discontinuity propagates into a large region behind the discontinuity. Their results do not apply in the vicinity of a discontinuity, and our goal is to discover the detailed behavior in this region. This information will be of use in constructing algorithms that attempt to accurately approximate solutions with discontinuities or shocks.

We analyze the behavior of finite difference approximations to a particular model problem with step function initial data. We use Fourier transforms to express the solution of the difference approximation as a Fourier integral. The behavior of this integral is then examined by using the theory of uniform asymptotic estimation of integrals. We show that the solution of the difference approximation is modeled by a particular class of integrals, which we call generalized Bessel functions. With these results, we are able to show that there is a "smearing" of the discontinuity which is the same as that which one obtains when approximating the scalar wave equation. Thus, the behavior near the discontinuity is qualitatively similiar to the near-front behavior of the scalar wave equation. These results show that the artifact discovered by Majda and Osher is overwhelmed near the discontinuity by the numerical dispersion and/or dissipation introduced by the difference approximation. Graphs of the generalized Bessel functions are provided. Finally, we discuss the relevance of our results to automatic mesh refinement and give an example.

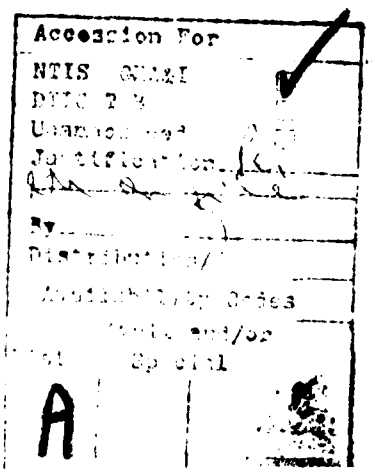

Approved for Publication:

By_____
For Major Department

By_____
Dean of Graduate Studies & Research

Acknowledgments

There are many people that I would like to thank.

First, I would like to thank Professor Joseph Oliger for his support and advice. He was always willing to help, whether to give a reference or to give encouragement. He gave me a good idea of what research is really like.

I wish to thank Doctor Gerald Hedstrom for originally suggesting this problem to me and for his valuable advice and guidance. Without his instruction on asymptotic analysis of integrals, this dissertation would never have been possible. He freely shared his insight into the behavior of difference schemes.

Professor Robert Schreiber gave of his time to serve on my reading committee. His comments on the organization of this dissertation were valuable.

Marsha Berger and Randall LeVeque made a number of valuable suggestions which improved the presentation in this dissertation. Lloyd Trefethen's careful reading of various versions of my dissertation improved both the presentation and the content.

The stimulating environment of the numerical analysis of group at Stanford made my stay there both productive and pleasant. Professor Gene Golub's enthusiasm and untiring efforts have this group what it is today. I would like to thank Professor Donald Knuth for the TEX typesetting system and the Stanford Linear Accelerator Center for the use of their computing facilities. The work in this dissertation was supported in part by the Office of Naval Research under Contract N00014-75-C-1132 and by the National Science Foundation under Grant MCS-7702082.

Finally, I thank my wife Marla for her constant support and encouragement.

Table of Contents

1. Introduction

In this dissertation we consider the numerical solution of the telegrapher's equation

$$\begin{aligned} \frac{\partial u}{\partial t} &= -\frac{\partial v}{\partial x} \\ \frac{\partial v}{\partial t} &= -\frac{\partial u}{\partial x} - v \end{aligned} \tag{1.1}$$

with step function initial data. This equation models wave propagation in a system of equations with coupling caused by the presence of undifferentiated or lower order terms. (If the lower order term were not present, it would be possible to diagonalize the system with a linear change of variables.) This equation is of interest because the solution to this equation is smooth away from discontinuities in the solution (Birkhoff and Lynch [1966]) but numerical approximations are not (Majda and Osher [1977]). Also, as we show below, the equation itself can be considered a model for transport phenomena, so that a better understanding of the behavior of approximate solutions to it will help in interpreting numerical results and in constructing numerical methods.

In this section we will first discuss some examples from engineering and physics of equations with coupling through lower order terms. These examples will help develop an intuition about what the exact solutions should look like. We will then give a brief historical overview of material on both the telegrapher's equation and on techniques for analyzing the behavior of approximations to hyperbolic partial differential equations (to which class the telegrapher's equation belongs). Finally, we will discuss in more detail the methods which we shall use to find the behavior of approximations to (1.1) near the discontinuity.

The following is an overview of this dissertation. The theoretical results are presented in sections 2, 3, and 4. In section 2, we find an asymptotic representation to the solution of (1.1) near the step discontinuity. The purpose of this section is to both show the behavior of (1.1) to which the approximate solutions will be compared and to illustrate the methods which will be used in later sections to analyze difference approximations to (1.1). In section 3, we analyze a semidiscrete second order centered difference approximation to (1.1). We first show that the width of the front in the approximation is $\mathcal{O}(h^{2/3})$. We then derive a form of integral (a generalized Bessel function) which represents the solution near the front. Finally, we compare the behavior of the approximation to (1.1) with the same type

of approximation to the scalar wave equation. In section 4, we analyze a model equation which represents a general difference approximation to (1.1). This section generalizes the results from section 3. Section 5 contains numerical results. We consider here four different difference approximations to (1.1). Graphs of the computed solutions and the observed widths of the front for each method are presented. These are followed by graphs of the generalized Bessel functions which we show in section 4 to represent the solution to a difference approximation to (1.1) near the front. Finally, an application of the results is made to a computation using mesh refinement.

Examples of Equations with Lower Order Terms

We begin with a brief discussion of a few examples of equations with lower order terms to show where the problem we address arises. The basic physical feature of all of these equations is a finite speed of propagation combined with decay of signal through, for example, absorption.

Perhaps the most familiar example is transmission along a resistive coaxial cable. This equation is usually written as

$$\frac{\partial^2 \psi}{\partial z^2} = \frac{\mu\epsilon}{c^2}\frac{\partial^2 \psi}{\partial t^2} + \frac{4\pi\mu\sigma}{c^2}\frac{\partial \psi}{\partial t}$$

(see Morse and Feshbach [1953], pp. 218-9). Here, μ, ϵ, and σ are physical constants of the cable, and c is the speed of light. ψ is a potential for the fields, t is time, and z is length along the cable. This equation may be rewritten as

$$\frac{\partial \psi}{\partial t} = -\frac{\partial \phi}{\partial z}$$
$$\frac{\mu\epsilon}{c^2}\frac{\partial \phi}{\partial t} = -\frac{\partial \psi}{\partial z} - \frac{4\pi\mu\sigma}{c^2}\phi$$

where ϕ is introduced only to convert the single second order equation into two first order equations. Another example is transmission of heat in one dimension in a gas. Here the equation is

$$\frac{\partial^2 \psi}{\partial x^2} = a^2\frac{\partial \psi}{\partial t} + \frac{1}{c^2}\frac{\partial^2 \psi}{\partial t^2}$$

(see Morse and Feshbach [1953], pp. 865-9). In this equation, ψ is absolute temperature, a is a property of the medium and c is the velocity of sound in the medium. This equation may disturb some who are used to the equation for transmission of heat being the traditional *Heat Equation*: $\psi_t = (1/a^2)\psi_{xx}$. The usual heat equation implies that heat moves infinitely

fast (John [1978], ch. 7), which is not physical. The equation given here has the property that heat can move no faster than the sound speed of the material (as is easily seen by writing the equation in characteristic form). The reason the heat equation is such a good approximation to the heat transmission problem is that it is the limit as $c \to \infty$ of the correct equation. That is, the transmission of heat is so slow relative to c that the finite speed of propagation has little effect on the solution.

We note that Morse and Feshbach [1953] provide a solution to this equation by means of Green's functions. This solution is not, however, very enlightening or generally useful.

Neutron transport provides another source for these equations. The actual equations are complicated integral equations; see Bell and Glasstone [1970] and Richtmyer and Morton [1967], chapter 9. A typical approximation to these equations assumes that the neutrons are confined to a small discrete set of energies. In this case, a coupled system of equations similiar to the telegrapher's equation arises. The lower order terms in this case model the loss of neutrons due to absorption.

Historical Background

The historical background for this thesis consists of two parts. First is a review of the work on lower order terms in constant coefficient hyperbolic partial differential equations. Second is an outline of some methods for studying the approximate solution to these equations analytically. As an introduction, we discuss the two main effects that the presence of lower order terms can have on the solution.

The first effect of a lower order term is the obvious one: changing the equation. In problems from physics, the lower order term represents a form of dissipation. For example, consider the equation $u_t = u_x + \alpha u$. It is easy to see that the solution to this is $u(x,t) = u(x+t,0)e^{\alpha t}$. Thus, if $\alpha < 0$, the lower order term damps the solution.

Another possible effect of lower order terms is the coupling that they provide among equations. Consider the hyperbolic system

$$\frac{\partial u}{\partial t} = A\frac{\partial u}{\partial x} + Bu. \tag{1.2}$$

Here, A and B are constant matrices, and u is the vector of dependent variables. For (1.2) to be hyberbolic, the eigenvalues of A must be real. This is the general constant coefficient case, since by the assumption of hyperbolicity, any matrix multiplying the $\partial u/\partial t$ term can be inverted and moved into A and B. Further, we assume that A is diagonalizable with

real eigenvalues so that the system will be hyperbolic. Now, if A and B do not commute, so that they are not simultaneously diagonalizable, this will cause coupling. (If A and B do commute, the coupling is apparent but not real. This will be clear in the following.) To see this, make a change of variable $Tu = v$, where $TAT^{-1} = D$, D a diagonal matrix. Then we are left with

$$\frac{\partial v}{\partial t} = D\frac{\partial v}{\partial x} + TBT^{-1}v.$$

This equation is as simple as possible while still exhibiting coupling. The TBT^{-1} term is not diagonal if A and B do not commute and thus couples the components of v.

There has not been much interest in the effect of lower order terms in approximations to constant coefficient hyperbolic partial differential equations until recently. A major reason for this is that, for the continuous problem, well-posedness is independent of the presence of lower order terms (Thomée [1969], sec. 2). This is also true for difference approximations. The lower order terms are unimportant in the question of stability of finite difference schemes, both for the Cauchy problem (Thomée [1969], sec. 5) and for the initial boundary value problem (Gustafsson, Kreiss, and Sundström [1972], Thm. 4.3).

There has been some work on equations with lower order terms. Early work by Apelkrans [1968] on scalar equations of the form

$$\frac{\partial u}{\partial t} = \rho(x,t)\frac{\partial u}{\partial x} + \phi(x,t)u$$

provides bounds on the size of errors made by difference approximations at a step discontinuity. These bounds are sharp for the general problem, but may be somewhat pessimistic for specific problems. The results are based on some concepts from stability theory for difference approximations to hyperbolic problems (see Kreiss and Lundqvist [1968]), and are difficult to extend to systems of coupled equations. Apelkrans' results show quite generally that for scalar (or uncoupled) equations, lower order terms have little effect on the accuracy of difference approximations. Later work by Brenner and Thomée [1971] sharpened these results; their arguments are also based on stability theory (Brenner and Thomée [1970]).

Recent work by Majda and Osher [1977] shows that lower order terms can have an enormous effect on the error in difference approximations by providing the kind of coupling discussed above. They analyze the problem

$$\frac{\partial}{\partial t}\begin{pmatrix}u_1\\u_2\end{pmatrix} = \begin{pmatrix}1 & 0\\0 & -1\end{pmatrix}\frac{\partial}{\partial x}\begin{pmatrix}u_1\\u_2\end{pmatrix} + \begin{pmatrix}0 & 1\\-1 & 0\end{pmatrix}\begin{pmatrix}u_1\\u_2\end{pmatrix}$$
$$u_1(x,0) = \begin{cases}1, & \text{if } x > 0\\ 0, & \text{if } x < 0\end{cases} \tag{1.3}$$
$$u_2(x,0) = 0.$$

Note that the matrices in this equation do not commute. They show that if U is a dissipative finite difference approximation to (1.3) which is at least second order accurate and satisfies certain technical conditions (which are satisfied by common methods), then for all $\delta > 0$ there exists a $C_\delta > 0$ such that

$$\max_{x,t\in R_\delta} |U - u| \le C_\delta h^2$$

where $R_\delta = \{(x,t) : |x| < t \text{ and } |x \pm t|/t > \delta\}$ and $0 < \delta \le t \le T_0$, T_0 the maximum time for the problem. This result is the best possible for arbitrarily accurate dissipative schemes. It is this fact, that the estimate is sharp, which is the interesting feature. This shows that over a large region, any reasonable dissipative method of order at least 2 is only second order accurate. Note that the solution to the continuous problem is smooth (C^∞) away from the fronts (at $x = -t$ and $x = t$) since the initial data is smooth. The results of Majda and Osher [1977] do not hold in the vicinity of the step discontinuity.

We now discuss some of the methods for studying the behavior of difference approximations to hyperbolic partial differential equations: stability theory, Fourier transforms of the difference approximation, model equations, and an *ad hoc* approach. Methods using stability theory are very powerful. General estimates on the accuracy of the solution can be found for a wide range of problems with this method. Examples are Lax [1961] for Cauchy problems and Gustafsson [1975] for initial-boundary value problems. The only drawback of this method is that it requires the solution to be sufficiently smooth. These methods do not say anything about the behavior of the difference scheme near a discontinuity. The results of Apelkrans [1968] and Brenner and Thomée [1971] mentioned above are an exception.

Most work on the behavior of difference approximations to hyperbolic problems by Fourier transform techniques has been restricted to scalar problems (see Hedstrom [1975] and Apelkrans [1968]). This is in contrast to stability theory for difference approximations, where general systems of linear equations can be treated (see Richtmyer and Morton [1967], ch. 4 and Coughran [1980]). The advantage of the Fourier technique is that it can treat nonsmooth solutions (such as step discontinuities).

For constant coefficient problems, methods using Fourier transforms of the difference scheme are practical. The inverse Fourier transform is then evaluated by the method of steepest descent. Hedstrom and Osterheld [1980] present a nice example of this procedure for a different problem. Pearson [1969], using a slightly different approach, studies the behavior of difference schemes for $u_{tt} = c^2 u_{xx}$.

The model or modified equation approach is another way to study the behavior of difference approximations to partial differential equations. In this method, a partial differential equation whose solutions model those of a difference approximation to a simpler differential equation are constructed. The model equation is then studied, rather than the original difference equation. This approach is discussed by Warming and Hyatt [1974] and in a review by Chin and Hedstrom [unpublished]. As we will use this approach to study the behavior of general difference schemes for (1.1), we will outline it below.

The form of the model equation for a hyperbolic problem $u_t + Lu = 0$, where L is a differential operator, is

$$\frac{\partial u}{\partial t} + Lu = c_p h^p \frac{\partial^{p+1} u}{\partial x^{p+1}} + c_q h^q \frac{\partial^{q+1} u}{\partial x^{q+1}}, \tag{1.4}$$

where p is odd and q is even. Given a hyperbolic differential equation $u_t + Lu = 0$ and a difference scheme, expand the finite differences in a formal Taylor series to get

$$\frac{\partial u}{\partial t} + Lu = \sum_{m=1}^{\infty} h^m P_{m+1} u. \tag{1.5}$$

Here, P_m is a homogenous differential operator in ∂_x and ∂_t of order m. Use the *ansatz*

$$\frac{\partial u}{\partial t} + Lu = \sum_{m=1}^{\infty} c_m h^m \frac{\partial^{m+1} u}{\partial x^{m+1}} \tag{1.6}$$

to replace all derivatives with respect to t in (1.5) with x-derivatives, and then match up the terms in (1.4) and (1.6), dropping higher order terms, to find the c_m in (1.4). This gives the model equation.

The behavior of the model equation can be studied with Fourier transform techniques. By using the model equation approach, we can avoid some of the algebra required when using the discrete Fourier transform. More important, the model equation approach allows us to identify the key features of the approximation, allowing us to consider general difference approximations. This approach has been taken by a number of authors. Using the model equation formulation, Hedstrom [1975] analyzed the behavior of step discontinuites

for the equation $u_t = u_x$. Work by Chin [1975] analyzes the detailed behavior near the front for the wave equation. Serdjukova [1971] considers the behavior near a step of a general scalar difference scheme for both explicit and implicit methods.

Finally, we mention an approach taken by Orszag and Jayne [1974]. They consider $u_t + u_x = 0$ and look for solutions with continuous derivatives of order up to n and discontinuous derivative of order $n + 1$. Through a clever choice of initial data with these properties, the difference between the appoximation and the true solution can then be estimated. Chin [1974] shows that this analysis is similiar to the Fourier analysis above and that their results are explained by model equation analysis.

Brief Introduction to Asymptotic Estimation of Integrals

We present here a brief outline of the method of steepest descent, on which most of our results are based. More complete and rigorous descriptions of this method can be found in Bleistein and Handelsman [1975], Erdélyi [1956], and Olver [1974]. Erdélyi [1956] in particular is a good first introduction to this material. We will first introduce the method of stationary phase because it may be more familiar.

We will need to find approximations to integrals of the form

$$\int_{-\infty}^{+\infty} g(x)e^{\phi(x)t}dx \tag{1.7}$$

when t is large. If $\phi(x) = i\psi(x)$, and $\psi(x)$ is real then we can use the method of *stationary phase*. The reason for this name will become clear in what follows.

We can think of $\psi(x)$ as a frequency of oscillation of the integrand, if we assume that $g(x)$ is slowly varying. Now, look for the extrema of $\psi(x)$ (these are points of stationary phase). Assume there is only one extremum, x_0. Expand both $g(x)$ and $\psi(x)$ around x_0:

$$\begin{aligned} g(x) &= g(x_0) + (x - x_0)\frac{dg}{dx}(x_0) + \cdots \\ \psi(x) &= \psi(x_0) + (x - x_0)^2\frac{d^2\psi}{dx^2}(x_0) + \cdots \end{aligned} \tag{1.8}$$

Using these expansions, we can rewrite (1.7) as

$$e^{i\psi(x_0)t}\left(g(x_0)\int_{-\infty}^{+\infty}\exp(it(x - x_0)^2\psi''(x_0))dx + \cdots\right).$$

The integral in the formula above can be evaluated exactly.

This works because, away from x_0, the integrand oscillates rapidly (since t is large) and hence nearly cancels out. Only near x_0 does the integrand oscillate slowly in x. We

can get more terms in the expansion simply by keeping more terms in the expansions (1.8) of g and ψ. There are, however, a number of restrictions to remember. First, it is very important that g vary slowly on the scale of $\exp(i\psi(x)t)$. For example, if g has a pole near an extremum of $\psi(x)$, the expansion (1.8) will be inaccurate. Also, in the case where $\psi(x)$ has several extrema, they must be well separated. Otherwise, there may be an interval, rather than a point, where the integrand oscillates slowly.

What if $\psi(x)$ or x_0 is not real? Then we must go to the *method of steepest descent.* We extend $\phi(x)$ (we will not use $\psi(x)$ again) to be a complex valued function $\phi(z)$ over the complex plane. This is usually a trivial step in practice. Since $\phi(z)$ is now complex valued, it is not possible to say that $e^{\phi(z)t}$ oscillates at all in general. Further, if $\phi(z)$ is analytic, it has no minima or maxima (by the maximum modulus principle).

We consider the following. If we could find a path of integration Γ such that $|e^{\phi}|/\max_{z\in\Gamma}|e^{\phi}| > \epsilon$ only along a few short intervals, then, just as before, we could expand g and ϕ about points on those intervals. Let us assume that there is only one such point, and call it z_0. We can then use the Cauchy integral theorem to deform the original path of integration to the new path Γ. Then as t increases, the contribution to the integral from points away from z_0 will decay exponentially.

A good way to look at this is in terms of a topographical map. Let $x + iy = z$ be the map coordinates, and let $\Re(\phi(z)) =$ real part of $\phi(z)$ be the height of the "ground." This map will normally have lots of valleys, hills, and, most importantly, saddle points (maybe only one). A simple saddle point is like a mountain pass — at the saddle point, you can either go downhill (along the pass) or uphill (at right angles to the pass). In our application, the path typically starts in a valley at $x = -\infty$, proceeds over one or more mountain ranges, and ends in a valley at $x = \infty$. When going over the mountain range, the best path to take is one going through the saddle points. The path then stays low except for a few peaks where it rises quickly to go though a pass (saddle point) and then falls again quickly. This is what we want, since the exponential will have small magnitude everywhere except in a small neighborhood of each pass (saddle point). This explains why the method is called the method of steepest descent, as the path descends as quickly as possible from each pass.

Given this geometric viewpoint, it is easy to find conditions for the passes and for the direction of the path. These conditions are derived in Bleistein and Handelsman [1975],

chapter 7. Basically, an n-th order saddle point z_0 is a point where the first n derivatives of $\phi(z)$ are zero and the $n+1$st derivative is non-zero. This condition is the same as for the method of stationary phase discussed above. Then it can be shown (see, e.g., Bleistein and Handlesman [1975], Thm 7.1) that the direction of the path of steepest descent from an n-th order saddle point at the saddle point is given by the following rule: If $d^{n+1}\phi(z_0)/dz^{n+1} = ae^{i\alpha}$, then the directions of steepest descent are given by $\theta = (-\alpha + (2p+1)\pi)/n$, for $p = 0, 1, \ldots, n-1$.

The above sketch of the method of steepest descent ignores a number of possible difficulties. Most important for our purposes is what happens if g is not slowly varying or if several saddle points come together. The proper way to handle this is discussed in section 2; basically it amounts to using better expansions for g and ϕ. The difficulty with these more accurate expansions is that the integrals in the expansion may no longer be recognizable as known special functions. Instead, they may define new special functions whose behavior must be investigated. We will encounter a new class of special functions in sections 3 and 4.

2. The Exact Solution

In this section we find the exact solution to the model problem

$$\begin{aligned} u_t &= -v_x \\ v_t &= -u_x - v \\ u(x,0) = v(x,0) &= \begin{cases} 1, & \text{if } x < 0 \\ \frac{1}{2}, & \text{if } x = 0 \\ 0, & \text{if } x > 0. \end{cases} \end{aligned} \tag{2.1}$$

We are only interested in u near the front ($x = t$). Our solution will be valid only in this region.

Our purposes for finding the exact solution to the model problem are manifold. First, we will need the exact solution to compare with the solutions of approximations to the problem. Second, in finding an asymptotic expression for the exact solution we will demonstrate many of the techniques that we will use in later sections. Most important, we will use the analysis in this section to motivate definitions and analysis in later sections.

We point out that for $x > t$, $u(x,t) = v(x,t) = 0$ from the theory of characteristics (John [1978]). Unless otherwise stated, all limits $x/t \to 1$ are from the left in the x-t plane.

The analysis will proceed as follows. First, we Fourier transform (2.1) in space to get a system of two ordinary differential equations. As these are linear constant coefficient equations, it is easy to solve for the inverse transform of the solution. The inverse transform does not represent any known special function, so we will use techniques from saddle point analysis to represent the inverse transform near the front $x = t$ as an asymptotic series in terms of modified Bessel functions.

Integral Form of the Solution

The Fourier transform of (2.1) is

$$\begin{aligned} \hat{u}_t &= -i\xi\hat{v} \\ \hat{v}_t &= -i\xi\hat{u} - \hat{v} \end{aligned} \tag{2.2}$$

where ξ is the dual variable. In matrix form, this is

$$\frac{d}{dt}\begin{pmatrix}\hat{u}\\ \hat{v}\end{pmatrix} = \begin{pmatrix} 0 & -i\xi \\ -i\xi & -1 \end{pmatrix}\begin{pmatrix}\hat{u}\\ \hat{v}\end{pmatrix}.$$

The eigenvalues λ of the matrix are given by $\lambda(\lambda+1)+\xi^2=0$, or

$$\lambda_\pm(\xi) = -\frac{1}{2} \pm \frac{i}{2}\sqrt{4\xi^2-1}.$$

The branch cut for the square root is the interval $[-\frac{1}{2}, \frac{1}{2}]$ in the ξ plane. This is the standard branch. The unnormalized eigenvectors of the matrix are

$$a_\pm = \begin{pmatrix} 1+\lambda_\pm \\ -i\xi \end{pmatrix}.$$

Therefore, the solution to (2.2) is

$$\begin{pmatrix} \hat{u} \\ \hat{v} \end{pmatrix} = \alpha_+(\xi)\begin{pmatrix} 1+\lambda_+ \\ -i\xi \end{pmatrix}e^{\lambda_+ t} + \alpha_-(\xi)\begin{pmatrix} 1+\lambda_- \\ -i\xi \end{pmatrix}e^{\lambda_- t}$$

where $\alpha_\pm(\xi)$ are determined by the Fourier transform of the initial conditions.

Now that we have the solution to the transform of (2.1), we can compute u and v by inverting the transform. The solution for u is thus

$$u(x,t) = \frac{1}{2\pi}\int_{-\infty}^{+\infty} [\alpha_+(\xi)(1+\lambda_+)e^{\lambda_+ t} + \alpha_-(\xi)(1+\lambda_-)e^{\lambda_- t}]e^{ix\xi}\,d\xi. \tag{2.3}$$

Here we choose the path of integration to pass over the branch cut between $-1/2$ and $1/2$ (an arbitrary choice).

To determine $\alpha_\pm$ we apply the initial conditions to the solution of the differential equation. At $t=0$, we have

$$\begin{aligned} \alpha_+(\xi)(1+\lambda_+) + \alpha_-(\xi)(1+\lambda_-) &= \hat{f}(\xi) \\ -i\alpha_+(\xi)\xi - i\alpha_-(\xi)\xi &= \hat{f}(\xi) \end{aligned}$$

where $\hat{u}(\xi,0) = \hat{v}(\xi,0) = \hat{f}(\xi)$. These imply

$$\begin{aligned} \alpha_-(\xi) &= \frac{i\hat{f}(\xi)}{\sqrt{4\xi^2-1}}\left(1 - \frac{i}{\xi}(1+\lambda_+)\right) \\ \alpha_+(\xi) &= \frac{i\hat{f}(\xi)}{\xi} - \alpha_-(\xi). \end{aligned} \tag{2.4}$$

For the initial data given by (2.1), we have $\hat{f}(\xi) = \frac{i}{2\xi} + \frac{\pi}{2}\delta(\xi)$.

Solution near the Front

We have now completely specified the solution to (2.1). We need only evaluate the integral (2.3) in order to determine the solution. However, there is no known special

function that this integral represents. To uncover the solution, we will turn to asymptotic evaluation of the integral by the method of steepest descent outlined in the introduction. We will outline the steps again, as we will see that there are new complications: converging saddle points and a pole in g. We write (2.3) as the sum of two integrals of the form

$$\int g(\xi)\, e^{\phi(\xi)t}\, d\xi.$$

Here, g does not contain an exponential factor in t or x.

The analysis of (2.3) takes place in five steps. First, the saddle points of ϕ are found. Next, the path of integration is deformed to the steepest descent path through some of the saddle points. We will call these the *important* saddles. This path will not necessarily pass through all of the saddle points. Care must be exercised at this point if the original path of integration passes through any singularities of the integrand. If the original path does pass through some simple poles and the new path does not, half the residues at those points will have to be added to the integral. Third, a change of variable is made to map ϕ onto a simpler function ψ that has the same number of important saddle points as ϕ has. Next, g is expanded *in* a power series about the saddle points of ψ and any critical points of g (in our case, we expand only about the critical points of g; this will be discussed later). Finally, the resulting integral is evaluated. In this section, these integrals can be evaluated in terms of known special functions. If this is not the case, as in the next section, then the integrals represent a new special function which must be examined. The result we now prove is:

Theorem 1: For $x \leq t$ and $x/t \approx 1$, the solution for u in (2.1) has the asymptotic representation

$$u(x,t) = \sum_{\nu=0}^{\infty} u_\nu \doteq \frac{1}{2} e^{-t/2} \sum_{\nu=0}^{\infty} \left(\frac{1-\omega}{1+\omega}\right)^{\frac{\nu}{2}} I_\nu\left(\frac{t}{2}\sqrt{1-\omega^2}\right). \tag{2.5}$$

Proof:

We first find the saddle points. Let $\omega = x/t$, and define $\phi_\pm(\xi) = \lambda_\pm(\xi) + i\omega\xi$. Then (2.3) can be written as

$$\int g_+ e^{\phi_+ t} d\xi + \int g_- e^{\phi_- t} d\xi.$$

Each of these is in the form discussed above. The condition for the saddle points of $\phi_\pm$ is

$$\frac{d\phi_\pm}{d\xi}(\xi) = \pm \frac{2i\xi}{\sqrt{1\xi^2 - 1}} + i\omega = 0. \tag{2.6}$$

The saddle points are

$$\xi_{\pm} = \pm \frac{\omega}{2\sqrt{\omega^2 - 1}}. \tag{2.7}$$

It is easy to show that $d^2\phi_{\pm}/d\xi^2 \neq 0$ for $\omega \neq 1$, so these saddles are simple for $\omega \neq 1$. At $\omega = 1$, the saddle points are both at infinity, and are of infinite order.

Now, we must be careful here as the formula (2.7) is the result of solving a quadratic formed by squaring (2.6). This means that we must check to see which choice of sign, if any, is a solution to the equation (2.6). This is equivalent to determining on which side of the branch cut of the square root the solutions (2.7) lie. Note that there are four conditions to check — $\xi_{\pm}$ in both ϕ_- and ϕ_+.

By substituting (2.7) into (2.6), we can show that for $\omega > 0$, ϕ_+ has *no* saddle points and ϕ_- has two saddle points. For $\omega < 0$ the situation is reversed.

It is thus natural to break the integral (2.3) into two parts

$$\begin{aligned} u_+ &= \frac{1}{2\pi} \int_{-\infty}^{+\infty} \alpha_+(1 + \lambda_+) e^{\phi + t}\, d\xi \\ u_- &= \frac{1}{2\pi} \int_{-\infty}^{+\infty} \alpha_-(1 + \lambda_-) e^{\phi - t}\, d\xi. \end{aligned} \tag{2.8}$$

We show in Appendix A that $u_+ = 0$ for $\omega > 0$. We therefore concentrate on the behavior of u_-, in particular for $\omega \approx 1$.

From (2.7), we see that as $\omega \to 1$, the saddle points go to $\pm i\infty$. The major contribution to the integral will come from two places. One is the region of the saddle points; the other is the pole in the integrand at $\xi = 0$. The path may be deformed away from the $(\xi \pm \frac{1}{2})^{-1/2}$ singularities in $\alpha_-(1 + \lambda_-)$ without changing the value of the integral, as these singularities are weaker than poles.

We first deform the path away from the pole at the origin. To correct for this (since the integral is the Cauchy Principle Value) we add πi times the residue at $\xi = 0$. From (2.4) and (2.8) it is easy to see that the residue is $i/4\pi$ (for the path of integration passing over, rather than under, the branch cut), yielding a term of $-1/4$ to be added to the integral over the new path.

We can now consider the effects of the saddle points. Since there are two saddle points, we will need to consider a uniform approximation to the integral which models the confluence of two saddle points to a saddle point of infinite order. Such a case is considered by Bleistein and Handlesman [1975] in section 9.5. We will use essentially the same approach as they use for this problem.

To make the analysis easier, we first map ξ onto $1/z$, and work in the z-plane. In the z-plane, the saddle points are converging to the origin as $\omega \to 1$.

Expanding $\phi_-(1/z)$ about $z = 0$, we see that

$$\begin{aligned}\phi_- &= -\frac{1}{2} - \frac{i}{z}\sqrt{1 - \frac{z^2}{4}} + \frac{i\omega}{z} \\ &\approx -\frac{1}{2} - \frac{i}{z}(1-\omega) + \frac{i}{8}z.\end{aligned}$$

Using this as motivation, we define a change of variables $p = p(z)$ by

$$\psi(p) = \frac{i}{8}p + b + \frac{a^2}{p} = \phi_-(\frac{1}{z}). \tag{2.9}$$

Here, a and b are numbers independent of p but perhaps depending on ω. It is important to note that this form is the simplest form which has the requisite properties. The requirements that ψ have exactly two saddle points which come together to a single saddle point of infinite order completely determines the simplest form of ψ.

To find a and b, let $z_\pm = 1/\xi_\pm$, $\xi_\pm$ the saddle points of $\phi(\xi)$, and let $p_\pm = p(z_\pm)$ be the saddle points in the p-plane. Since $p(z)$ is locally 1-1 (see Guillemin and Sternberg [1977], page 441-2), we have

$$\frac{dp}{dz} = \frac{d\phi_-}{dz} \Big/ \frac{d\psi}{dp} = \frac{\dfrac{d\phi_-}{dz}}{\dfrac{i}{8} - \dfrac{a^2}{p^2}} \neq 0.$$

The fact that $p(z)$ is locally one-to-one everywhere means that, in particular, it is one-to-one at the saddle points. Thus we must have $dz/dp \neq 0$ at the saddle points. Since by definition $d\phi_-/dz = 0$ at the saddle points, we must have

$$\frac{i}{8} - \frac{a^2}{p(z_\pm)^2} = 0$$

or $p^2(z_\pm) = -8ia^2$. Applying these two equations to (2.9) gives $\pm 2\sqrt{i/8}a + b = \phi_-(\xi_\pm)$ or

$$\begin{aligned}b &= \frac{\phi_-(\xi_+) + \phi_-(\xi_-)}{2} \\ a &= \frac{\phi_-(\xi_+) - \phi_-(\xi_-)}{4\sqrt{\frac{i}{8}}}.\end{aligned}$$

Being careful with the branch of the square root, it is easy to show that $\phi_-(\xi_\pm) = -\frac{1}{2} \pm \frac{i}{2}\sqrt{\omega^2 - 1}$, and hence that

$$\begin{aligned}b &= -\frac{1}{2} \\ a^2 &= \frac{i(\omega^2 - 1)}{2}.\end{aligned}$$

Thus $\psi(p)$, the *canonical form*, is

$$\psi(p) = \frac{i}{8}p - \frac{1}{2} - \frac{i(1-\omega^2)}{2}\frac{1}{p}. \tag{2.10}$$

Note that for $\omega \approx 1$, this is very close to the $z \to 0$ limit of ϕ_-.

The unexponentiated part of the integral has three components. First is the $\beta(1+\lambda_-)$ from (2.3). Second is a $-1/z^2$ term coming from the change of variables $\xi = 1/z$. Finally, there is the dz/dp term coming from the change of variables $p = p(z)$. To determine these in terms of p, we need to find a representation for $p = p(z)$. We also need to find dz/dp. In a general case, we can find this information from (2.9); however, in this case, we can find the map explicitly.

Now, (2.9) may be thought of as a quadratic equation in z, whose coefficients depend on p:

$$\frac{ip}{8} + \frac{i(\omega^2-1)}{2p} - \frac{i\omega}{z} = -\frac{i}{z}\sqrt{1-\frac{z^2}{4}}$$

or

$$z^2\left(\frac{p}{8} + \frac{(\omega^2-1)}{2p} + \frac{\omega}{z}\right)^2 = 1 - \frac{z^2}{4}$$

With some algebraic manipulation, we may rewrite this as

$$z = \frac{8p(\omega \mp 1)}{p^2 + 4(\omega \mp 1)^2}.$$

To pick between the two solutions for z, we insist that for ω near 1, $z \approx p$, with both p and z near 0. This requirement just says that $p = p(z)$ is one-to-one in the neighborhood of the saddle points near $z = 0$. This is satisfied by the $+$ choice in $\mp$, and we have finally

$$z = \frac{2p}{\omega+1}\frac{1}{1+\left(\frac{p}{2(\omega+1)}\right)^2}.$$

It will be useful to expand this about $p = 0$; the result is:

$$z = \frac{2p}{\omega+1}\sum_{\nu=0}^{\infty}(-1)^\nu\left(\frac{p}{2(\omega+1)}\right)^{2\nu}. \tag{2.11}$$

Differentiating (2.11), we find that

$$\begin{aligned}\frac{dz}{dp} &= \frac{2}{\omega+1}\sum_{\nu=0}^{\infty}(-1)^\nu(1+2\nu)\left(\frac{p}{2(\omega+1)}\right)^{2\nu} \\ &\approx \frac{2}{1+\omega}\left(1 - \frac{3p^2}{4(\omega+1)^2} + O(p^4)\right).\end{aligned}$$

This is the appropriate form of dz/dp, since the saddle points are converging to the origin, and the unexponentiated term has a pole at $p = 0$. (We have used the form recommended by van der Waerden [1951] for saddle points near a pole. Other expansions are possible; see Bleistein [1966] and Olver [1974].)

Next, we find the unexponentiated part of the integrand. It is convenient to consider $\alpha_-(1+\lambda_-)(-1/z^2) \equiv h(p)$ together. Neglecting the δ-function term in $\alpha_-(1+\lambda_+)$, this is

$$h(p) = \frac{1}{8\sqrt{1-\frac{z^2}{4}}}\left(1 - \frac{2i}{z}\left(1+\sqrt{1-\frac{z^2}{4}}\right)\right).$$

Now, we need to convert this to the p variable. We handle the square root first.

$$\begin{aligned}\sqrt{1-\frac{z^2}{4}} &= \sqrt{1 - \frac{16p^2(\omega+1)^2}{(p^2+4(\omega+1)^2)^2}} \\ &= \frac{4(\omega+1)^2 - p^2}{4(\omega+1)^2 + p^2}\end{aligned}$$

where the branch of the square root was chosen for p small. Using this formula, we find after some manipulation that

$$h(p) = \frac{p^2 + 4(\omega+1)^2}{8(4(\omega+1)-p^2)}\left(1 - \frac{2i(\omega+1)}{p}\right).$$

Multiplying this by the last part of the unexponentiated term, dz/dp, we get

$$\frac{1}{4(\omega+1)}\left(1 - \frac{2i(\omega+1)}{p}\right)\frac{1}{\frac{p^2}{4(\omega+1)^2}+1}.$$

Finally, as a power series, this is

$$\frac{1}{4(\omega+1)}\sum_{\nu=-1}^{\infty}\left(\frac{-p}{2i(\omega+1)}\right)^{\nu}. \tag{2.12}$$

We are now ready to write u as an asymptotic series. Combining (2.10) and (2.12), we have

$$u(x,t) = -\frac{1}{8\pi(\omega+1)}\sum_{\nu=-1}^{\infty}\int_{-\infty}^{+\infty}\left(\frac{-p}{2i(\omega+1)}\right)^{\nu}\exp\left(\left(\frac{i}{8}p - \frac{1}{2} - \frac{i(1-\omega^2)}{2p}\right)t\right)dp.$$

Again, we have deformed the path of integration. The $\delta(\xi)$ term in $\hat{f}$ which we have been neglecting cancels the $-\frac{1}{4}$ term from the pole at $\xi = 0$ (which is $z = \infty$). This pole is not

present in our expansion of the unexponentiated term because we broke the integral u_- in (2.8) into two parts: one part about the saddle points near $z = 0$, and the other part near the pole at $z = \infty$. We can deform the path away from the pole at $z = \infty$, including the contribution from the pole. This leaves us with just the integral above. (Note that there is also a pole at $p = 0$. This pole is handled as part of the integral — see the second integral identity in Appendix A.)

The first term in this expansion is

$$u \approx u_0 = -\frac{1}{2\pi}\int_{-\infty}^{+\infty} \frac{i}{2p} \exp\left(\left(\frac{i}{8}p - \frac{1}{2} - \frac{i(1-\omega^2)}{2p}\right)t\right) dp.$$

The second integral identity in Appendix A tells us that this is

$$u_0 = \frac{1}{2}e^{-t/2} I_0\left(\frac{t}{2}\sqrt{1-\omega^2}\right),$$

where I_ν is the regular special Bessel function of order ν. This is a good approximation for ω less than and near 1.

The next term is just

$$u_1 = -\frac{1}{2\pi}\int_{-\infty}^{+\infty} \frac{1}{4(\omega+1)} \exp\left(\left(\frac{i}{8}p - \frac{1}{2} - \frac{i(1-\omega^2)}{2p}\right)t\right) dp.$$

From the formula in Appendix A, this is

$$u_1(x,t) = \frac{1}{2}e^{-t/2}\sqrt{\frac{1-\omega}{1+\omega}}\, I_1\left(\frac{t}{2}\sqrt{1-\omega^2}\right).$$

This process may be carried out repeatedly; this completes the proof. ∎

It is interesting to consider the behavior of the first few terms in the approximation (2.5) near the front ($\omega \approx 1$). First we note that for $\omega = 1$, the $\nu > 0$ terms are all zero since $I_\nu(0) = 0$ for $\nu \geq 1$ (see Abramowitz and Stegun [1972]). In general, at $\omega = 1$, the $\nu > k$ terms are 0 for $u(x,t)$ and its first k derivatives in x. Thus, the first k terms give u and its first $k-1$ derivatives in x exactly at $t = x$. We expect, therefore, that the first few terms would give us a good approximation to the solution for $x \approx t$.

Asymptotic Behavior near the Front

We can get a better idea of behavior of the solution near the front $x = t$ by looking at the small argument behavior of $I_\nu(z)$. Using the small argument form, (2.5) gives

$$u(x,t) = \frac{1}{2}e^{-t/2}\left(1 + \frac{t-x}{4} + \frac{t^2-x^2}{16} + \frac{(t-x)^2}{32} + \cdots\right)$$

$$\frac{\partial u}{\partial x} = -\frac{1}{8}e^{-t/2}\left(1 + \frac{x}{2} + \cdots\right).$$

It is clear from the power series for I_ν that $u_\nu = b_\nu(t-x)^\nu \exp(-t/2) + O((t-x)^{\nu+2})\exp(-t/2)$ for $\omega \approx 1$. At $t = 1$ and $x = 1$ these give $u = \frac{1}{2}e^{-1/2}$ and $u_x = -\frac{3}{16}e^{-1/2}$ exactly. We can compare these with the computed solution given in figure 1. The method used for computing the exact solution is given in Appendix B.

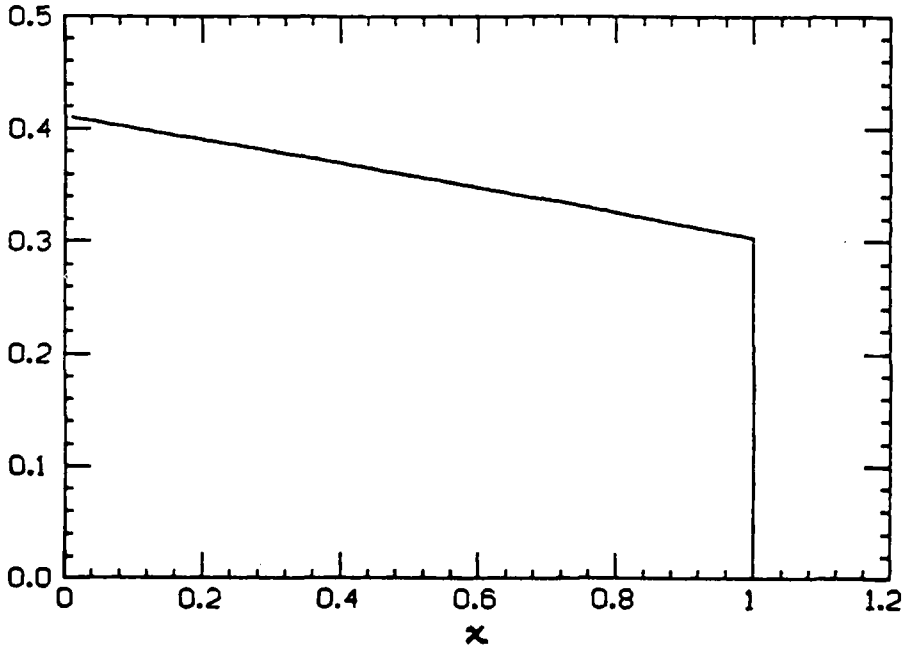

Figure 1: Exact solution for u for $t = 1$.

As we can see from figure 1, these match our results. In particular, note that the height of the front is roughly 0.3, which agrees with the computed value of $\frac{1}{2}e^{-1/2} \approx 0.303$. Also, the slope near the front can be estimated as $0.3 - 0.41 = -0.11$, which matches the calculated value of $-3e^{-1/2}/16 \approx -0.114$.

Finally, we discuss the range of validity of the expansion (2.5). The limitation comes from the fact that the expansion (2.12) is valid only for $|z| < 2$. Thus, as ω decreases from 1, we can expect the $(z \pm 2)^{-1/2}$ terms to have an increasing effect. As a rule of thumb, since $|z_\pm| = 2$ at $\omega = (1/2)^{1/2} \approx 0.707$, the approximation will be valid for a range of ω

near 1, such as $1/2 + 1/2(1/2)^{1/2} < \omega \leq 1$. If we wanted an expansion that was valid over a greater range of ω, we would have to either use an expansion of $\alpha_-(1 + \lambda_-)$ with a greater radius of convergence or use the method of matched asymptotics. In this case, the method of matched asymptotics would be the more fruitful approach. In this approach, as the saddle points approach the branch cut, the path of steepest descent begins to be affected by the branch cut. At the same time, the saddle points are moving apart and hence interacting less and less strongly. Thus we could use an expansion valid for two saddle points approaching a branch cut. In the transition region, we would match these two asymptotic expansions. Since we are interested in the solution only near the front $\omega = 1$, we will not consider either of these further.

3. Behavior of Difference Approximations near the Discontinuity: Second Order Method of Lines

In this section we analyze a particular difference approximation to the model problem. For simplicity in the discussion, we consider the method of lines (or semi-discrete) second order centered difference approximation

$$\begin{aligned} \frac{dU_j}{dt} &= -\frac{V_{j+1} - V_{j-1}}{2h} \\ \frac{dV_j}{dt} &= -\frac{U_{j+1} - U_{j-1}}{2h} - V_j \\ U_j(0) = V_j(0) &= \begin{cases} \frac{1}{2}, & \text{if } j < 0 \\ 0, & \text{if } j = 0 \\ -\frac{1}{2}, & \text{if } j > 0. \end{cases} \end{aligned} \tag{3.1}$$

This is a second order non-dissipative difference approximation to our model problem. The space step size is h. The grid is not staggered. For simplicity of analysis, the undifferentiated term is not averaged. Also for simplicity of analysis, the initial conditions are slightly different from those in the previous section. However, this will not affect the behavior of the difference scheme, since both the equation and the difference scheme are linear. Of course, this change in initial data changes the solution everywhere by $\frac{1}{2}$ for U and by $\frac{1}{2}e^{-t}$ for V for both the continuous and the semi-discrete problem, but we can ignore this since the change is the same for all x.

Our analysis will illustrate the behavior of the approximate solution to $U_j(t)$ near the front $x = t$. We are particularly interested in the asymptotic behavior of the width of the front as $h \to 0$. In addition, we will show that the behavior of the difference scheme near the front is very similiar to that of the wave equation.

Since this section is the longest, we will provide a more detailed summary of it. We first find the inverse Fourier transform which represents the solution to (3.1). We will see that the inverse transform is more complicated than that in section 2; in fact, its canonical form represents a new special function. At this point the analysis diverges from that in the previous section. We take up the question of the width of the front in (3.1) (since the discontinuity in the solution to (2.1) is smeared out by the approximation (3.1)). First we discuss the behavior of the exponential in the inverse transform integral. This leads us to

a definition for the width of the front. We then go on to state and prove a theorem that the width of the front is $O(h^{2/3})$. After the proof is complete, we turn to the canonical form of the inverse tranform. From the canonical form, we can show the behavior of the solution to (3.1) near the front (mostly through graphs displayed in section 5). We close with a few secondary issues which may be skipped on a first reading. The first is the behavior of the solution away from the front. The other discusses the size of a term that was neglected in the analysis.

Integral Form of Solution

We start with the discrete Fourier transform of (3.1):

$$\begin{aligned} \frac{d\hat{U}}{dt} &= -\frac{i}{h}\sin(h\xi)\hat{V} \\ \frac{d\hat{V}}{dt} &= -\frac{i}{h}\sin(h\xi)\hat{U} - \hat{V} \end{aligned} \tag{3.2}$$

where ξ is the dual variable. Let $\theta = h\xi$. In matrix form, this is

$$\frac{d}{dt}\begin{pmatrix}\hat{U}\\ \hat{V}\end{pmatrix} = \begin{pmatrix}0 & -\frac{i}{h}\sin\theta\\ -\frac{i}{h}\sin\theta & -1\end{pmatrix}\begin{pmatrix}\hat{U}\\ \hat{V}\end{pmatrix}.$$

The eigenvalues λ of the matrix are given by $\lambda(\lambda+1) + \sin^2\theta/h^2 = 0$, or

$$\lambda_\pm(\xi) = -\frac{1}{2} \pm \frac{i}{2}\sqrt{\frac{4\sin^2\theta}{h^2} - 1}.$$

The branch cut for the square root is the interval $[-\mathrm{Arcsin}(h/2)/h, \mathrm{Arcsin}(h/2)/h]$ in the ξ plane. This is the standard branch. The unnormalized eigenvectors of the matrix are

$$a_\pm = \begin{pmatrix}1+\lambda_\pm\\ -\frac{i}{h}\sin\theta\end{pmatrix}.$$

Therefore, the solution to (3.2) is

$$\begin{pmatrix}\hat{U}\\ \hat{V}\end{pmatrix} = \alpha_+(\xi)\begin{pmatrix}1+\lambda_+\\ -\frac{i}{h}\sin\theta\end{pmatrix}e^{\lambda_+ t} + \alpha_-(\xi)\begin{pmatrix}1+\lambda_-\\ -\frac{i}{h}\sin\theta\end{pmatrix}e^{\lambda_- t}$$

where $\alpha_\pm(\xi)$ are determined by the discrete Fourier transform of the initial data. The solution for U is then just the inverse transform

$$U(x,t) = \frac{1}{2\pi}\int_{-\pi/h}^{+\pi/h}[\alpha_+(\xi)(1+\lambda_+)e^{\lambda_+ t} + \alpha_-(\xi)(1+\lambda_-)e^{\lambda_- t}]e^{ix\xi}\,d\xi. \tag{3.3}$$

As in section 2, the path of integration passes above the branch cut. Let $\phi_\pm = \lambda_\pm + i(x/t)$. We will write the two terms in (3.3) corresponding to ϕ_+ and ϕ_- as U_+ and U_- respectively,

as in (2.8). We note that this formula defines U for all real x, even though U was originally defined only for $x = jh$ for integer j. The inverse transform (3.3) provides, however, a natural interpolation to real x, and we will use this in the rest of this section.

To determine $\alpha_\pm$ we apply the initial conditions to the solution of the differential equation (3.2). At $t = 0$, we have

$$\alpha_+(\xi)(1+\lambda_+) + \alpha_-(\xi)(1+\lambda_-) = \hat{f}(\xi)$$
$$\alpha_+(\xi)\frac{\sin\theta}{h} + \alpha_-(\xi)\frac{\sin\theta}{h} = i\hat{f}(\xi)$$

where $\hat{U}(\xi,0) = \hat{V}(\xi,0) = \hat{f}(\xi)$. These imply

$$\alpha_-(\xi) = \frac{i\hat{f}}{\sqrt{\frac{4\sin^2\theta}{h^2} - 1}}\left(1 - \frac{ih}{\sin\theta}(1+\lambda_+)\right)$$
$$\alpha_+(\xi) = \frac{ih\hat{f}}{\sin\theta} - \alpha_-(\xi)$$

or

$$\begin{aligned}\alpha_-(\xi)(1+\lambda_-) &= \frac{i\hat{f}}{2\sqrt{\frac{4\sin^2\theta}{h^2} - 1}}\left(1 - \frac{2i\sin\theta}{h} - i\sqrt{\frac{4\sin^2\theta}{h^2} - 1}\right)\\ \alpha_+(\xi)(1+\lambda_+) &= -\frac{i\hat{f}}{2\sqrt{\frac{4\sin^2\theta}{h^2} - 1}}\left(1 - \frac{2i\sin\theta}{h} + i\sqrt{\frac{4\sin^2\theta}{h^2} - 1}\right).\end{aligned} \tag{3.4}$$

For the initial data given by (3.1), we have $\hat{f}(\xi) = ih\cot(\theta/2)/2$.

We need now to investigate the behavior of (3.3) with (3.4) in the vicinity of $x = t$. We start by defining $\omega = x/t$ and $\phi_\pm(\xi) = \lambda_\pm(\xi) + i\omega\xi$. (Where it is more convienent, we will write $\phi(\theta)$ for $\phi(\xi)$.) The condition for the saddle points is then

$$\frac{d\phi_\pm}{d\xi}(\xi) = \pm\frac{2i\sin\theta\cos\theta}{h\sqrt{\frac{4\sin^2\theta}{h^2} - 1}} + i\omega = 0. \tag{3.5}$$

The solution for the saddle points $\theta_\pm$ is

$$s_\pm^2 \equiv \sin^2\theta_\pm = \frac{1-\omega^2}{2} \pm \frac{1}{2}\sqrt{(1-\omega^2)^2 + \omega^2 h^2}. \tag{3.6}$$

There are clearly eight solutions ξ to this equation in the rectangle $(-\pi/h, \pi/h] \times (-\infty, \infty)$. Let $\theta_\pm = \sin^{-1} s_\pm$, with $0 \le \theta_+ < \pi/2$ and $\Re\theta_- = 0$, $\theta_-/i > 0$. ($\Re z$ is the real part of z.) Then the other six roots are $-\theta_+$, $\pi - \theta_+$, $-\pi + \theta_+$, $-\theta_-$, $\pi + \theta_-$, and $\pi - \theta_-$. To see which of these solutions are zeros of $\phi'_-(\xi)$ and which are zeros of $\phi'_+(\xi)$, we plug (3.6)

into (3.5). Again, we must be careful with the branch of the square root. We first note that $\text{sign}(\Re \sin\theta) = \text{sign}(\Re(4\sin^2\theta/h^2 - 1)^{1/2})$. Thus, by considering the sign of $\Re\cos\theta$, we see that $\phi'_-(\xi)$ has roots $h\xi = \pm\theta_+$ and $\pm\theta_-$, and $\phi'_+(\xi)$ has roots $\pm\pi \mp \theta_+$ and $\pi \pm \theta_-$.

Note that the location of the saddle points is substantially more complicated than for the integral in section 2. This complication makes it impossible to obtain an asymptotic expansion for (3.3) in terms of known special functions. We will have to be content with some estimates of its behavior. Note also that the integral of the ϕ_+ term is not zero, in contrast to the continuous case. However, we will show later that it is of the same size as the first neglected term in the asymptotic expansion. For the moment, though, we will ignore the ϕ_+ term.

Width of the Front

Perhaps the most interesting information that we can look for is the width of the front. Serdjukova [1971] and Hedstrom [1975] have shown that for the scalar wave equation, the width of the approximation to a step discontinuity by a difference method of order p is $O(h^{p/(p+1)})$. This smearing out of the front can be thought of as the result of numerical dispersion or dissipation or both, introduced by the approximation. In this section we will show that the same relation holds for the second order method (3.1) under consideration. We show this as follows. First, we study the path of steepest descent. This will show us that the saddle point θ_- controls the width of the front. Next, we use perturbation techniques to find θ_- and $\phi_-(\theta_-)$ for $x/t = \omega = 1 + ch^\gamma$. By studying the behavior of $\phi_-(\theta_-)$ as a function of γ, we will see that the width of the front is indeed $O(h^{2/3})$.

In passing, we note that the width of the front is not a well defined concept. This is because there are a number of other phenonema which interfere with any measurments of a width of the front. For example, the oscillations which are present in almost any difference approximation can mask the width of the front. Despite this, it is sometimes possible to define a width for the front that matches the observations. For the scalar wave equation (Hedstrom [1975]), dimensional analysis reveals the width of the front. We can not use the same technique here. Thus, we must motivate a "definition" of width of front which matches what we observe when we look at a graph of the solution. We will show that $\phi_-(\theta_-)$ provides us with a definition for the width of the front.

We will start by presenting some computations of the path of steepest descent and the height of that path for a particular value of h. These computations are only used to provide

motivation for both a definition of width of the front and the theorem that follows, and are not used for proof. However, the geometry of the surface $\Re\phi_-$ is complicated enough that a specific example will help in understanding the proof.

Since we are interested in the behavior in the vicinity of $x = t$, we look at contour plots of $\Re\phi_-$ for ω near 1. From the topographical interpretation of saddle points, we define $\Re\phi_-$ as the *height* of ϕ_-, since $|e^{\phi}| = e^{\Re\phi}$.

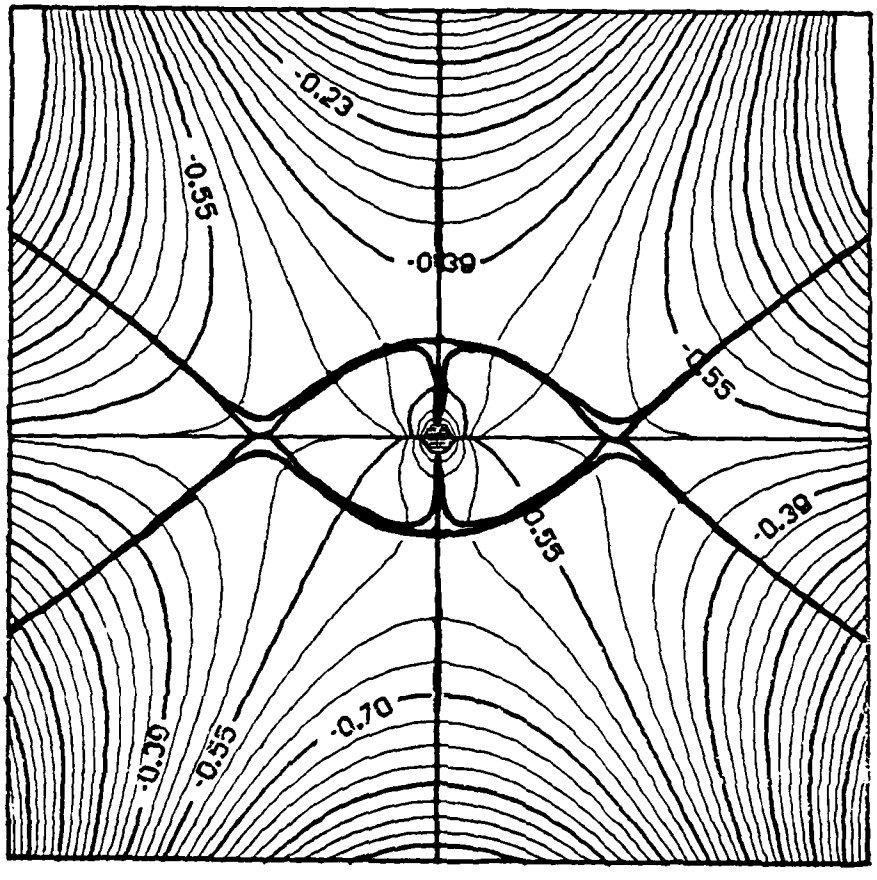

Figure 2: Contour plot of ϕ_- for $\omega = 0.985$ and $h = 0.05$. Boldface lines are lines of steepest descent (constant $\Im\phi_-$), others are lines of constant height ($\Re\phi_-$).

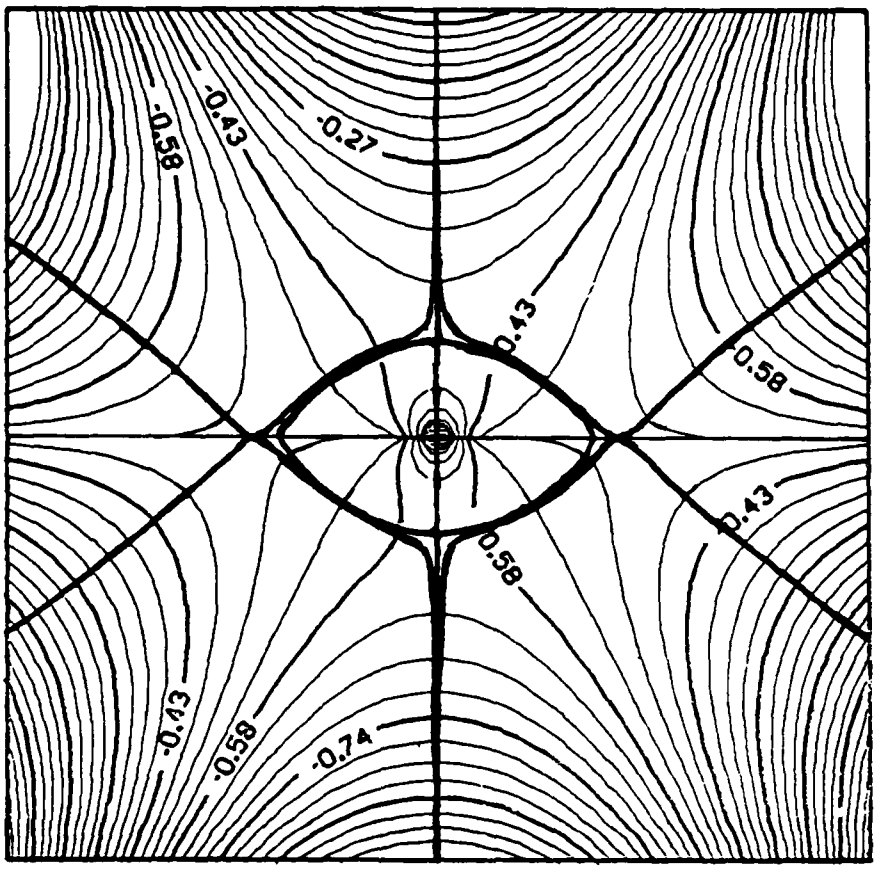

Figure 3: Contour plot of ϕ_- for $\omega = 0.986$ and $h = 0.05$. Lines have the same meaning as the previous figure.

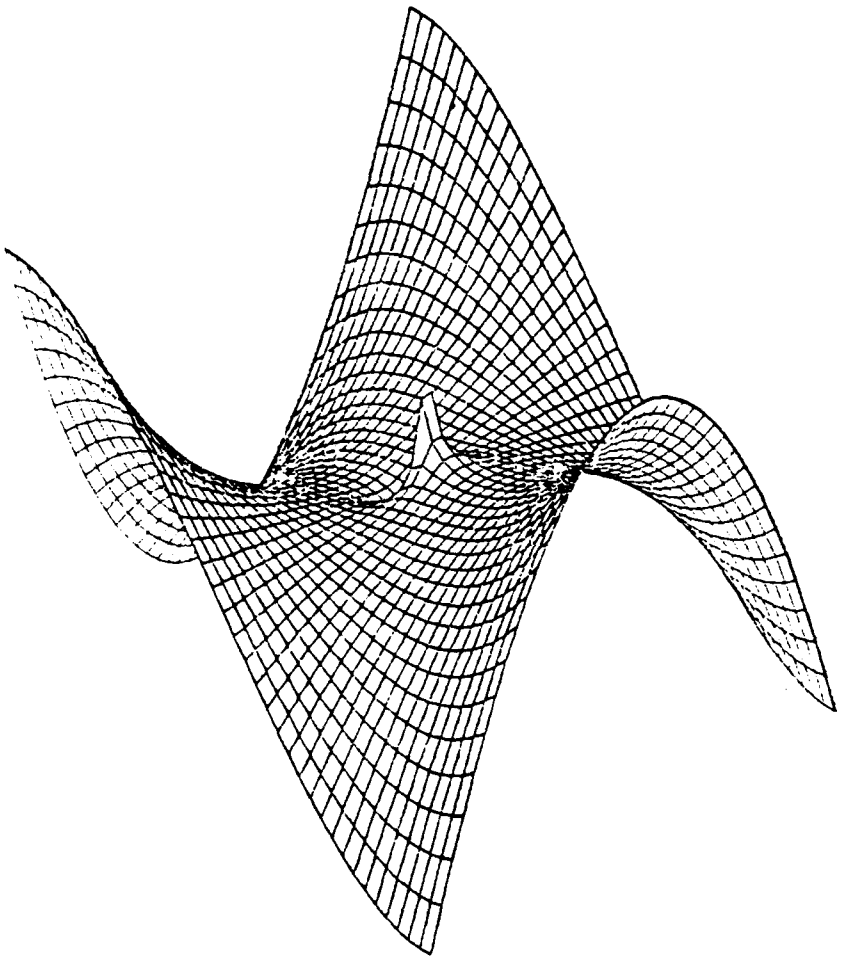

Figure 4: Surface plot corresponding to figure 2. The direction of view is from the upper right corner of figure 2 to the lower left, viewed from above. Note the branch cut in the center of the plot.

Note how the path of steepest descent changes between figures 2 and 3. The path in figure 2 has three components. Two parts of the path pass through the saddle points on the real axis, and the other part loops around the branch cut at $[-\frac{1}{2}, \frac{1}{2}]$. In figure 3, the path of steepest descent passes only through the principal saddle on the imaginary axis (the paths through the other saddle points are forbidden because they pass on the wrong side of the branch cut). What we are seeing here is a complicated interaction of four saddle points. Well behind the front, the path of steepest descent has two features. First is the part of the path that mimics the path for the continuous problem. This is the part that

loops around the branch cut. The other part consists of the paths that pass through the two saddle points on the real line. These explain the oscillations that are known to extend well behind the front (see the subsection, 'Behavior Away from the Front').

As we near the front, the paths come closer together, eventually crossing at a value of ω of about 0.985. It is interesting to look at the height of the path in this critical region. If the path has humps at each saddle point, then the saddle points may be treated separately. If not, then we must consider all the saddle points together. The next two figures answer this question.

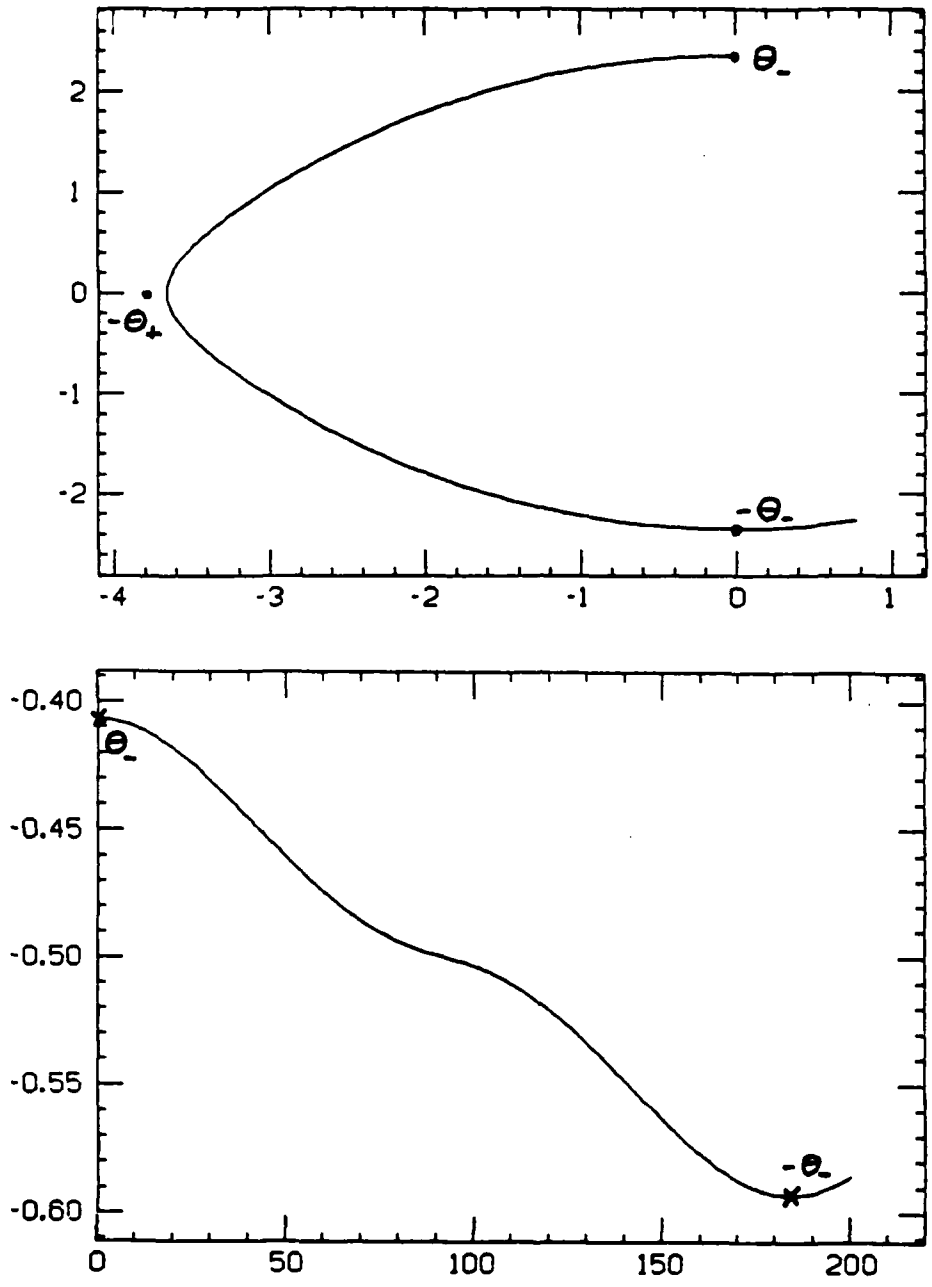

Figure 5: Plot of the left side of the path from the principal saddle and the height of the path for $\omega = 0.985$ and $h = 0.05$. Note how the height of the path flattens out in the neighborhood of the saddles $-\theta_+$, $-\theta_-$, and θ_-. The abscissa in the second graph is an arclength along the path.

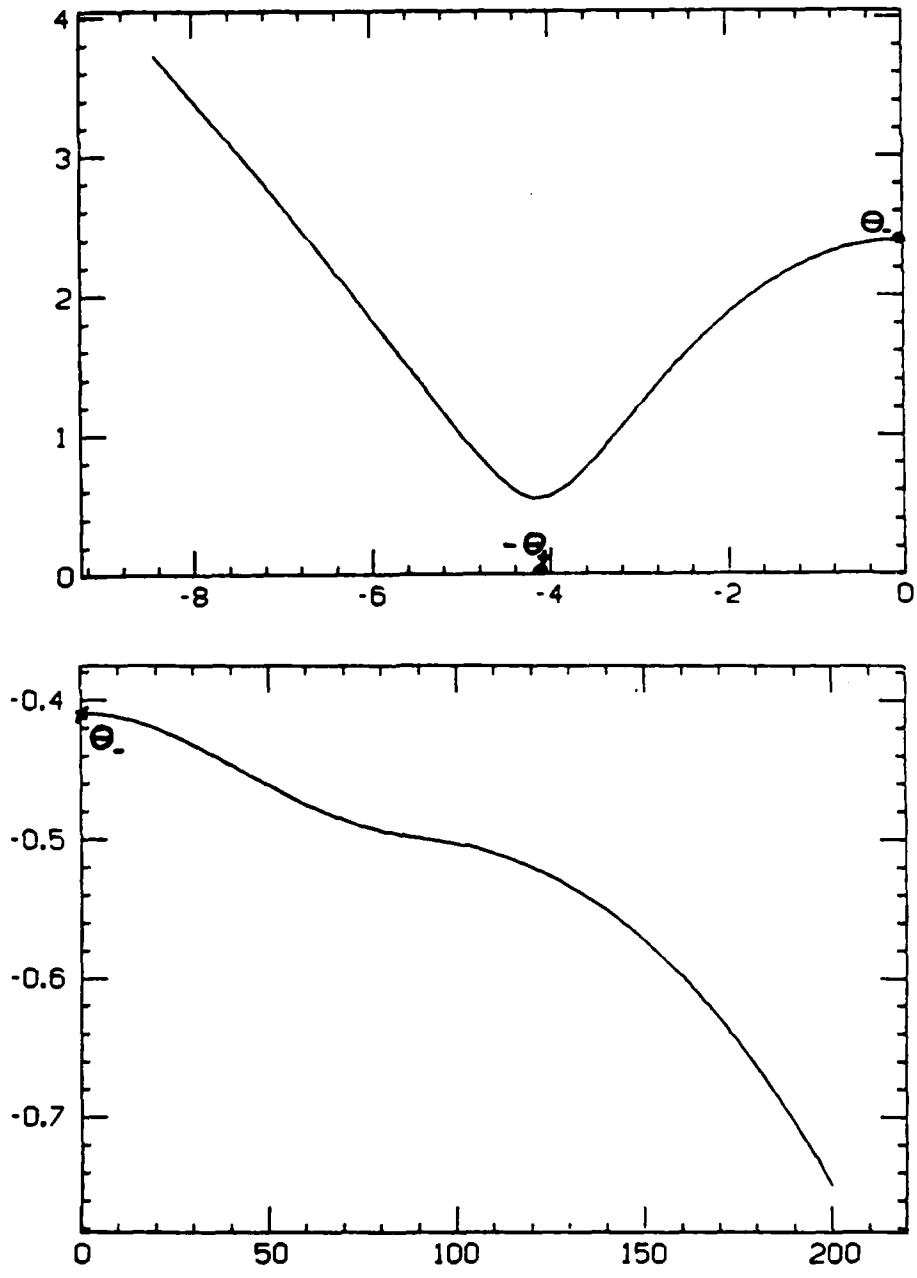

Figure 6: Plot of the left side of the path from the principal saddle and the height of the path for $\omega = 0.986$ and $h = 0.05$. Note how quickly the height falls as the path moves away from the saddle points.

These figures show that we must consider all of the saddle points simultaneously in the neighborhood of the front. However, note that the principal saddle point θ_- is always higher than the other saddle points. This means that the principal saddle controls the gross features of the solution. In particular, we expect the width of the front to be reflected in the behavior of the principal saddle. The next figure shows the behavior of the height of the principal saddle.

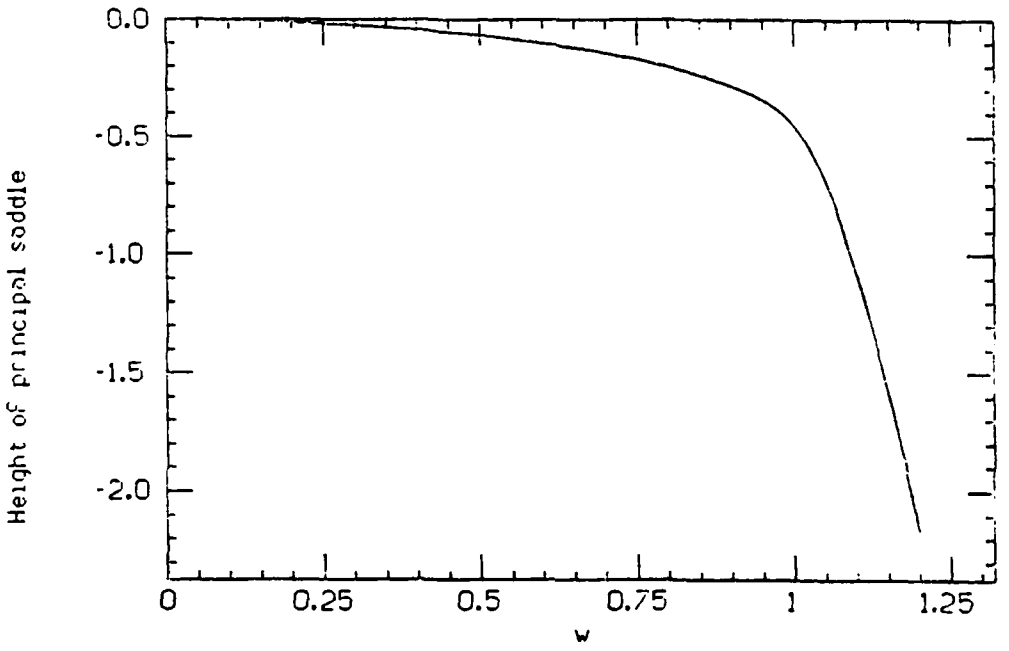

Figure 7: Height of the principal saddle θ_- as a function of ω; $h = 0.05$. Note how rapidly the height falls as ω increases past 1.

Since $\Re\phi_-(\theta_-)$ falls off so quickly, we can expect that by considering how $\Re\phi_-(\theta_-)$ behaves ahead of the front, we should be able to find the width of the front. This leads to the following definition:

Definition 1: Given $c > 0$ and some $\gamma_c > 0$, IF the height of the principle (highest) saddle point tends to $-\infty$ for $\omega = 1 + ch^\gamma$, for $\gamma < \gamma_c$, and the height of the principle saddle is bounded below for $\omega = 1 + ch^\gamma$, for $\gamma > \gamma_c$, THEN the width of the front is $O(h^{\gamma_c})$.

This definition is based on the following estimate of the inverse transform integral. Under the conditions in the definition, we can write the inverse transform integral as

$$\int g(\xi)e^{\phi(\xi)}\,d\xi \sim Ae^{-f(h)}\int e^{B(\xi-\xi_0)^2}\,d\xi$$

where $1/f(h) = o(1)$, $\Re f(h) > 0$, and ξ_0 is the principal saddle point. Then, as $h \to 0$, the integral vanishes (discarding contributions from poles near the path; these give the $-\frac{1}{2}$ in the solution ahead of the front). We do not need to consider the effects of the other saddle points because of the exponential importance of ϕ at the principal saddle point. Note that this definition does not say that the width of the front is asymptotically equal to $h^{\gamma c}$, only that the width of the front is at most $h^{\gamma c}$.

The restriction in definition 1 to $c > 0$ is based on the before-mentioned difficulty in defining a width of the front. For $c < 0$, we have $\omega < 1$ and hence we are looking behind the front. But behind the front there is no clear way to measure the width of the front (see the graphs of the computed solution in section 5).

For more detail of the behavior of the solution near the front we must take into consideration the interaction of all four saddle points. This is discussed below in the subsection on the canonical form. We proceed below to find the width of the front, proving the conjectures above about the behavior of the path and the height of the principal saddle.

Theorem 2: The width of the front in the solution to (3.1) is $O(h^{2/3})$, where h is the spatial step size.

Proof:

First, we need to know something about the path of steepest descent (henceforth *path*). We actually will need only qualitative information on the behavior of the path. For this, we look at $\phi''_-(\xi)$ for ξ a saddle point. Now,

$$\phi''_-(\xi) = \frac{2ih^2(1-2\sin^2\theta) + 8i\sin^4\theta}{h^2\left(\frac{4\sin^2\theta}{h^2}-1\right)^{3/2}}.$$

Since $4\sin^2(\theta)/h^2 - 1$ is negative for $\theta = \theta_-$ and positive for $\theta = \theta_+$, we can easily evaluate ϕ''_- at the saddle points. At the upper saddle, θ_-, it is negative. At the lower saddle, $-\theta_-$, it is positive, and at the left and right saddles, $\mp\theta_+$, it is $\mp i\gamma$, for some real positive γ. These facts allow us to determine the direction of the path of steepest descent at the saddle points; see, for example, Bleistein and Handelsman [1975], ch. 7.

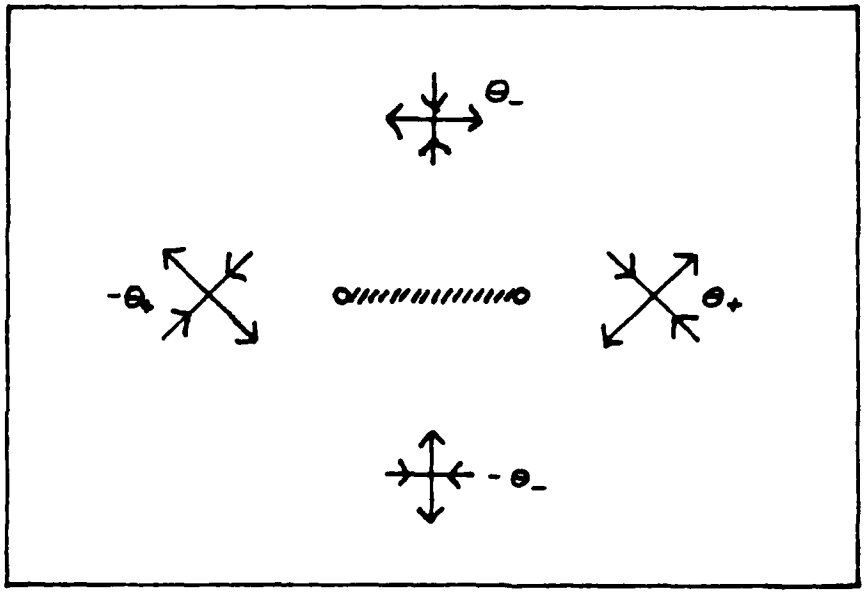

Figure 8: Saddle points of ϕ_-. Arrows point downhill. The branch cut is indicated by the shaded line.

Figure 8 shows the behavior of $\Re\phi_-$ in the neighborhood of its saddle points. Recall that the domain is the strip $[-\pi/h, \pi/h] \times [-\infty, \infty]$ in the ξ plane. Clearly, the path of steepest descent is one of three forms in the next figure.

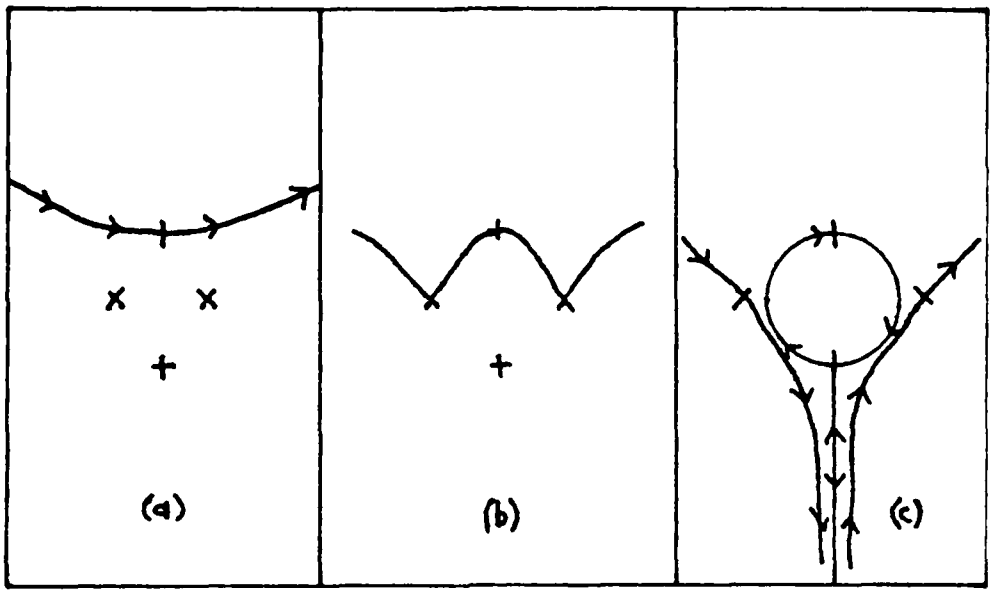

Figure 9: Possible paths of steepest descent for ϕ_-. Arrows show the direction of integration.

We first study the possible paths of steepest descent illustrated in the previous two figures. Determining which of these three choices is correct for all values of h and ω is very difficult, and we will not do it. Fortunately, by purely geometric considerations, we can show that the saddle point at θ_- dominates all of the possible paths.

Recall that the definition of the height of a saddle point at θ is $\Re\phi(\theta)$. Figure 9a shows the path which passes only through θ_-; this is the correct path if $\Re\phi_-(\theta_-)$ is less than the heights of the right and left saddle points. Of course, figure 9a may be the right path even if this is not the case, but we will see in a moment that that is not important to us here. In the other cases (figures 9b and 9c), the saddle at θ_- must be higher than the other saddle points, for otherwise the path in figure 9a would be a lower, and hence better, path. Therefore, because the heights of the saddles enter as $e^{\phi(\theta)}$, the saddle at θ_- is always the most important term. We will call this saddle point the *principal* saddle point. This is not to say that the other saddle points are unimportant; we will see that the left and right saddle points lead to the oscillations that are observed in the solution of (3.1). The lower saddle point $-\theta_-$ is also important to the detailed behavior of the solution.

We will have to deform the path of integration to pass through the principal saddle point before we proceed. In doing so, we will pick up a term from the singularities along the path of integration. In deforming the original path of integration passing along the real axis above the branch cut to the path of steepest descent, we move the path off of singularities at 0 and $\pm \sin^{-1}(h/2)/2$. Only the pole at zero contributes anything. As with the continuous problem, we must add $i\pi$ times the residue of this pole to the integral. It is easy to see that this is just $-\frac{1}{2}$ by making a Taylor expansion of the integrand. We will ignore this constant term in what follows.

We now find the behavior of θ_- and $\phi_-(\theta_-)$ for $\omega = 1 + ch^\gamma$, as functions of γ and as h goes to zero. To discover what sort of perturbation expansion we will need, we consider an expansion for $\omega = 1$. We have $\sin^2\theta_- = -\frac{1}{2}h$, or $h\xi_- = \theta_- \approx i\sqrt{h/2}$. Thus we see that as $h \to 0$, ξ_- is large and θ_- is small. We thus proceed by making expansions with ξ large and θ small. We will use the notation $O(h^\alpha; \ldots; h^\omega)$ to mean $O(h^{\min(\alpha,\ldots,\omega)})$.

Using this result as a guide, we let $\omega = 1 + ch^\gamma$, where c and γ are positive. In addition, we will assume that $\gamma < 1$. It is easy to show that $\phi_-(\theta_-)$ tends to $-\frac{1}{2}$ as $h \to 0$ for $\gamma \geq 1$.

We start with (3.6):

$$\sin^2\theta_- = \frac{1-\omega^2}{2} - \frac{\omega^2-1}{2}\sqrt{1 + \frac{\omega^2 h^2}{(1-\omega^2)^2}}$$

$$= \frac{1}{2}\left[-(1+\omega)ch^\gamma - (1+\omega)ch^\gamma\left(1 + \frac{1}{2}\frac{\omega^2 h^{2-2\gamma}}{(1+\omega)^2c^2} + O(h^{4-4\gamma})\right)\right].$$

To simplify the notation, we will replace $(1+\omega)c$ with c. Then we have

$$\sin^2\theta_- = -ch^\gamma\left(1 + \frac{1}{4}\frac{\omega^2 h^{2-2\gamma}}{c^2} + O(h^{4-4\gamma})\right)$$

or

$$\sin\theta_- = i\sqrt{ch^\gamma}\left(1 + \frac{1}{8}\frac{\omega^2 h^{2-2\gamma}}{c^2} + O(h^{4-4\gamma})\right).$$

Since θ_- is small, we may expand the inverse sine to get

$$\theta_- = i\sqrt{ch^\gamma}\left(1 + \frac{1}{8}\frac{\omega^2 h^{2-2\gamma}}{c^2}\right) - \frac{i\sqrt{c^3h^{3\gamma}}}{6} + O(h^{4-7\gamma/2}; h^{5\gamma/2}). \tag{3.7}$$

Now, we can find $\phi_-(\theta_-)$. First, we need to know

$$\frac{4\sin^2\theta_-}{h^2} - 1 = -4ch^{\gamma-2}\left(1 + \frac{1}{4}\frac{\omega^2 h^{2-2\gamma}}{c^2}\right) + O(h^{2-3\gamma}) - 1$$

$$\sqrt{\frac{4\sin^2\theta_-}{h^2} - 1} = 2i\sqrt{ch^{\gamma-2}}\left(1 + \frac{1}{8}\frac{\omega^2 h^{2-2\gamma}}{c^2}\right)\left(1 + O(h^{4-4\gamma}; h^{2-\gamma})\right).$$

Thus, for $\phi_-(\theta_-)$, we plug these in to get

$$\begin{aligned}\phi_-(\theta_-) = -\frac{1}{2} - \frac{i}{2}2i\sqrt{ch^{\gamma-2}}\left(1 + \frac{1}{8}\frac{\omega^2 h^{2-2\gamma}}{c^2}\right) \\ + i\omega\left[i\sqrt{ch^{\gamma-2}}\left(1 + \frac{1}{8}\frac{\omega^2 h^{2-2\gamma}}{c^2}\right) - \frac{i(ch^\gamma)^{3/2}h^{-1}}{6}\right] \\ + \mathcal{O}(h^{3-7\gamma/2}; h^{1-\gamma/2}; h^{5\gamma/2-1})\end{aligned}$$

Collecting terms, this is

$$\begin{aligned}\phi_-(\theta_-) = -\frac{1}{2} + (1-\omega)\left[\sqrt{ch^{\gamma-2}}\left(1 + \frac{1}{8}\frac{\omega^2 h^{2-2\gamma}}{c^2}\right)\right] + \frac{\omega c^{3/2}h^{3\gamma/2-1}}{6} \\ + \mathcal{O}(h^{3-7\gamma/2}; h^{1-\gamma/2}; h^{5\gamma/2-1})\end{aligned}$$

Now, we replace $1-\omega$ by $-ch^\gamma/(1+\omega)$ (since we redefined c above) and get

$$\begin{aligned}\phi_-(\theta_-) &= -\frac{1}{2} - c^{3/2}h^{3\gamma/2-1}\left(\frac{1}{1+\omega} - \frac{\omega}{6}\right) + \mathcal{O}(h^{3-7\gamma/2}; h^{1-\gamma/2}; h^{5\gamma/2-1}) \\ &= -\frac{1}{2} - (\text{positive quantity})h^{3\gamma/2-1} + \mathcal{O}(h^{3-7\gamma/2}; h^{1-\gamma/2}; h^{5\gamma/2-1})\end{aligned} \tag{3.8}$$

From this we can see that for $\gamma > 2/3$, $\phi_-(\theta_-) \to -\frac{1}{2}$ as $h \to 0$. For $\gamma < 2/3$, $\phi_-(\theta_-) \to -\infty$ as $h \to 0$. Thus, for $\gamma < 2/3$, $U \to -\frac{1}{2}$ as $h \to 0$ ($-\frac{1}{2}$ comes from the pole; the contribution from the path tends to zero, as does the ϕ_+ term). For $\gamma > 2/3$ the contribution from the path does not tend to zero. ∎

Note that we have not shown that U is different from $-\frac{1}{2}$ for $\gamma > 2/3$, since we would need a lower bound on the integral. Thus we can only say that the width of the front is $\mathcal{O}(h^{2/3})$ rather than the stronger statement that the width is asymptotically proportional to $h^{2/3}$. Section 5 will present computations that demonstrate that the width is indeed proportional to $h^{2/3}$. Also, this result is good for t small and positive as well, since the behavior is so strong.

The limited form of this result is caused by the complicated behavior of the saddle points and is not an inherent limitation of the method. With better information about the location of the saddle points and the path of steepest descent, we could describe the behavior of the front in more detail. In particular, for any given h and ω, we could work out the detailed behavior. Since we are interested in general results, however, we will not do this.

This sort of analysis may seem contrary to the analysis in section 2, where great care was exercised to get the contributions from all of the saddle points along the path of

steepest descent. This is because this section and the previous one have somewhat different objectives. In the previous section, it was important both to introduce the techniques of uniform asymptotics and to show the solution to the continuous problem. Here, we are interested in finding the width of the front as a function of h. To compute the solution near the front, we would have to determine the correct path of steepest descent and use a uniform expansion to calculate the behavior near the front. Using the canonical form, we do this computation in section 5.

The Canonical Form

In section 2 we saw that the integral representing the solution of the continuous problem could be transformed into an integral with a simpler form. We did this by simplifying the argument of the exponential in the integral into a form which represented the saddle point behavior. This form is the canonical form, and by studying these integrals we can gain a better understanding of the exact solution to the difference equations.

For the difference approximation of this section, we will use the canonical form to discuss the behavior of the principal terms in the asymptotic expansion near the front.

The canonical form chosen depends on the region of interest. Near the front, we know from above that $\Re\phi_-(\theta_-) \approx -\frac{1}{2}$. It is easy to see that $\Re\phi_-(\theta_+) = \Re\phi_-(-\theta_+) = -\frac{1}{2}$ everywhere. Therefore, we expect the path of steepest descent to be more like figure 9b or 9c than 9a. In this case, we will need to consider the interaction of four saddle points. As in the continuous problem, we will be guided to a canonical form by considering an expansion of ϕ_-. We recall that the saddle points are $\theta_\pm = O(h^{1/2})$ near the front. Thus, in contrast to the derivation in section two, we will remain in the θ plane (rather than going to the $1/\xi$ plane).

The small h, small θ expansion of ϕ_- (in terms of ξ) is

$$\phi_-(\xi) \approx -\frac{1}{2} + \frac{i}{8\xi} + i(\omega - 1)\xi + \frac{i\xi^3 h^2}{6} + O(\xi^5 h^4). \tag{3.9}$$

(In this expansion, it is important to expand the sine inside the square root, rather than expanding the square root and then the sin, because the first term in $\sin^2\theta/h^2$ is large, while the succeeding terms are small.)

Note that since for $\omega \approx 1$, $\xi \approx h^{-1/2}$, and hence the $h^2\xi^3$ term is not smaller than the first two terms. However, the next term, $\xi^5 h^4$, is smaller. This suggests the canonical

form

$$\psi(p) = \frac{a}{p} + b + cp + dp^3 = \phi_-(\xi). \tag{3.10}$$

Here we have already applied the requirement of symmetry of the saddle points to eliminate the p^2 term. By setting $b = -\frac{1}{2}$, we do not affect the saddle points of ψ. We may also normalize the mapping by setting one of the remaining parameters; we set $a = i/8$ so that $d\xi/dp \approx 1$. We are then left with the two parameters c and d. To determine these, we need two and only two conditions. These two conditions are provided by the fact that the mapping (3.10) is locally one-to-one at the saddle points. This means that the saddle points correspond. That is, if ξ is a saddle point, then so is $p(\xi)$. Since, by symmetry, the saddle points are described by two parameters, we have the two conditions that we need to determine (3.10).

Now, $\psi(p)$ has four saddle points $p_\pm$ and $-p_\pm$ which satisfy

$$p_\pm^2 = \frac{-c \pm \sqrt{c^2 + \frac{3id}{2}}}{6d}. \tag{3.11}$$

We expect (3.11) to have two real and two imaginary solutions. This will be the case if $c^2 + 3id/2 < 0$. There are many ways to satisfy this condition; it is clearly satisfied if c and d are pure imaginary and d is small enough or has positive imaginary part. This is just the case for ϕ_-. Also note that the behavior of the saddle points follows that of $\phi_-(\xi)$ as $h \to 0$. In particular, the saddle points of $\psi(p)$ go toward infinity for $\omega = 1$ as h tends to zero. All we have to do is to determine c and d such that $\psi(p_\pm) = \phi_-(\xi_\pm)$.

Unfortunately, it is too difficult to analytically determine c and d. We can solve for them numerically, however, and compare them to (3.9). A fixed point iteration suggested by Hedstrom [1979] for the scalar wave equation can be adapted for this problem:

1 Pick $c^{(0)}$ and $d^{(0)}$. Set $n = 0$. Define $\psi^{(n)}(p)$ by (3.10), with $c^{(n)}$ and $d^{(n)}$ replacing c and d.

2 Repeat steps 3-4 until $c^{(n)}$ and $d^{(n)}$ converge.

3 Find the saddle points of $\psi^{(n)}$. Find a correspondence between these saddle points and the saddle points of ϕ_-.

4 Solve the two (linear) equations $\psi^{(n+1)}(p_\pm) = \phi_-(\xi_\pm)$ for the coefficients $c^{(n+1)}$ and $d^{(n+1)}$. Set $n \leftarrow n + 1$.

We use this algorithm to find c and d for ω in a neighborhood of 1. Good choices of $c^{(0)}$ and $d^{(0)}$ are needed. We can start at $\omega = 1$ by taking c and d from (3.9). With the $\omega = 1$ values of c and d, we can proceed to nearby values of ω by continuation.

This canonical form defines a new special function, which is a generalized regular special Bessel function. Graphs of this function are displayed in section 5. The following two figures show c/i and d/ih^2 for $h = 0.001$. The figures compare these to the values from (3.9) for c and d.

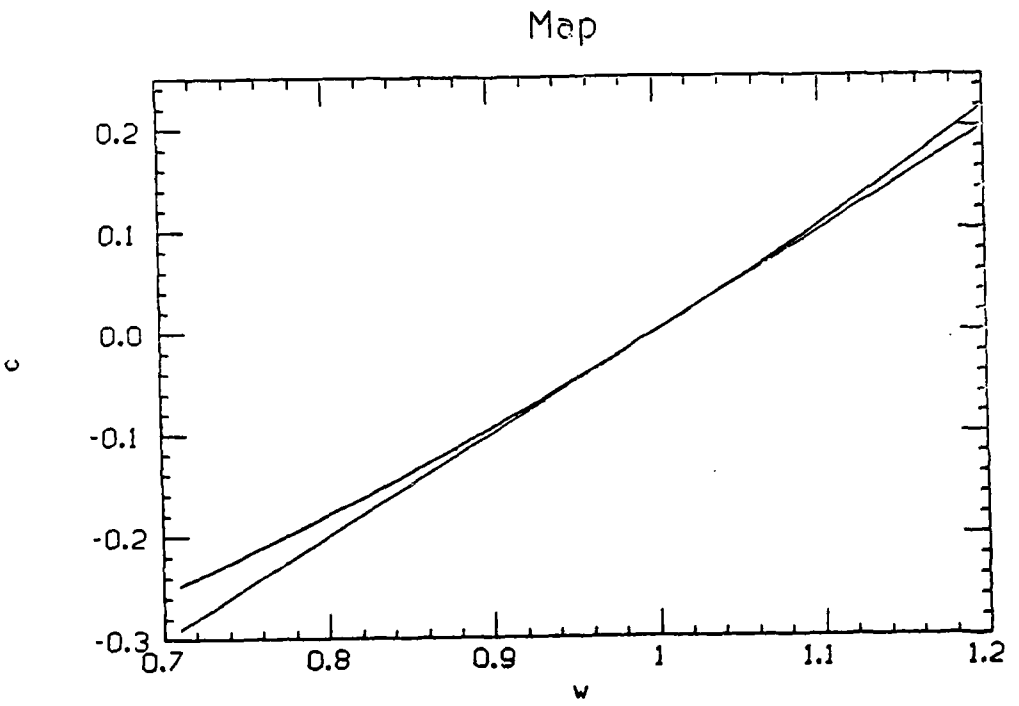

Figure 10: Comparison of coefficients for model equation with coefficients for map. Curved line is c/i for $h = 0.001$. Straight line is the value from (3.9).

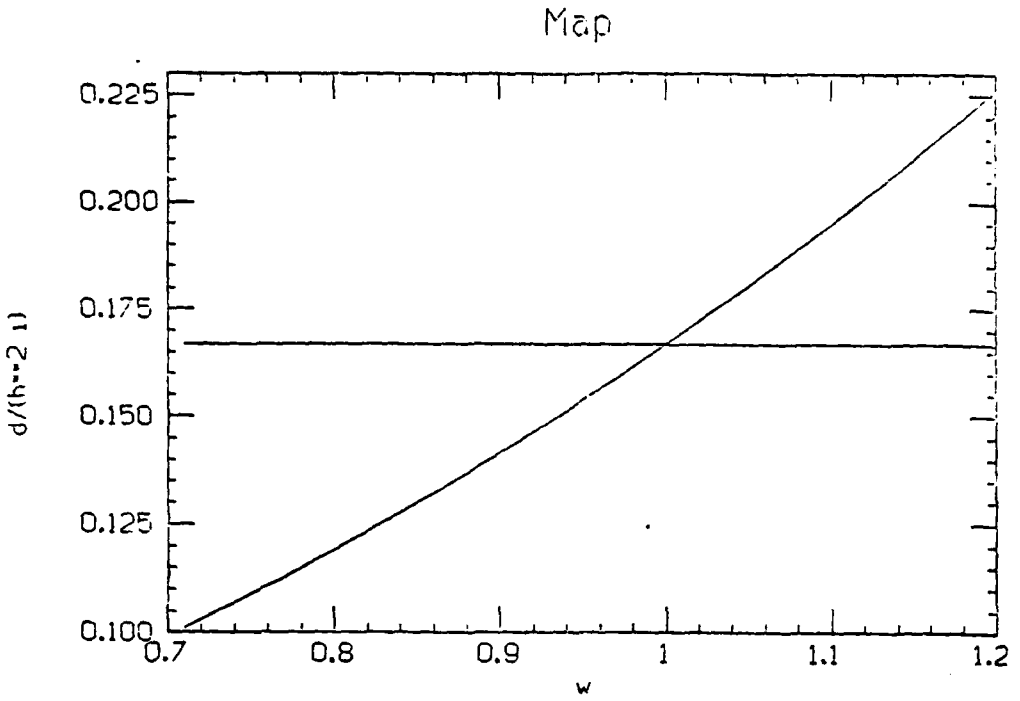

Figure 11: Comparison of coefficients for model equation with coefficients for map. Curved line is d/ih^2 for $h = 0.001$. Horizontal line (at $1/6$) is the value from (3.9).

These figures show that near the front the form in (3.9) (really a model equation) is a good approximation. Away from the front the neglected terms in the Taylor series in (3.9) become important, and (3.9) is no longer as good an approximation. Fortunately, we are interested only in the near-front behavior, so we will use the (3.9) form of the mapping.

We can use the above result to look at the behavior of the canonical form near the discontinuity. Because the form in (3.9) is so close to the canonical form near the discontinuity, we will look only at the form in (3.9).

Written with (3.9), the form of the integral for the solution to (3.1) is

$$\int_{-\pi/h}^{\pi/h} g \exp\left\{\left(\frac{i}{8\xi} + i(\omega - 1) + \frac{i\xi^3 h^2}{6}\right)t\right\} d\xi.$$

We now consider various scalings of ξ which reveal the importance of the terms in the exponential. If we define $h^\alpha \eta = \xi$, the integral is

$$\int_{-\pi h^{-\alpha-1}}^{\pi h^{-\alpha-1}} g \exp\left\{\left(\frac{i}{8h^\alpha \eta} + i(\omega - 1)h^\alpha \eta + \frac{ih^{3\alpha+2}\eta^3}{6}\right)t\right\} h^\alpha d\eta.$$

If (3.1) were the scalar wave equation, $\alpha = -1$ would be the natural scaling (see Hedstrom [1975]). Writing the above with $\alpha = -1$, we have

$$\int_{-\pi}^{\pi} g \exp\left\{\left(\frac{ih^2}{8\eta} + i(\omega - 1)\eta + \frac{i\eta^3}{6}\right)\frac{t}{h}\right\} h^{-1} d\eta. \tag{3.12}$$

The integral (3.12) is useful when we may neglect the $ih^2/8\eta$ term, for then (3.12) may be written in terms of the well understood Airy functions. For that term to be negligible, we must have $|h^2/\eta| \ll |(\omega - 1)\eta|$ and $|h^2/\eta| \ll |\eta^3|$ at the saddle points. We may rewrite these conditions as

$$\begin{aligned} |\omega - 1| &\gg \left|\frac{h^2}{\eta^2}\right| \\ |\eta| &\gg \sqrt{h}. \end{aligned} \tag{3.13}$$

Now, near the front we know that $\xi \approx 1/\sqrt{h}$, so $\eta = h\xi = \sqrt{h}$ and the condition $|\eta| \gg \sqrt{h}$ is not satisfied. Thus (3.12) is not useful near the discontinuity. As we move away from the front, $\eta = h\xi \approx$constant (from (3.6)), and both of the conditions (3.13) are satisfied.

In particular, (3.12) and (3.13) show that the term in the integral due to the coupling (the $ih^2/8\eta$ term) becomes less and less important away from the front. From this, we can conclude that in a region near (near for expansion (3.9) to be valid) but bounded away from the discontinuity, the behavior of the U_- term is similiar to the behavior of the centered difference approximation to the scalar wave equation.

It is important to note that the U_+ term is important away from the front (Majda and Osher [1977]), so we may not exclude it in discussing the behavior of the solution to (3.1).

Another useful scaling of ξ is $\alpha = -1/2$. With this scaling, the positions of the saddle points stay nearly fixed in the η-plane (as functions of h) for ω near 1. The integral then looks like

$$\int_{-\pi/\sqrt{h}}^{\pi/\sqrt{h}} g \exp\left\{\left(\frac{i}{8\eta} + \frac{i(\omega - 1)\eta}{h} + \frac{i\eta^3}{6}\right)t\sqrt{h}\right\} h^{-\frac{1}{2}} d\eta. \tag{3.14}$$

For (3.14), we want the term $i(\omega - 1)\eta/h$ to be unimportant and $t\sqrt{h}$ large. For this, we have $|1/\eta| \gg |(\omega - 1)\eta/h|$ and $|\eta^3| \gg |(\omega - 1)\eta/h|$, or

$$\begin{aligned} \left|\frac{1}{\eta^2}\right| &\gg \left|\frac{(\omega - 1)}{h}\right| \\ |\eta^2| &\gg \left|\frac{(\omega - 1)}{h}\right|. \end{aligned} \tag{3.15}$$

From (3.7) and $\eta = \xi/\sqrt{h}$, we have $\eta \approx h^{(\gamma-1)/2}$ at $\omega - 1 = ch^\gamma$. Inserting these into (3.15) shows (3.15) satisfied for $\gamma < 1$ ((3.7) is valid only for $\gamma < 1$). Note that the argument

of the exponential (dropping the $i(\omega - 1)/h$ term) has 4 saddle points equally distributed about the unit circle. This shows us that very near the discontinuity, all four saddle points are important.

Note also that this scaling makes asymptotic analysis difficult, as we would need $t\sqrt{h}$ to be large as h tends to zero.

Behavior away from the Front

We may use the integral representation (3.3) to get some information about the behavior of the solution away from the front as well. Let us consider the effect of the two real saddle points in figure 7. There is some $\omega_c < 1$ such that for $\omega < \omega_c$, the two saddle points on the real line are *isolated*; the path of steepest descent through each of these two saddles starts at infinity and passes through only one of them before going back out to infinity (cf. figure 8c). Thus, we may use classical saddle point theory to estimate the contributions of these terms. Considering just the contributions from these terms, we have

$$U_{osc} = g(\theta_+)\frac{1}{\sqrt{t|\phi_-''(\theta_+)|}}e^{\phi_-(\theta_+)t}C + g(-\theta_+)\frac{1}{\sqrt{t|\phi_-''(-\theta_+)|}}e^{\phi_-(-\theta_+)t}C + \cdots$$

where g is the unexponentiated part of the integral in (3.3). We may use the fact that θ_+ is real to relate $g(\theta_+)$ to $g(-\theta_+)$ and $\phi_-(\theta_+)$ to $\phi_-(-\theta_+)$. The leading term in $g(\theta_+)$ is h/θ, so to leading order, g is odd in θ. We also have

$$\phi_-(\pm\theta_+) = -\frac{1}{2} \mp \sqrt{\frac{4\sin^2\theta_+}{h^2} - 1} \pm \omega\theta_+.$$

Combining these, we may write U_{osc} as

$$U_{osc} \approx \frac{g(\theta_+)C}{\sqrt{t|\phi_-''(\theta_+)|}}e^{-t/2}\sin\left(\left(\sqrt{\frac{4\sin^2\theta_+}{h^2} - 1} - \omega\theta_+\right)t\right).$$

This shows where the oscillations in the solution to (3.1) come from. They are artifacts caused by the presence of the spurious saddle points on the real line (spurious in the sense that they are not present in the continuous problem in section 2).

While the above analysis shows where the oscillations come from, it does not give the frequency of those oscillations. Since θ_+ is a function of ω and hence of x and t, both $g(\theta_+)$ and $\phi_-''(\theta_+)$ contribute to the oscillations. Still, this does show where the oscillations in the solution come from, and a more careful analysis, such as those in Hedstrom [1975] and Pearson [1969] for the scalar wave equation, would show the observed frequency.

Size of the U_+ term

In closing this section, we show that the U_+ term in (3.3) is asymptotically negligible as we have claimed. For the region away from the front (ω bounded away from 1), we can use the same basic techniques as before. First, we determine the path of steepest descent. Second, we determine the appropriate canonical form. The canonical form near the front will be different from the canonical form away from the front. Finally, we get estimates on the size of the terms in the resulting integrals. For the region near the front, the situation is more complicated. In this region, we will show that the U_+ term is of the order of the first neglected term in the U_- expansion.

First, for the region away from the front, we look at the saddle points. To discover the path of steepest descent, we consider the relation between $\phi_-(\xi_\pm)$ and $\phi_+(\xi_\pm)$. Let $\tilde{\theta} = \theta + \pi$. Clearly,

$$\begin{aligned}\phi_+(\tilde{\theta}) &= \frac{1}{2} + \frac{i}{2}\sqrt{\frac{4\sin^2(\tilde{\theta})}{h^2} - 1} + i\omega\frac{\tilde{\theta}}{h} \\ &= \frac{1}{2} + \frac{i}{2}\sqrt{\frac{4(-\sin\theta)^2}{h^2} - 1} + i\omega\frac{\theta}{h} + i\omega\frac{\pi}{h} \\ &= \phi_-(\theta) + i\omega\frac{\pi}{h}\end{aligned}$$

since the sign of the sine changes the sign of the square root. Hence, $\Re\phi_+(\tilde{\theta}) = \Re\phi_-(\theta)$. Thus the behavior of the saddle points and the path of steepest descent is the same as that for ϕ_- found earlier in this section.

There are then two cases to consider: ω away from 1, where the saddle points are well separated, and ω near 1, where the saddle points are coming together (at infinity). We will first consider the simpler case of ω away from 1.

In this region of ω, we can use classical saddle point analysis to get an estimate on U_+. Following Erdélyi [1956] we have that

$$U_+ \approx g(\tilde{\theta}_-)\frac{1}{\sqrt{t|\phi_+''(\tilde{\theta}_-)|}}e^{\phi_+(\tilde{\theta}_-)t}C + \text{asymptotically smaller terms.}$$

Here, $g(\tilde{\theta}_-) = \alpha(\tilde{\theta}_-)(1+\lambda_+)$ (see (3.3)). We can investigate the small h behavior of this by making Taylor expansions in h of g and ϕ_+''. We already know that $\Re\phi_+(\tilde{\theta}_-) \approx -\frac{1}{2}$. The first terms in the expansions for g and ϕ_+'' are ($h\xi = 0$, $\tilde{\theta} = \theta + \pi$, ξ is $O(1)$ away from the

front)

$$g(\tilde{\theta}) \approx \frac{h^2\xi\left(1+2i\xi-i\sqrt{4\xi^2-1}\right)}{8\sqrt{4\xi^2-1}}$$

$$\phi_+''(\tilde{\theta}) \approx \frac{2i}{(4\xi^2-1)^{3/2}}.$$

Thus, U_+ is $O(h^2)$. This is just what we would expect, since the method that we are considering is second order accurate. Note also that the exponential is like

$$e^{\phi_+(\tilde{\theta}_-)t} = e^{\phi_-(\theta_-)t+ix\pi/h}$$

$$= \text{slowly varying part} \times e^{ix\pi/h}$$

so we would expect U_+ to have a wavelength of $2h$ in x. These oscillations are observed in practice.

As a demonstration of this analysis, the following table presents the results of computing U_+ numerically for $h = 2^{-n}$, $n = 5, 6, \ldots, 15$.

n	U_+	ratio
5	1.44E-2	NA
6	3.88E-3	1.89727
7	9.49E-4	2.03098
8	2.32E-4	2.03180
9	5.71E-5	2.02369
10	1.41E-5	2.01370
11	3.52E-6	2.00731
12	8.77E-7	2.00377
13	2.19E-7	2.00191
14	5.47E-8	2.00096
15	1.37E-8	2.00048

Table 1: U_+ for $h = 2^{-n}$ and $x = 2t = \frac{1}{2}$. Ratio column is the log of the ratios of successive rows divided by log(1/2). Note how quickly U_+ approaches $O(h^2)$. The value for U_+ was taken as the maximum over two periods (each period is $2h$ long) and a constant factor was divided out. Of course, there is no ratio for the first entry.

It is instructive to note that as ω goes to 1, ϕ_+'' becomes $O(h^{3/2})$. Thus, as ω nears 1, it is no longer sufficient to consider just the effect of the principal saddle point. We look then at the canonical form (3.10). By the above analysis, $\phi_+(\tilde{\theta}_-)$ and $\phi_-(\theta_-)$ are essentially

the same (they differ by a term constant in θ). Thus we can use the same canonical form for estimating the size of th U_+ term.

The behavior of the canonical form integral is very complicated for $\omega \approx 1$. The best that we can do with it is to show that it is comparable to the first neglected term in the previous analysis. Define g_+ to be the unexponentiated part of the U_+ integral in (3.3) and g_- to be the unexponentiated part of the U_- integral. Because of the behavior of the saddle points of ϕ_+ and ϕ_- near the front, we need to know the behavior of $g_+(\tilde{\theta})$ for $\tilde{\theta}$ near π and the behavior of $g_-(\theta)$ for θ near 0. Let $\tilde{\theta} = \pi + \theta$, θ small. This gives us:

$$g_+(\tilde{\theta}) = \frac{\hat{f}(\tilde{\theta})}{2} + \frac{i\hat{f}(\tilde{\theta})}{2}\left(\frac{1 + \frac{2i\sin\theta}{h}}{\sqrt{\frac{4\sin^2\theta}{h^2} - 1}}\right)$$

$$g_-(\theta) = \frac{\hat{f}(\theta)}{2} + \frac{\hat{f}(\theta)}{2}\left(\frac{1 - \frac{2i\sin\theta}{h}}{\sqrt{\frac{4\sin^2\theta}{h^2} - 1}}\right)$$

Now, $\hat{f}(\tilde{\theta}) = ih\cot(\tilde{\theta}/2)/2$, so $\hat{f}(\theta + \pi) = -ih\tan(\theta/2)/2$. From this we can see that $g_+(\tilde{\theta})$ is smaller than $g_-(\theta)$, since both are $\hat{f} \times$ similiar functions, and $\tan\theta \ll \cot\theta$ for θ small.

We have not shown that this term is small; indeed we will not. It is a recognized problem in asymptotic analysis that estimating the higher order terms in an expansion for arbitrary h and ω can be very difficult. For specific h and ω, however, these terms could be estimated by preforming the integration numerically with a method with a known error bound. See Wong [1980] for a clear discussion of error estimates for asymptotic expansions of integrals.

To get a good estimate of U_+, we would need to know both the location of the saddle points and the path of steepest descent. Since both the computations of the path of steepest descent and the integral (3.14) show that all of the saddle points are important, we must be able to estimate the canonical form integral corresponding to these features. As the canonical form integral represents a new special function, this analysis reduces to tabulating the integral which the canonical form (3.10) represents and using the resulting tables to estimate U_+.

We can, however, provide computations to show that the term is in fact as inconsequential as claimed. For this specific problem, we can look at the following table:

n	U_+	ratio
5	2.02E-4	NA
6	9.77E-5	1.04968
7	2.57E-5	1.92524
8	8.09E-6	1.66781
9	4.34E-6	0.89907
10	1.61E-6	1.42923
11	5.09E-7	1.66131
12	2.26E-7	1.17489
13	8.16E-8	1.46689
14	3.19E-8	1.35582
15	1.28E-8	1.31484

Table 2: U_+ for $h = 2^{-n}$, $t = 1$, and $\omega = 1 + h^{2/3}$. Columns have the same meaning as in the previous table. The lack of an obvious limit in the ratio column is due to the need to average over the oscillations. Unfortunately, the predicted ratio changes over the length of one oscillation, thereby contaminating the results.

For more general problems (such as the next section), we can look at the graphs of the appropriate canonical form which are presented in section 5.

4. Behavior of Difference Approximations near the Discontinuity: General Difference Schemes

In this section we analyze a model equation for the model problem. This approach was discussed in section 1. Our model equation is

$$\begin{aligned}
\frac{\partial u}{\partial t} &= -\frac{\partial v}{\partial x} + ah^p \frac{\partial^{p+1} v}{\partial x^{p+1}} + bh^q \frac{\partial^{q+1} v}{\partial x^{q+1}} \\
\frac{\partial v}{\partial t} &= -\frac{\partial u}{\partial x} + ah^p \frac{\partial^{p+1} u}{\partial x^{p+1}} + bh^q \frac{\partial^{q+1} u}{\partial x^{q+1}} - \rho v \\
u(x,0) = v(x,0) &= \begin{cases} \frac{1}{4}, & \text{if } x < 0 \\ 0, & \text{if } x = 0 \\ -\frac{1}{4}, & \text{if } x > 0 \end{cases} \qquad (4.1) \\
1 \leq p &< q.
\end{aligned}$$

Here, p and q are integers, and one of p and q is even, the other is odd. For example, for $p = 2$, $a = -1/6$, $\rho = 1$, and $b = 0$, this equation models the nondissipative second order scheme studied in section 3. We will use ρ to allow us to see what effect the lower order term has near the discontinuity. For $\rho = 0$, (4.1) is just the model equation for difference approximations to the ordinary wave equation; $\rho = 1$ is the telegrapher's equation, and it is this case that should be kept in mind for most of the analysis.

That this model equation is a good model can be proved by techniques similar to those in section 3. In fact, section 3 can be taken as proof of this model equation for the case of the second order difference approximation in (3.1).

Averaging of the undifferentiated term has not been included in order to simplify the analysis. The techniques used here can be used to find the behavior of difference schemes which average the undifferentiated terms.

Our analysis will proceed along the same lines as in the previous section. We represent the solution to (4.1) as an inverse Fourier integral. We then study the behavior of the saddle points of this integral, and show that the width of the front is $O(h^{p/(p+1)})$. The calculations for this are very similiar to those in section 3 and we will compare the results there to the results in this section. We then use ρ to show in which regions near the front the undifferentiated term is important. Finally, we present a generalization of (4.1) which shows exactly what dimensionless quantity must be small for our analysis.

Integral Form of the Solution

We start with the Fourier transform of (4.1):

$$\begin{aligned}\frac{d\hat{u}}{dt} &= -i\xi\hat{v} + ai\xi(ih\xi)^p\hat{v} + bi\xi(ih\xi)^q\hat{v} \\ \frac{d\hat{v}}{dt} &= -i\xi\hat{u} + ai\xi(ih\xi)^p\hat{u} + bi\xi(ih\xi)^q\hat{u} - \rho\hat{v}\end{aligned} \tag{4.2}$$

where ξ is the dual variable. In matrix form, this is

$$\frac{d}{dt}\begin{pmatrix}\hat{u}\\ \hat{v}\end{pmatrix} = \begin{pmatrix}0 & -i\xi(1 - a(ih\xi)^p - b(ih\xi)^q)\\ -i\xi(1 - a(ih\xi)^p - b(ih\xi)^q) & -\rho\end{pmatrix}\begin{pmatrix}\hat{u}\\ \hat{v}\end{pmatrix}.$$

Then the eigenvalues of this matrix are

$$\lambda_\pm = -\frac{\rho}{2} \pm \frac{i}{2}\sqrt{4\xi^2(1 - a(ih\xi)^p - b(ih\xi)^q)^2 - \rho^2}$$

Let $\phi_\pm = \lambda_\pm + i\omega\xi$, where $\omega = x/t$. The branch cuts (there are many of them) are chosen so that the $h = 0$ limit has saddle points with the same behavior as for the continuous problem. The other branch cuts are chosen to be well away from the origin (the region of interest) for $\omega \approx 1$. If we let $a_\pm$ be the unnormalized eigenvectors of the matrix, we can write the solution to (4.2) as

$$\begin{pmatrix}\hat{u}\\ \hat{v}\end{pmatrix} = \alpha_+(\xi)a_+e^{\lambda_+ t} + \alpha_-(\xi)a_-e^{\lambda_- t}$$

where $\alpha_\pm(\xi)$ are determined by the Fourier transform of the initial data. Then the solution of (4.1) is the inverse transform

$$u(x,t) = \frac{1}{2\pi}\int_{-\infty}^{+\infty}\left[\alpha_+(\xi)a_{1+}e^{\lambda_+ t} + \alpha_-(\xi)a_{1-}e^{\lambda_- t}\right]e^{ix\xi}d\xi \tag{4.3}$$

where $a_{1\pm}$ are the first components of $a_\pm$.

It is possible to express $\alpha_\pm(\xi)$ in terms of the initial data and $\lambda_\pm$, but it shows nothing new. We will therefore assume that $\alpha_-(\xi) \approx 1/2\xi$ for ξ near 0, and that the λ_+ term is negligible compared to the λ_- term for $x \approx t$. The arguments for these assertions follow the same pattern as those in the previous section, and they will not be repeated here.

Width of the Front

To determine the asymptotic behavior of the width of the front, we will follow the procedure used in the previous section. Specifically, we first find the saddle points of $\phi_-(\xi)$. We then show that the saddle point corresponding to the principal saddle of the

continuous problem controls the width of the front. Finally, we show how ϕ $(\xi_-(\omega + ch^\gamma))$ behaves as a function of γ.

Consistency of the difference approximation will be used to guide and justify the steps in the analysis. We require that the $h \to 0$ limit of the equations below must give the respective equations from the continuous problem. In particular, we will use our knowledge of the behavior of the principal saddle point to pick an appropriate perturbation expansion.

Theorem 3: The width of the front, as defined by definition 3.1, under a general difference scheme with model equation (4.1) is $h^{p/(p+1)}$.

Proof:

The saddle points satisfy the equation

$$0 = \pm 2i \frac{\xi(1 - a(ih\xi)^p - b(ih\xi)^q)(1 - (1+p)a(ih\xi)^p - (1+q)b(ih\xi)^q)}{\sqrt{4\xi^2(1 - a(ih\xi)^p - b(ih\xi)^q)^2 - \rho^2}} + i\omega. \qquad (4.4)$$

Now, from section 2 we expect that while ξ tends to infinity as ω approaches 1, $h\xi$ will remain bounded. We define a new variable $\eta = ih\xi$, including the i to simplify the notation. We are now looking for solutions η to (4.4), where η is small for ω near 1. Expanding (4.4) as a polynomial by moving the $i\omega$ term to the left hand side and then squaring both sides, we can now drop the terms in the polynomial from (4.4) with η to powers greater than $q+2$. This leaves us with:

$$8(2 + p - \omega^2)a\eta^{p+2} + 8(2 + q - \omega^2)b\eta^{q+2} + 4\eta^2(\omega^2 - 1) + h^2\omega^2\rho^2 = o(\eta^{q+2}). \qquad (4.5)$$

This equation is clearly too complicated to solve analytically. We thus turn to perturbation techniques. Our interest is in $h \approx 0$ and $\omega \approx 1$. Starting with a perturbation series in h for the solutions η to (4.5), we have as the equation for the zeroth order term

$$8(2 + p - \omega^2)a\eta_0^{2+p} + 8(2 + p - \omega^2)b\eta_0^{2+q} + 4\eta_0^2(\omega^2 - 1) = 0.$$

The first $p+2$ roots of this are

$$\eta_0 = \begin{cases} 0 \text{ twice} \\ p \text{ roots of } \sqrt[p]{\dfrac{1-\omega^2}{2a(2+p-\omega^2)}} = \sqrt[p]{\dfrac{1-\omega}{a(1+p)}} \end{cases} + \text{higher order terms}$$

The remaining $q - p$ roots we may ignore because they do not approach zero as $\omega \to 1$.

We can make an identification of these saddle points by comparing with the scalar wave equation case (Serdjukova [1971] and Hedstrom [1975]). In that problem, there are

p saddle points due to the difference approximation about the origin; they correspond, to first order, to the p saddle points found above. The other two saddle points correspond to the two saddle points in the continuous problem discussed in section two. We will need to know more precisely the location of these last two saddle points, as we use the behavior of the height of the principal saddle point as our definition of width of front. To get the next term in the perturbation expansion for $\eta \approx \eta_0 = 0$, we let $\eta = -dh^\alpha$. Here, d has been chosen real and positive (so that $\xi = idh^{\alpha-1}$ will be the principal saddle point). Also, since we are interested in the width of the front, we need to know how η changes as a function of ω, with $\omega = 1 + ch^\gamma$. Making both of these substitutions in (4.4), we get

$$8(2+p-\omega^2)a(-d)^{2+p}h^{(2+p)\alpha} + 8(2+q-\omega^2)b(-d)^{q+2}h^{(2+q)\alpha} + 4(\omega+1)c(-d)^2h^{2\alpha+\gamma} + h^2\omega^2\rho^2 = 0.$$

Now, since $q > p$, we may drop the h^{2+q} term. This leaves us with

$$8(2+p-\omega^2)a(-d)^{2+p}h^{(2+p)\alpha} + 4(\omega+1)c(-d)^2h^{2\alpha+\gamma} + h^2\omega^2\rho^2 = 0. \qquad (4.6)$$

There are three cases.

case	condition	exponents	α	$-d$
1	$2\alpha+\gamma < 2$	$(2+p)\alpha = 2\alpha+\gamma$	γ/γ	$\sqrt[p]{\frac{-(\omega+1)c}{2a(2+p-\omega^2)}}$
2	$2\alpha+\gamma > 2$	$(2+p)\alpha = 2$	$2/(2+p)$	$\sqrt[p+2]{\frac{-\omega^2\rho^2}{8a(2+p-\omega^2)}}$
3	$2\alpha+\gamma = 2$	all equal	$\frac{2}{2+p} = \frac{2-\gamma}{2}$	*

Table 3: Three cases for η. The condition column gives the condition for that case to hold. The terms column gives the powers of h in (4.6) for that case, and the last two columns give α and $-d$ for that case. The * value of $-d$ is the solution to a $p+2$-th order polynomial, and is omitted.

Each of the cases in table 3 is valid for a range on γ, or, equivalently, for a region near the front. Case 1 is valid for $\gamma < 2/(1+2/p)$. Since this bounds γ from above, the region where case 1 is valid is asymptotically further from the front than cases 2 or 3. Note from (4.6) that in case 1, the $h^2\omega^2\rho^2$ term may be dropped, and hence this is the region where the undifferentiated part of (4.1) does not affect the solution (to first order) Case 2 is valid

for $\gamma > 2/(1+2/p)$. Since this bounds γ from below, this region is asymptotically closer to the front than the region in case 1. In this case, the $4(\omega+1)c(-d)^2h^{2\alpha+\gamma}$ term in (4.6) (the term from the convective or x-derivative) is less important than the ρ term. We note that this case is for ω very near the discontinuity, closer than we expect the approximation to the front to be. Case 3 is the transition region between cases 1 and 2. In this region, all parts of (4.1) are equally important.

Now that we know something about the behavior of the principal saddle points for $\omega \approx 1$, we can look at the path of steepest descent. As in the previous section, we will need very little information about the path in order to find the width of the front. The following figure shows the situation for the methods in this section.

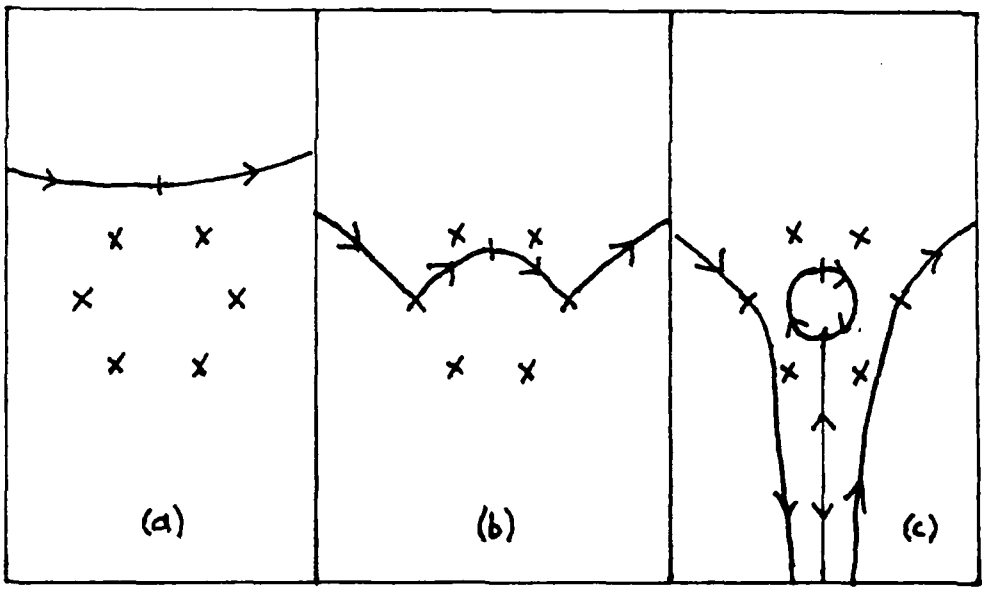

Figure 12: Possible paths of steepest descent for ϕ_- near the saddle points. Arrows show the direction of integration.

As before, the path always passes through the principal saddle point.

We now look at the value of ϕ_- at the principal saddle point $\eta = -dh^\alpha$. It will be useful to expand ϕ_- at this point for ξ large and η small

$$\phi_-(\xi) = -\frac{1}{2} - \frac{i}{2}\sqrt{4\xi^2(1 - a(ih\xi)^p - b(ih\xi)^q)^2 - 1} + i\omega\xi$$
$$= -\frac{1}{2} - i\xi\sqrt{(1 - a(ih\xi)^p - b(ih\xi)^q)^2 - \frac{1}{4\xi^2}} + i\omega\xi.$$

Expanding the argument of the square root we get

$$\phi_-(\xi) = -\frac{1}{2} - i\xi\sqrt{1 - 2a\eta^p - 2b\eta^q - \frac{1}{4\xi^2} + \mathcal{O}(\eta^{2p})} + i\omega\xi$$
$$= -\frac{1}{2} - i\xi\left(1 - a\eta^p - b\eta^q - \frac{1}{8\xi^2} + \mathcal{O}(\eta^{2p})\right) + i\omega\xi$$

Collecting terms, we have finally

$$\phi_-(\xi) = -\frac{1}{2} - i\xi(1 - \omega) + i\xi\left(a\eta^p + b\eta^q + \frac{1}{8\xi^2} + \mathcal{O}(\eta^{2p})\right)$$

or

$$\phi_-(\xi) = -\frac{1}{2} - i\xi(1 - \omega - a\eta^p) + \mathcal{O}(\xi\eta^q; \frac{1}{\xi^2}; \eta^{2p})$$

Now we substitute $-i\eta/h$ for ξ and $-ch^\gamma$ for $1 - \omega$ to get

$$\phi_-(\xi) = -\frac{1}{2} - \eta h^{-1}(-ch^\gamma - a\eta^p) + \mathcal{O}(\eta^{q+1}h^{-1}; h^2\eta^{-2}; \eta^{2q}).$$

Finally, we have $\eta = -dh^\alpha$, or

$$\phi_-(\xi) = -\frac{1}{2} - dh^{\alpha-1}(ch^\gamma + a(-d)^p h^{p\alpha}) + \mathcal{O}(h^{\alpha(q+1)-1}; h^{2-2\alpha}; h^{2p\alpha}).$$

Since $d > 0$, we clearly need only look at the behavior of $h^{\alpha-1}(ch^\gamma + a(-d)^p h^{p\alpha})$. We wish to find the critical γ_c such that this term (which controls the height of the principal saddle point for $\omega \approx 1$) approaches $-\infty$ for $\gamma < \gamma_c$ and 0 for $\gamma > \gamma_c$. However, we can get no further without assuming something about η. We will first take case 1 from above. In this case, $p\alpha = \gamma$ so both terms are equally important. We then have

$$\phi_-(\xi) = -\frac{1}{2} - dch^{(\alpha-1)\gamma}\left(1 - \frac{1+\omega}{2(2+p-\omega^2)}\right) + \cdots \tag{4.7}$$

where we have used the formula for $-d$ above. The quantity in parenthesis is always positive, so this term has the critical gamma $\gamma_c = 1 - \alpha$. From table 3, we see that case 1 implies that $(2+\gamma)\alpha = 2\alpha + \gamma$, so we have finally $\gamma_c = p/(p+1)$.

We need only show that the other two cases in table 3 are excluded. First, we have $p\alpha > \gamma$ in cases 2 and 3. Since we are looking for the critical γ, this means that we

must have $\gamma = 1 - \alpha$. From table 3 we know that in cases 2 and 3, $\alpha = 2/(2+p)$, so $\gamma = 1/(2+p)$ and hence that $2\alpha + \gamma < 2$. But for both cases 2 and 3, the condition on γ is $2\alpha + \gamma \geq 2$. Hence for $\gamma = \gamma_c$, case 1 is the only case that applies. ∎

In the proof, we again expanded about $h\xi = 0$. (Recall that in the continuous problem we expanded about $1/\xi = 0$.) If we could not have done this, then we would not have been able to use the model equation (4.1), since it is essentially an expanssion in $h\xi$ for a difference approximation to (2.1).

Results of Section 3 as an Example

To illustrate the results above, we will briefly sketch out the analysis for the difference method analyzed in section 3. The parameters for the centered second order difference method considered there are $p = 2$, $a = -1/6$, $\rho = 1$, and $b = 0$. Then for case 1 in table 3, we have

$$-d = \sqrt{\frac{-c(\omega+1)}{2(-1/6)(2+2-\omega^2)}} \approx \sqrt{(1+\omega)c}$$

since $\omega^2 \approx 1$. With this, we may write (4.7) as

$$\phi_-(\xi) = -\frac{1}{2} - (c(1+\omega))^{3/2} h^{(\alpha-1)\gamma}\left(\frac{1}{1+\omega} - \frac{1}{6}\right) + \cdots.$$

(Recall that $c(1+\omega)$ here is c in section 3.) This is the same as (3.8). Finally, case 1 is valid for $\gamma < 2/2 = 1$, and the width of the front is $O(h^{2/3})$.

The Canonical Form

As in the previous section, it will be very useful to construct the canonical form for the solution (4.3) to (4.1). By producing graphs of the canonical form, we will be able to show the near-front behavior for a wide range of difference approximations.

Near the front, we have the following small h, small η expansion for $\phi_-(\xi)$

$$\phi_-(\xi) \approx -\frac{1}{2} - i\xi(1-\omega) + \frac{i}{8\xi} + ai\xi(ih\xi)^p + bi\xi(ih\xi)^q.$$

Following the example in section 3, we expect the canonical form to be

$$\psi(r) = \frac{a}{r} + b + cr + \cdots + dr^{p+1} + er^{q+1}.$$

The parameters may be determined by the method outlined in section 3. However, the exact form of ψ is less interesting than the simpler approximation

$$\psi(r) = -\frac{1}{2} - ir(1-\omega) + \frac{i}{8r} + air(ihr)^p + bir(ihr)^q$$

which is just the leading terms in $\phi_-(r)$. It is straightforward to show that this form has the required properties; $p+2$ saddle points which converge to a saddle point of infinite order as $h \to 0$ and $\omega \to 1$. The $q-p$ saddle points are much further from the origin than the first $p+1$ saddle points and are unimportant to first order.

Because of the complexity of even the approximate $\phi(r)$, we will not analyze it here. Instead, the reader is refered to section 5, where graphs of the canonical form integral are presented. These graphs show both the behavior of difference schemes that fit the framework of (4.1) near the front, and the qualitative similiarity between the finite difference solutions to the scalar wave equation $u_t = u_x$ and the telegrapher's equation.

The Cell Wave-Coupling Number

Consider the generalization to (4.1)

$$\begin{aligned} \frac{\partial u}{\partial t} &= -c\frac{\partial v}{\partial x} + ah^p \frac{\partial^{p+1} v}{\partial x^{p+1}} + bh^q \frac{\partial^{q+1} v}{\partial x^{q+1}} \\ \frac{\partial v}{\partial t} &= -c\frac{\partial u}{\partial x} + ah^p \frac{\partial^{p+1} u}{\partial x^{p+1}} + bh^q \frac{\partial^{q+1} v}{\partial x^{q+1}} - \rho v. \end{aligned} \tag{4.8}$$

All we have done here is to add a propagation speed c to (4.1). The advantage of this is that now (4.8) is in dimensional form if a, b, and c have the dimensions of a speed and ρ has dimension $1/t$. Now, we chose a change of variable to put (4.8) into nondimensional form. Let $x = cx'/\rho$ and $t = t'/\rho$. Define $R = h\rho/c$. We will call this the cell (from the h) wave-coupling (from the ρ) number. Then (4.8) may be written as

$$\begin{aligned} \frac{\partial u}{\partial t'} &= -\frac{\partial v}{\partial x'} + \frac{a}{c} R^p \frac{\partial^{p+1} v}{\partial x'^{p+1}} + \frac{b}{c} R^q \frac{\partial^{q+1} v}{\partial x'^{q+1}} \\ \frac{\partial v}{\partial t'} &= -\frac{\partial u}{\partial x'} + \frac{a}{c} R^p \frac{\partial^{p+1} u}{\partial x'^{p+1}} + \frac{b}{c} R^q \frac{\partial^{q+1} u}{\partial x'^{q+1}} - v. \end{aligned}$$

This shows that the appropriate dimensionless quantity which must be small in our analysis is R, the cell wave-coupling number. This is illuminating, as it shows that if the cellsize is small or the coupling coefficient is small, then the solution to (4.8) will behave near the front like the solution to the scalar wave equation ($\rho = 0$ in (4.1)).

5. Numerical Results

We present in this section two distinct numerical results. The first set of computations is used to illustrate the theory. They show that the width of the front is as predicted for a number of schemes, both semi and fully discrete. The second set of computations presents graphs of the generalized Bessel functions described in section 4. These show that the qualitative behavior of approximations to the telegraph equation for small $\rho h/c$ (recall that this is the cell wave-coupling number) is the same as the behavior for the scalar wave equation.

Behavior near the Discontinuity for Various Difference Schemes

The following graphs show the width of the front for two method-of-lines (MOL) schemes and two fully discrete schemes. The MOL schemes are the centered second (5.1) and fourth order (5.2) schemes

$$\begin{aligned} \frac{dU_i}{dt} &= -\frac{V_{i+1} - V_{i-1}}{2h} \\ \frac{dV_i}{dt} &= -\frac{U_{i+1} - U_{i-1}}{2h} - V_i \end{aligned} \tag{5.1}$$

and

$$\begin{aligned} \frac{dU_i}{dt} &= -\frac{8(V_{i+1} - V_{i-1}) - (V_{i+2} - V_{i-2})}{12h} \\ \frac{dV_i}{dt} &= -\frac{8(U_{i+1} - U_{i-1}) - (U_{i+2} - U_{i-2})}{12h} - V_i \end{aligned} \tag{5.2}$$

for $i = 0, \pm 1, \pm 2, \ldots$ and h the space step size. The fully discrete schemes are Leapfrog (5.3) and Lax-Wendroff (5.4). Let k and h be the time and space step size respectively, and let $\lambda = k/h$. Then the schemes are

$$\begin{aligned} U_i^{n+1} &= U_i^{n-1} - \lambda(V_{i+1}^n - V_{i-1}^n) \\ V_i^{n+1} &= V_i^{n-1} - \lambda(U_{i+1}^n - U_{i-1}^n) - 2kV_i^n \end{aligned} \tag{5.3}$$

and

$$\begin{aligned} U_i^{n+1} &= \tfrac{1}{2}\lambda(\lambda U_{I+1}^n + (\tfrac{1}{2}k - 1)V_{i+1}^n) + (1 - \lambda^2)U_i^n + \tfrac{1}{2}\lambda(\lambda U_{i-1}^n + (1 - \tfrac{1}{2}k)V_{i-1}^n) \\ V_i^{n+1} &= \tfrac{1}{2}\lambda(\lambda V_{i+1}^n + (\tfrac{1}{2}k - 1)U_{i+1}^n) + (1 - k - \lambda^2 + \tfrac{1}{2}k^2)V_i^n \\ &\quad + \tfrac{1}{2}\lambda(\lambda V_{i-1}^n + (1 - \tfrac{1}{2}k)U_{i-1}^n) \end{aligned} \tag{5.4}$$

Each method was integrated to $t = 1/4$ for $h = 1/2^n$ for $n = 5, \ldots, 10$. For each value of h, the width was determined by finding the value a x where the solution U was equal to U_0. The values of U_0 used were .05 and .001. These were chosen to measure the width in two different areas: inside the front ($U_0 = .05$) and in the tail ahead of the front ($U_0 = .001$). By chosing two different values of U_0, we show that the width behaves as predicted over the entire front. Since U is defined only at discrete points, we used linear interpolation to find the value of x.

First, we show the computed solution for $h = 1/512$ and $t = 1/4$ for each method. The MOL schemes were integrated with RKF45 (see Shampine, Watts, and Davenport [1976] for a discussion of the merits of RKF45; Forsythe, Malcolm, and Moler [1977] for the code); the fully discrete schemes used $k = h/1.25$. Following graphs of the computed solution are eight graphs showing the width of the front for these four schemes.

Centered, H= 1.953125D-03

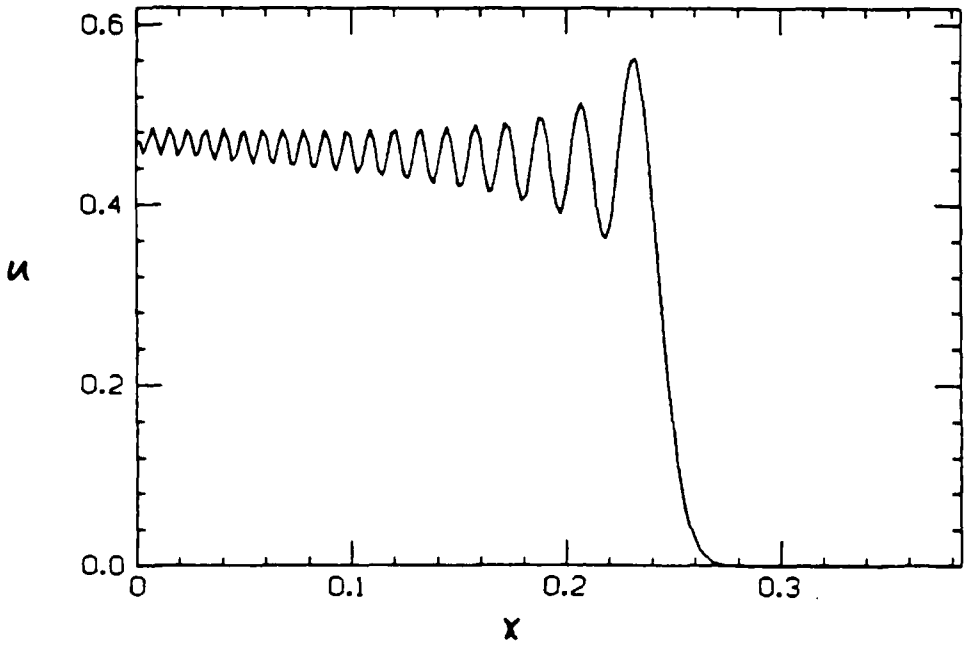

4th Order Centered, H= 1.953125D-03

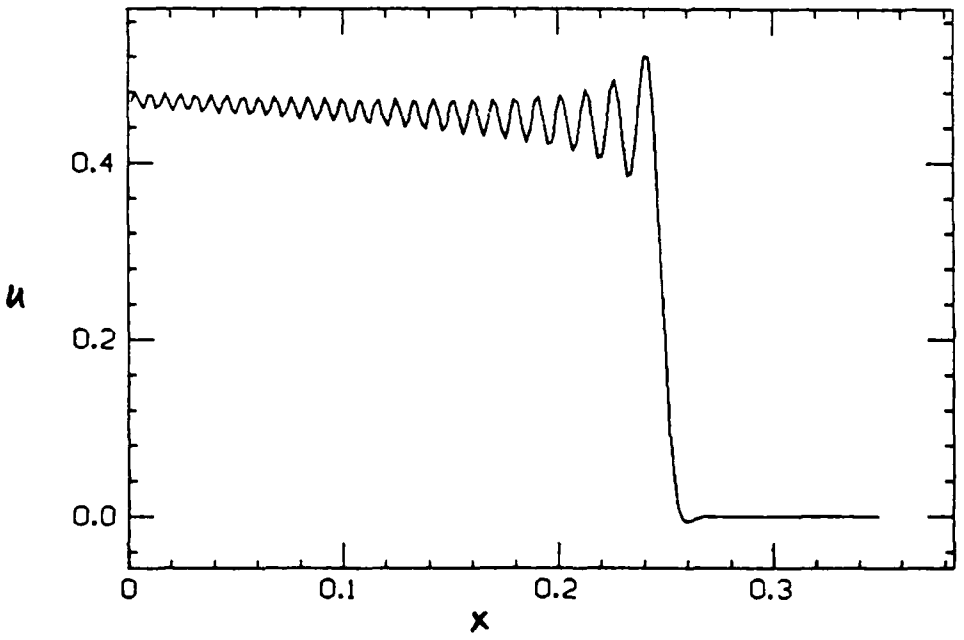

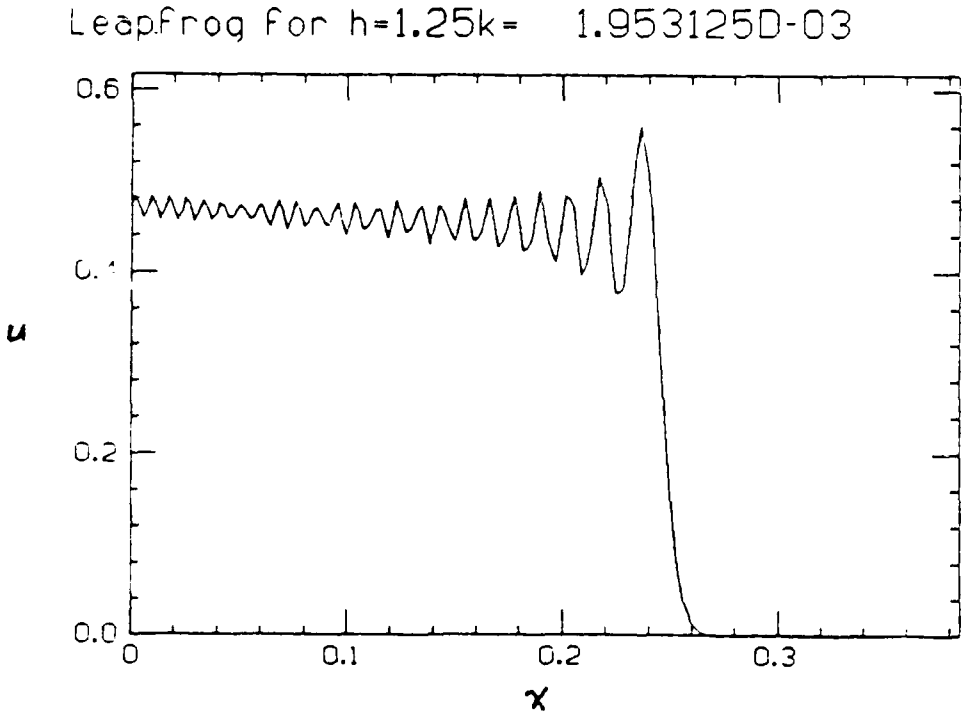
Leapfrog for h=1.25k= 1.953125D-03
0.6
0.4
0.2
0.0
u
0
0.1
0.2
0.3
x

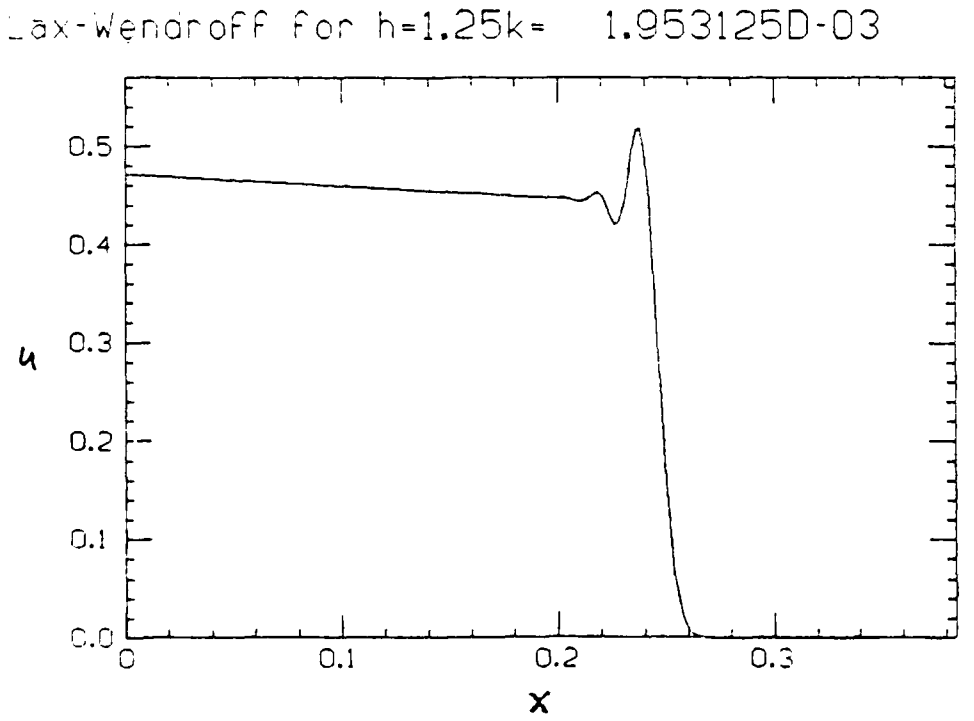
Lax-Wendroff for h=1.25k= 1.953125D-03
0.5
0.4
0.3
0.2
0.1
0.0
u
0
0.1
0.2
0.3
x

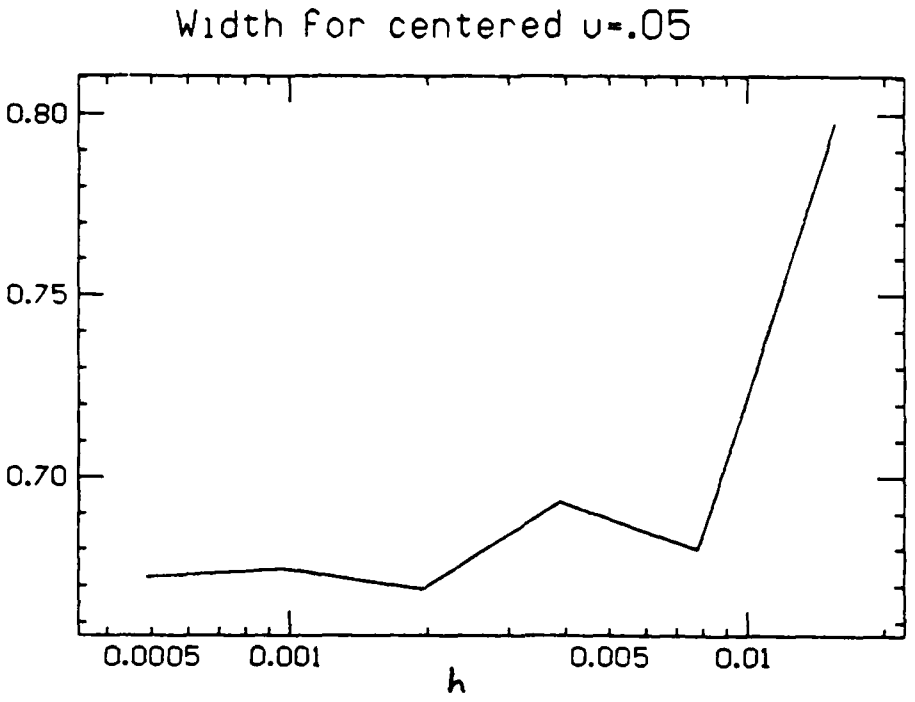
Width for centered u=.05
0.80
0.75
0.70
0.0005
0.001
0.005
0.01
h

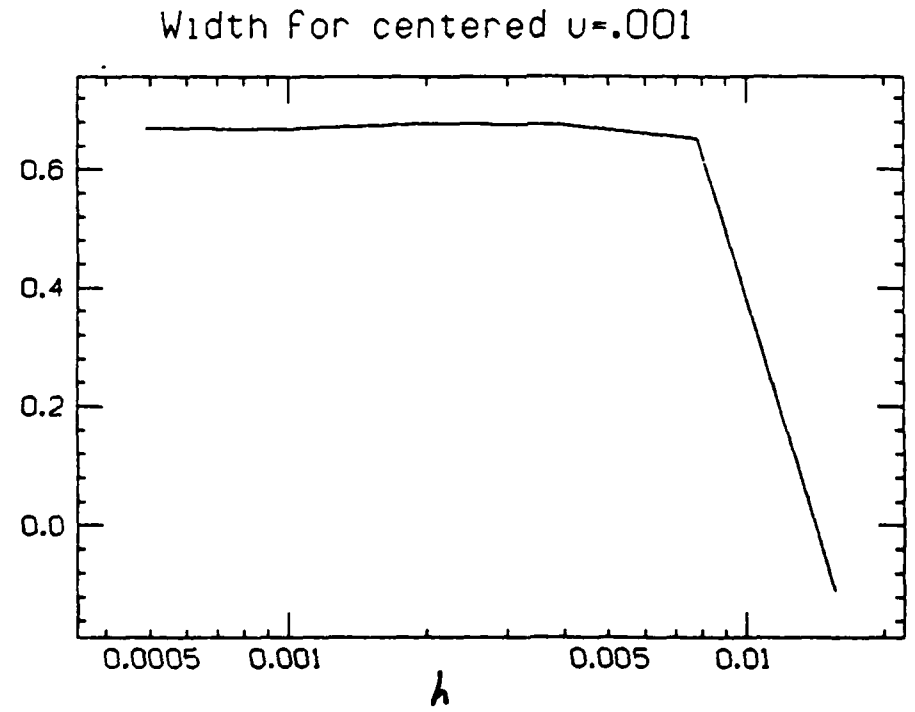
Width for centered u=.001
0.6
0.4
0.2
0.0
0.0005
0.001
0.005
0.01
h

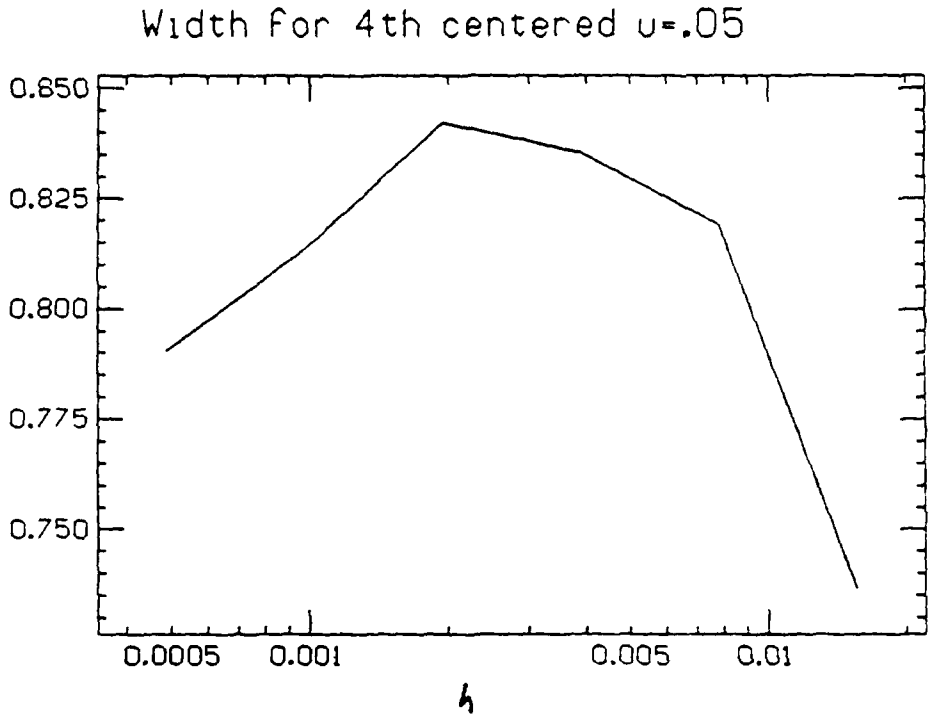
Width for 4th centered u=.05
0.850
0.825
0.800
0.775
0.750
0.0005
0.001
0.005
0.01
h

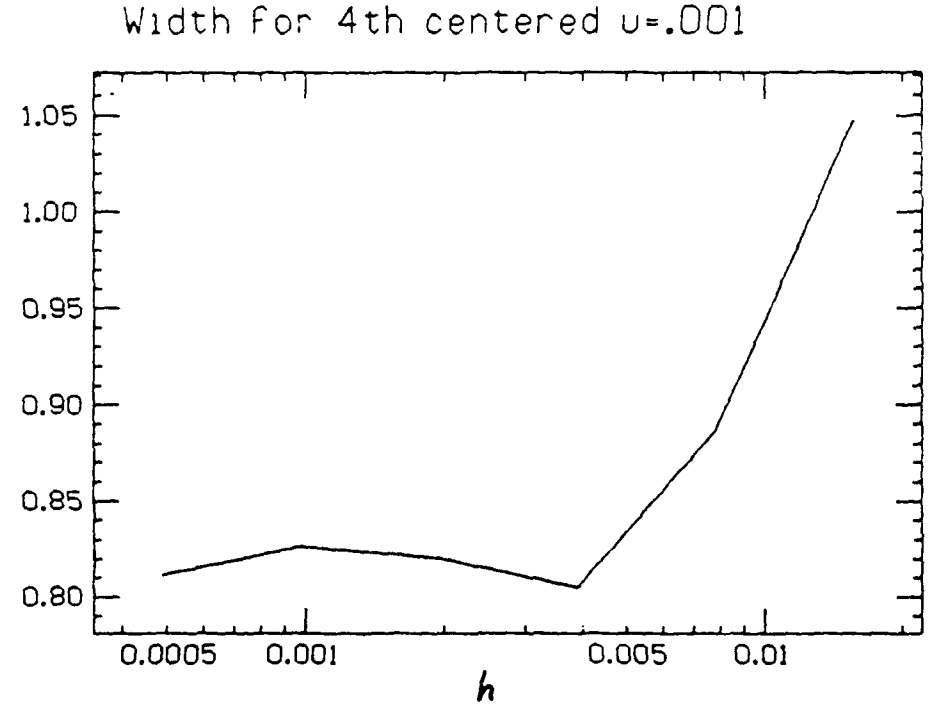
Width for 4th centered u=.001
1.05
1.00
0.95
0.90
0.85
0.80
0.0005
0.001
0.005
0.01
h

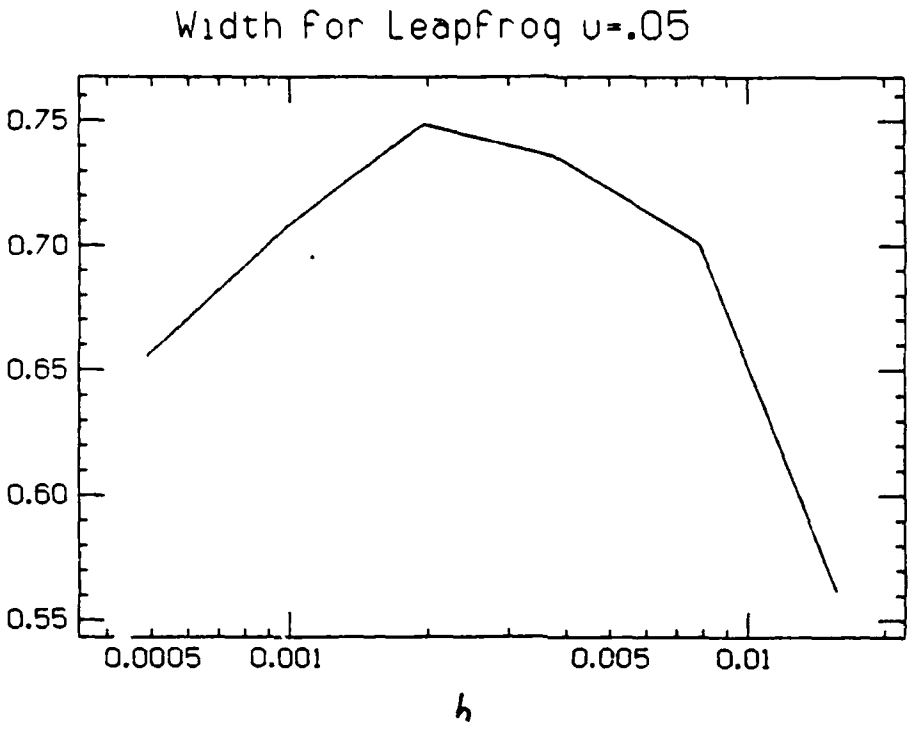
Width for Leapfrog υ=.05
0.75
0.70
0.65
0.60
0.55
0.0005
0.001
0.005
0.01
h

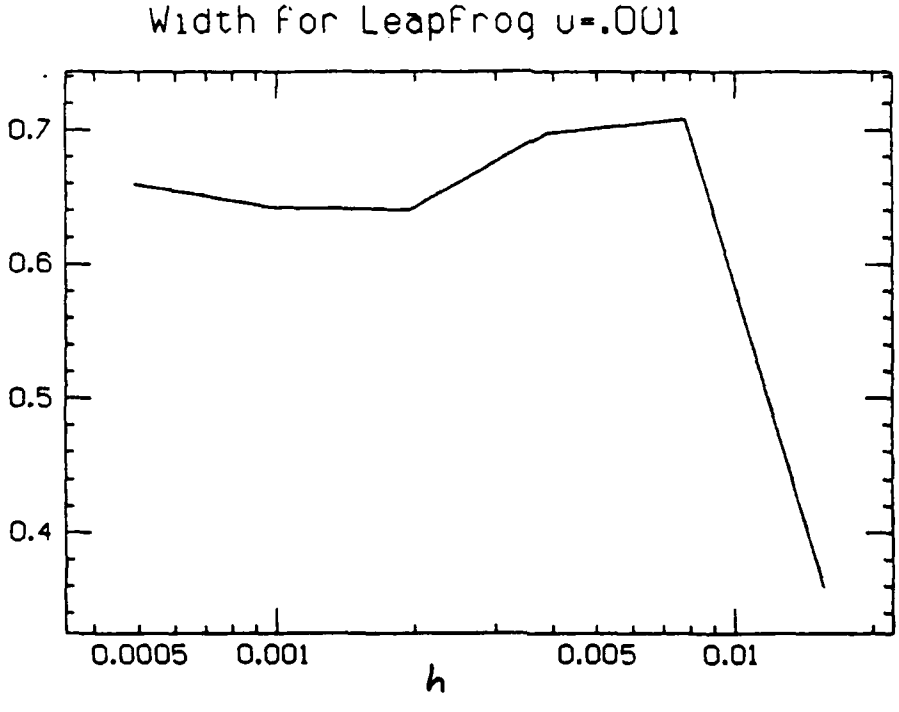
Width for Leapfrog υ=.001
0.7
0.6
0.5
0.4
0.0005
0.001
0.005
0.01
h

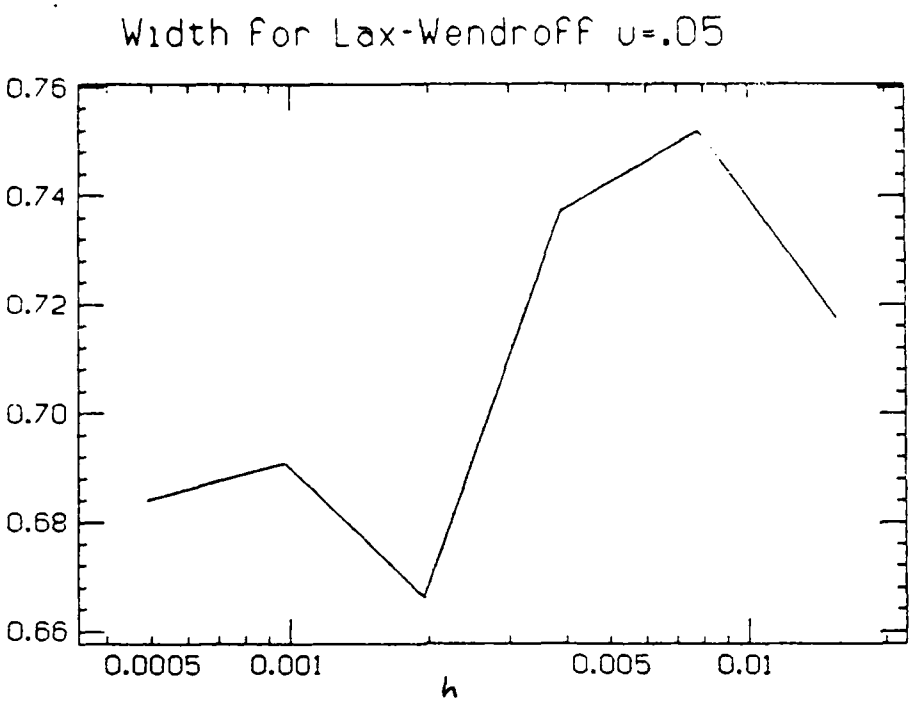
Width for Lax-Wendroff u=.05
0.76
0.74
0.72
0.70
0.68
0.66
0.0005
0.001
0.005
0.01
h

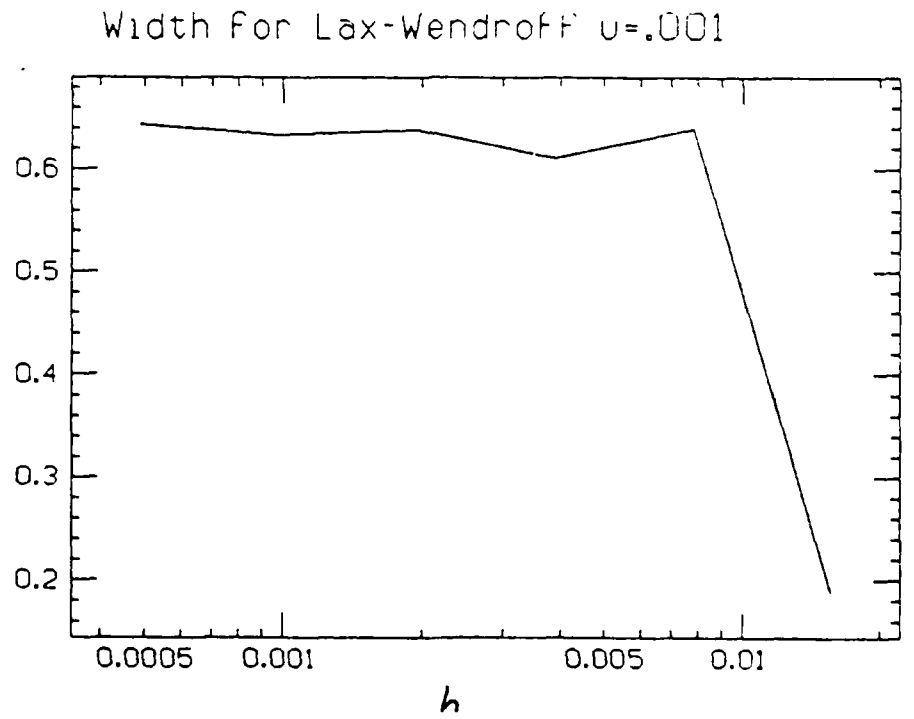
Width for Lax-Wendroff u=.001
0.6
0.5
0.4
0.3
0.2
0.0005
0.001
0.005
0.01
h

The graphs of the width of the fronts verify the predictions of the theory developed in sections 3 and 4. The second order method of lines calculations verify the results in section 3; the others confirm the results in section 4. Notice that for the fourth order method of lines the width of the front is $O(h^{4/5})$ as expected. Note also that for the finite difference methods (Lax-Wendroff and Leapfrog) the rate of convergence to $h^{2/3}$ is slower than for the semidiscrete approximations. This points out the asymptotic nature of the theory: the results are applicable only for large t/h.

Graphs of Generalized Bessel Functions

We have seen in previous sections that the behavior of difference approximations to the telegrapher's equation may be represented by a class of integrals. The most useful information for our purpose (understanding the behavior of the difference approximations) is contained in graphs of these integrals, since the solution of a difference approximation is closely modeled by these integrals.

We will first transform the general canonical form given in section 4 to both bring out the independent parameters and to place it in a form with convenient limits. Specifically, we would like to show the scalar wave equation limit as a way of showing the similarities in the behavior of approximations to the two problems.

The canonical form integral in section 4 is

$$I = \frac{1}{2\pi}\int_{-\pi/h}^{\pi/h} \xi^{-s}\exp\left[\left(\frac{i\rho^2}{8\xi} + i\xi(\omega-1) + ia\xi(ih\xi)^p + ib\xi(ih\xi)^q\right)t\right]d\xi.$$

We will take p even and q odd, and $s = 1$ or 0. After a little bit of algebraic manipulation, we may write this as

$$I = \frac{1}{2\pi}\int_{-\infty}^{\infty} y^{-s}\exp\left[\frac{i\beta}{y} + ixy + \frac{iy^{p+1}}{p+1} - \frac{\alpha y^{q+1}}{q+1}\right]dy.$$

(The limits of integration have been extended to $\pm\infty$.) The values for α, β, and x are

$$\alpha = \tilde{b}\left(\frac{t}{h}\right)^{\frac{p-q}{p+1}}\tilde{a}^{-\frac{q+1}{p+1}}$$

$$\beta = \left(\frac{t}{h}\right)^{\frac{p+2}{p+1}}\rho^2h^2\tilde{a}^{\frac{1}{p+1}}$$

$$x = \left(\frac{t}{h}\right)^{\frac{p}{p+1}}(\omega-1)w\tilde{a}^{-\frac{1}{p+1}}$$

where

$$\tilde{a} = (p+1)a(-1)^{\frac{p}{2}}$$
$$\tilde{b} = -(q+1)b(-1)^{\frac{q+1}{2}}.$$

($\tilde{a}$ corresponds to c and $\tilde{b}$ corresponds to ϵ in Chin and Hedstrom [1978].) Note that β is proportional to the square of the cell wave-coupling number k discussed in section 4, and that only β contains any contribution from ρ. Thus the coupling in the telegrapher's equation shows up only in the β term. Further, we have dropped leading constants. We define $I_{1-s}(\alpha, \beta, p, q; x)$ as this integral. The advantage of this form is that $I_{1-s}(\alpha, 0, p, q; x)$ is equal to the generalized Airy functions tabulated by Chin and Hedstrom [1978] for the scalar wave equation (our p is their $p-1$, our q is their $q-1$). This will allow us to both check our graphs against their published solutions and to see how the β term changes the behavior of $I_{1-s}(\alpha, \beta, p, q; x)$.

The graphs are organized as follows. Each page has graphs for fixed α, p and q. The left column shows $I_0(\alpha, \beta, p, q; x)$ for $\beta = 0$, 0.01, and 0.05. The right column gives $I_1(\alpha, \beta, p, q; x)$ for the same values of β. The left column represents the leading term in the asymptotic expansion for the difference solution.

The last two pages of these graphs show the special case where there is no p term. These represent the odd order methods (such as upstream differencing).

To use these graphs, the following should be kept in mind. First, in comparing the I_0 graphs with the computed solutions, the left column should be multiplied by -1 (flipped over) since the integral for the solution in sections 3 and 4 is the negative of the form used here. Second, except for the last two pages (the 'p-term missing' graphs), these graphs are appropriate for even order methods with artificial viscosity (or no viscosity if $\alpha = 0$). Increasing values of α represent increasing artificial viscosity.

$p=2 \quad q=1 \quad \alpha=0.50$

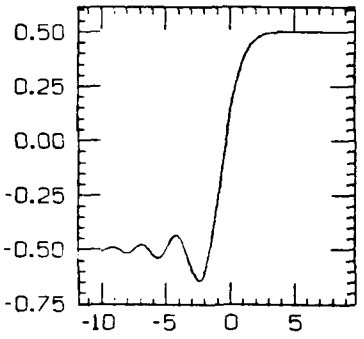

$\beta=0$

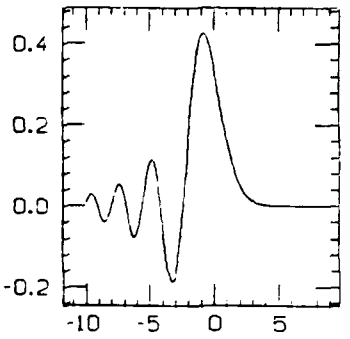

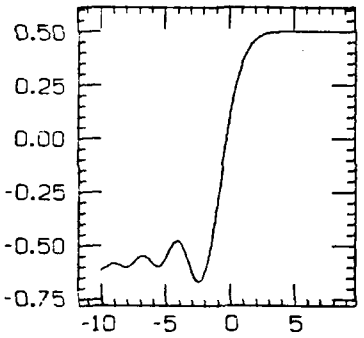

$\beta=.01$

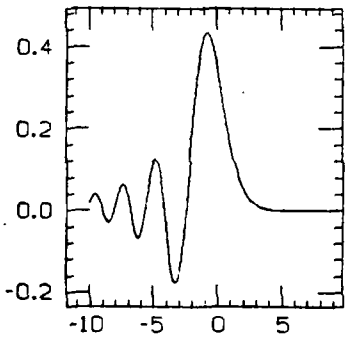

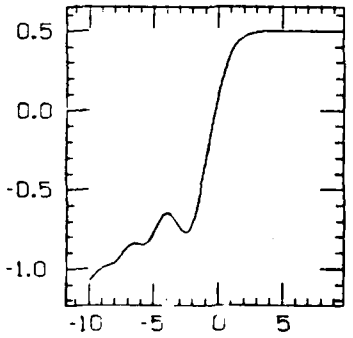

$\beta=.05$

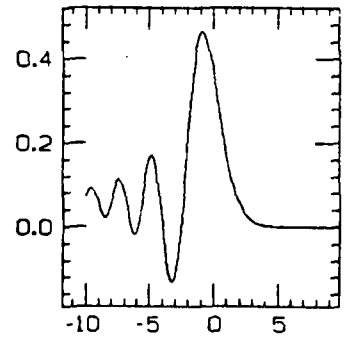

I_0 I_1

p=2 q=1 α=1.00

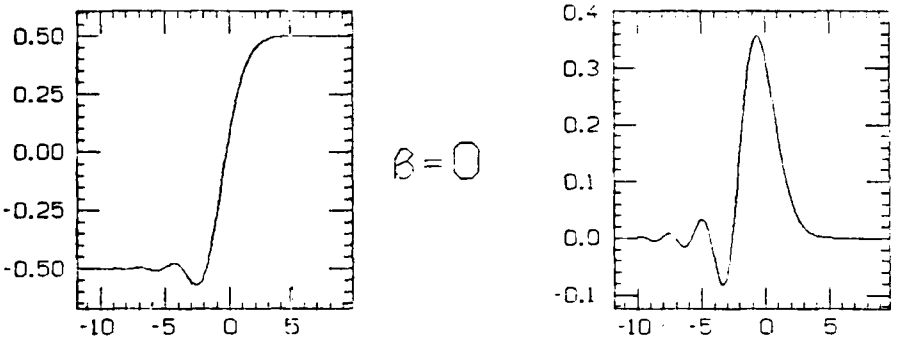

β=0

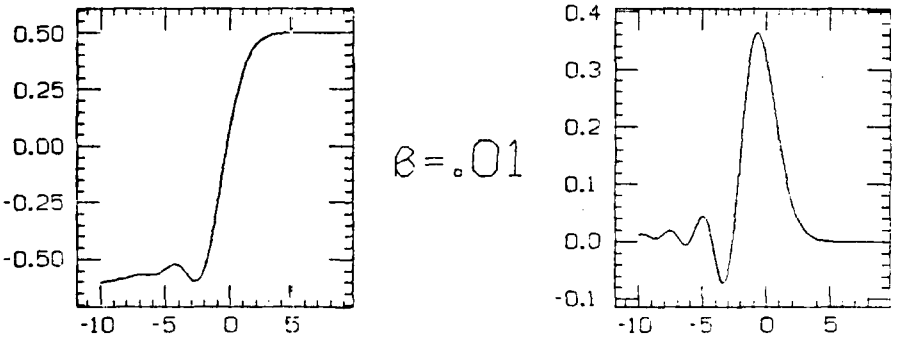

β=.01

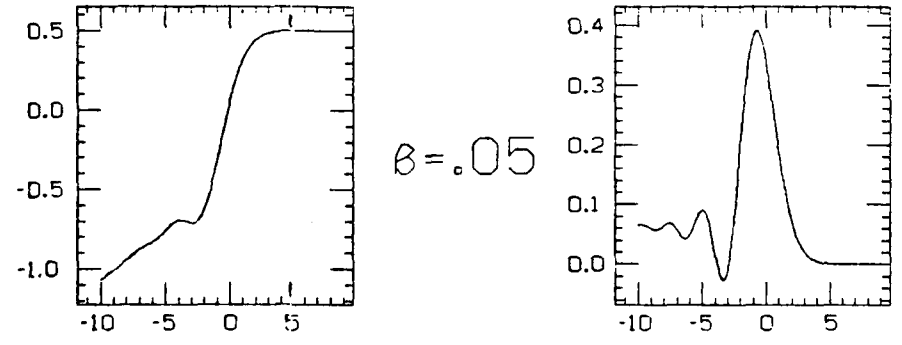

β=.05

I_0 I_1

p=2 q=1 α=2.00

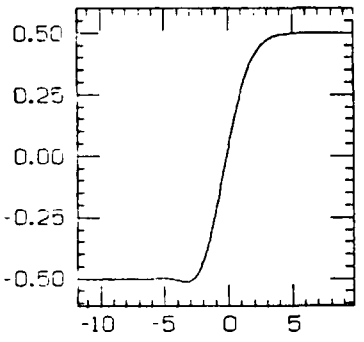

β=0

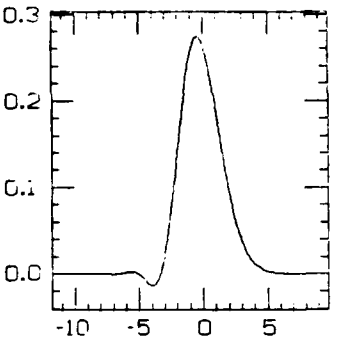

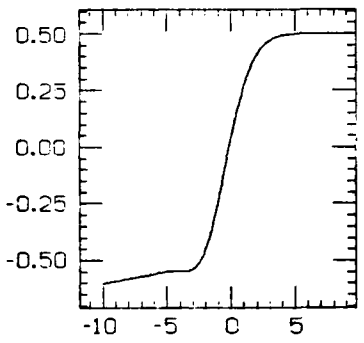

β=.01

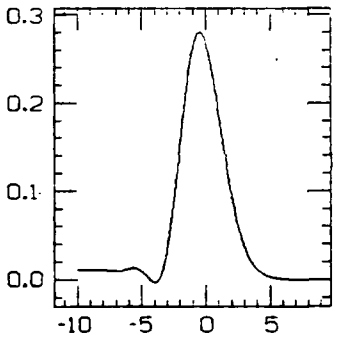

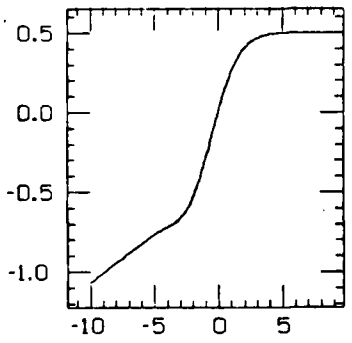

I_0

β=.05

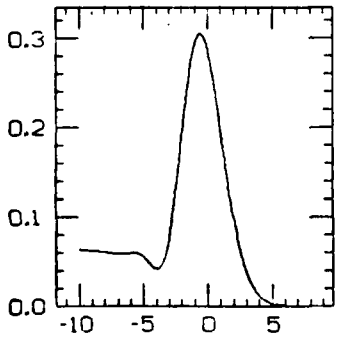

I_1

p=2 q=3 α=0.50

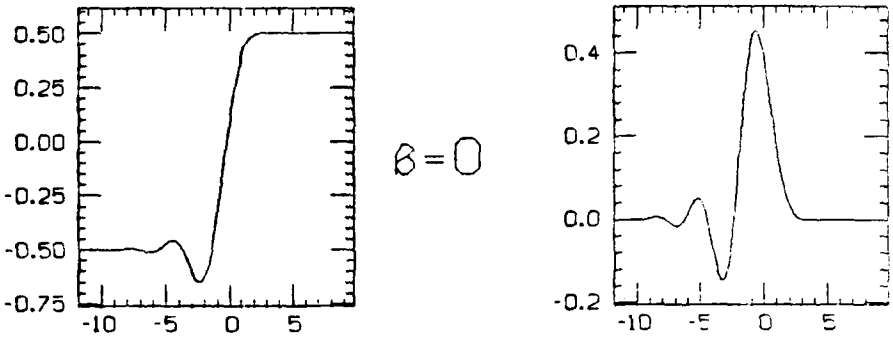

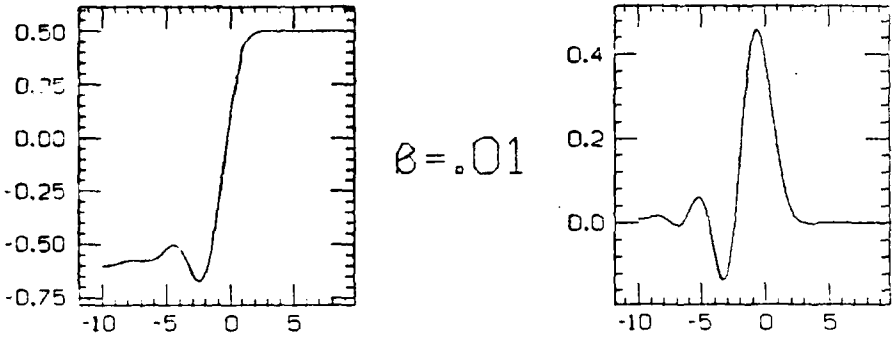

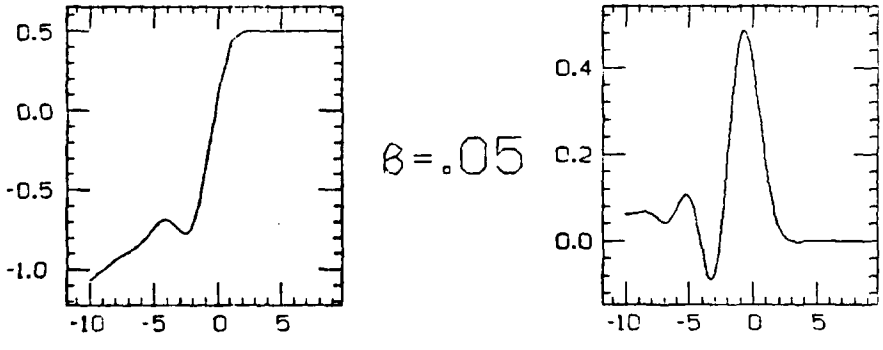

I_0 I_1

p=2 q=3 α=1.00

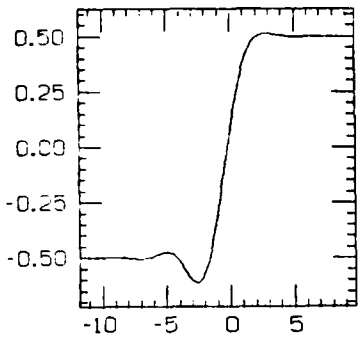

β=0

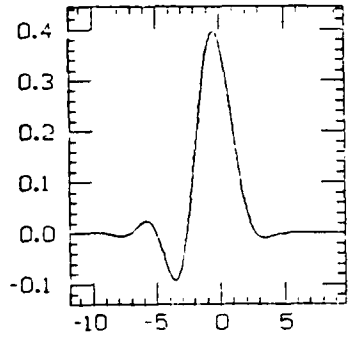

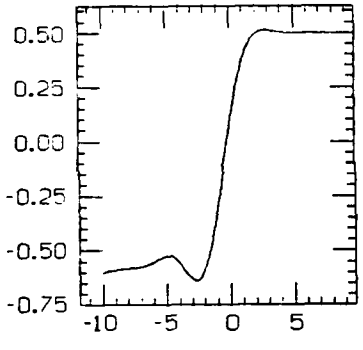

β=.01

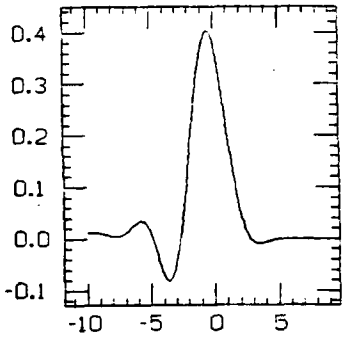

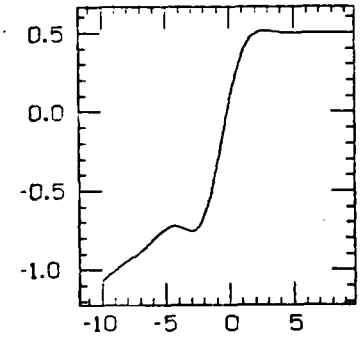

β=.05

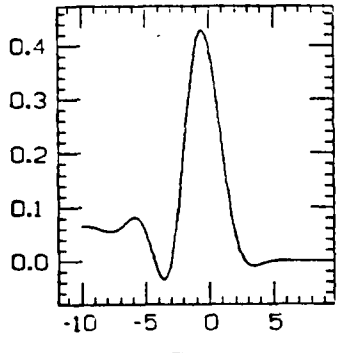

I_0 I_1

p=2 q=3 α=2.00

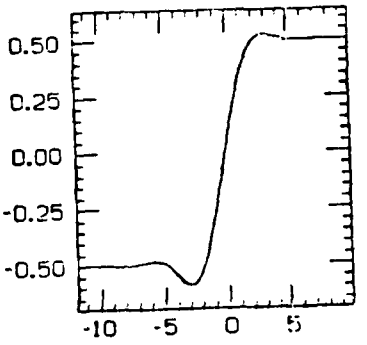

β=0

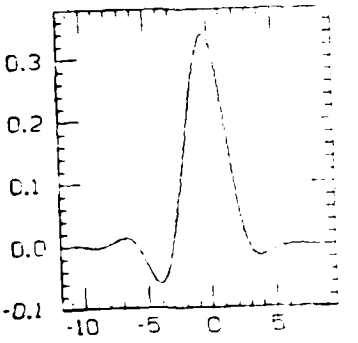

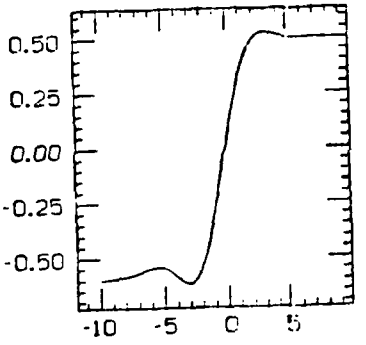

β=.01

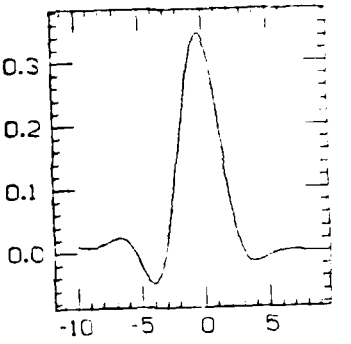

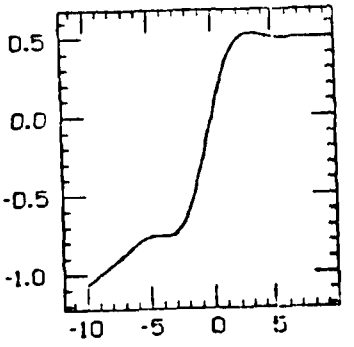

I_0

β=.05

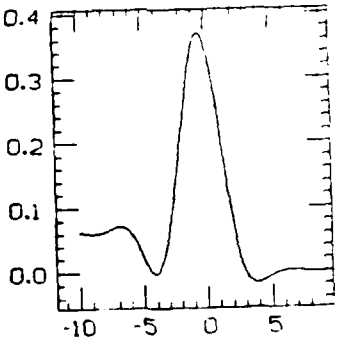

I_1

$p=2 \quad q=5 \quad \alpha=0.50$

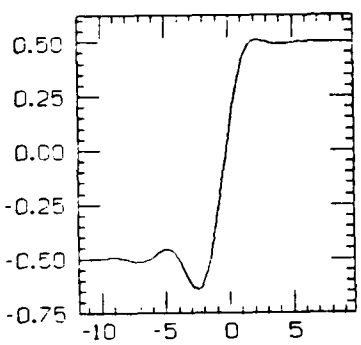

$\beta=0$

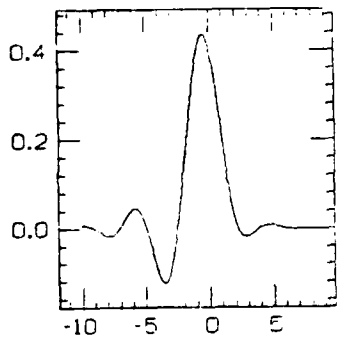

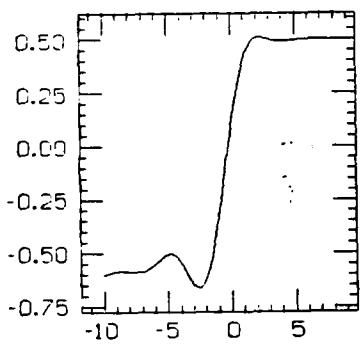

$\beta=.01$

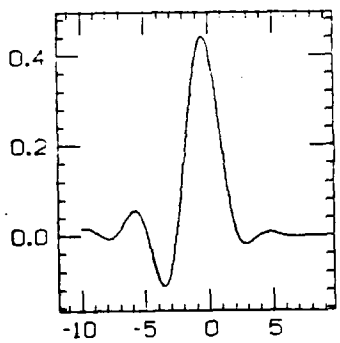

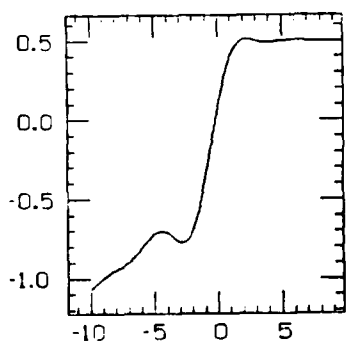

I_0

$\beta=.05$

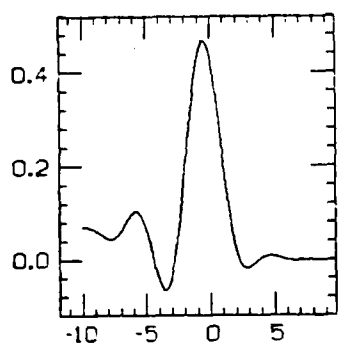

I_1

p=2 q=5 α=1.00

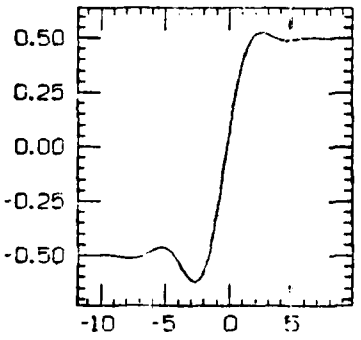

β=0

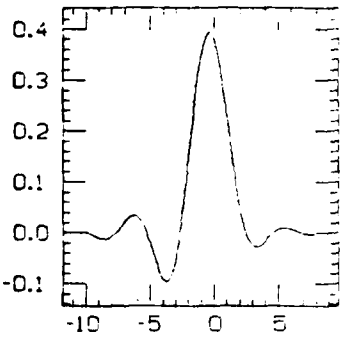

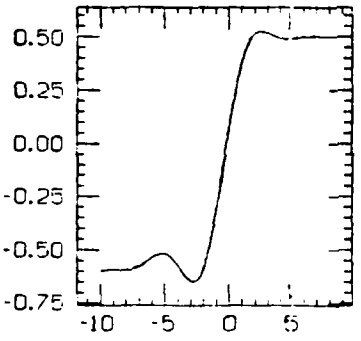

β=.01

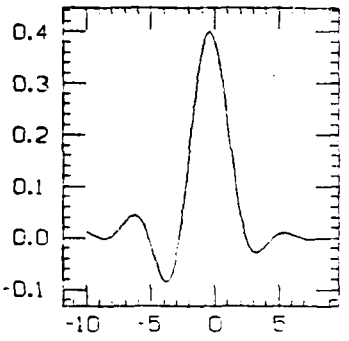

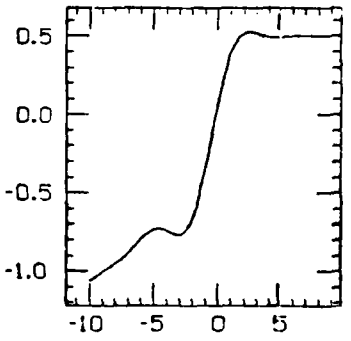

β=.05

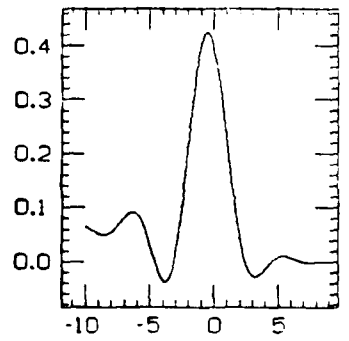

I_0 I_1

p=2 q=5 α=2.00

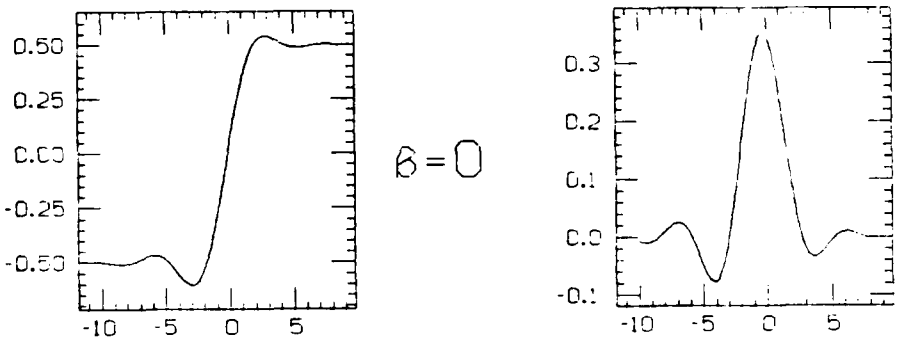

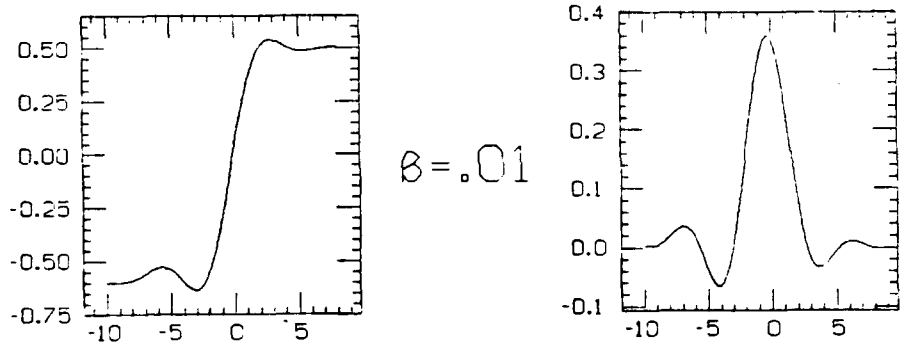

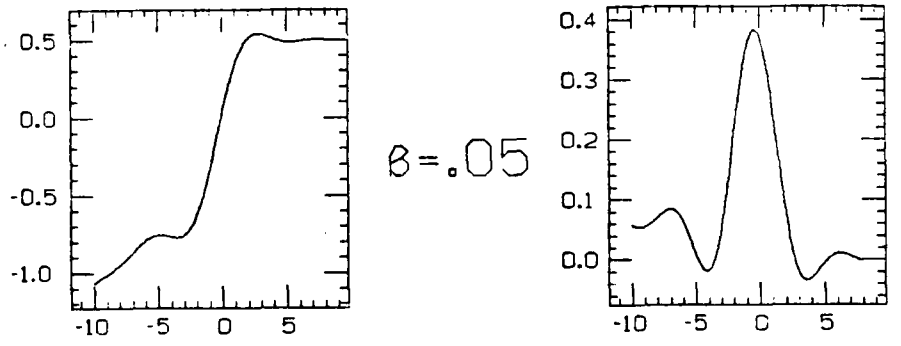

I_0 I_1

p=4 q=1 α=0.50

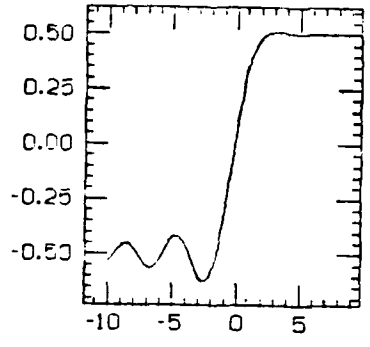

β=0

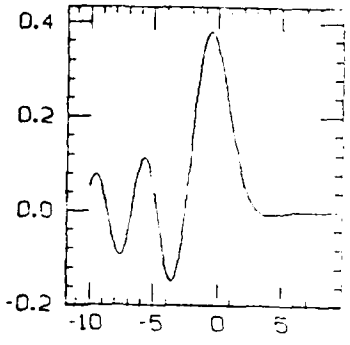

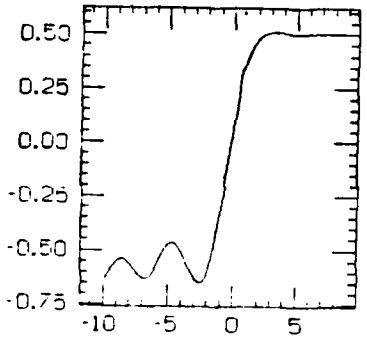

β=.01

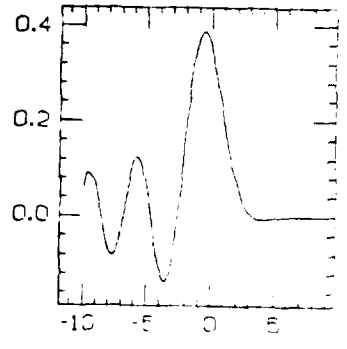

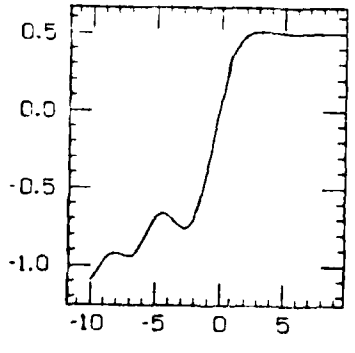

β=.05

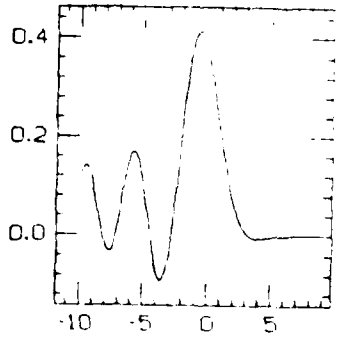

I_0 I_1

p=4 q=1 α=1.00

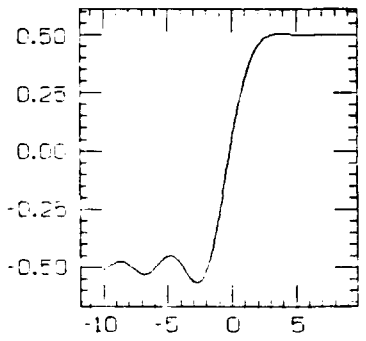

β=0

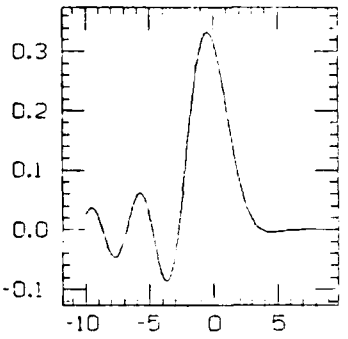

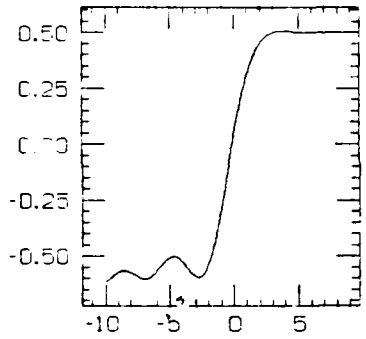

β=.01

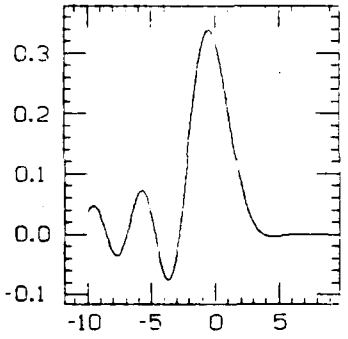

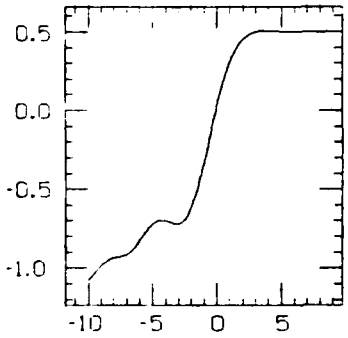

I_0

β=.05

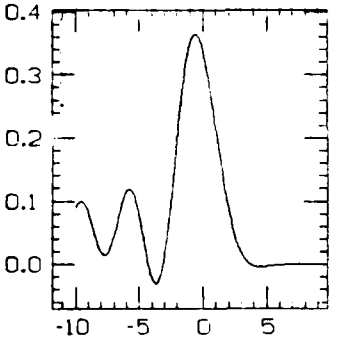

I_1

p=4 q=1 α=2.00

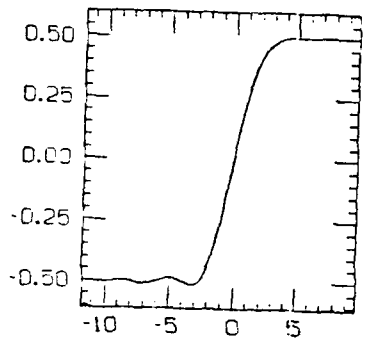

β=0

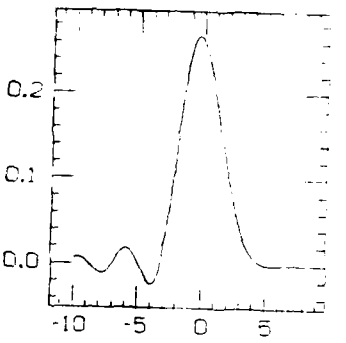

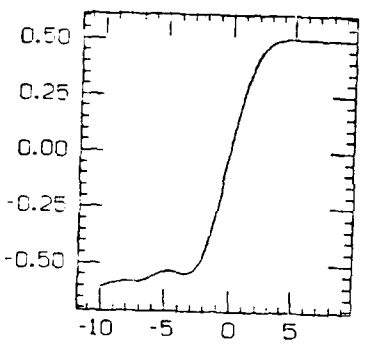

β=.01

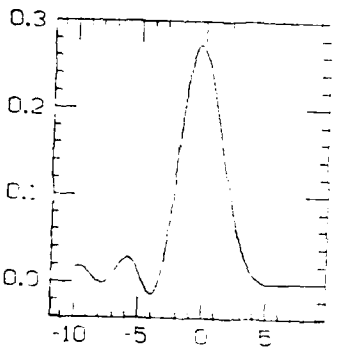

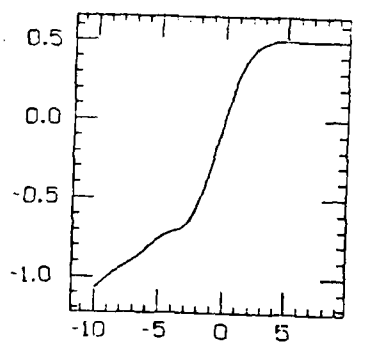

I_0

β=.05

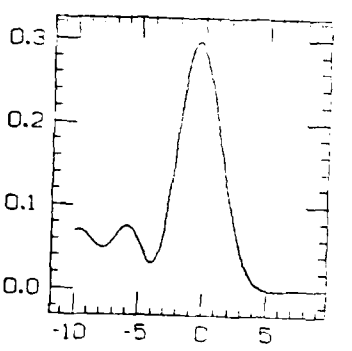

I_1

p=4 q=3 α=0.5

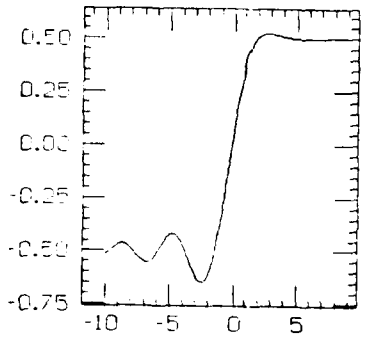

β=0

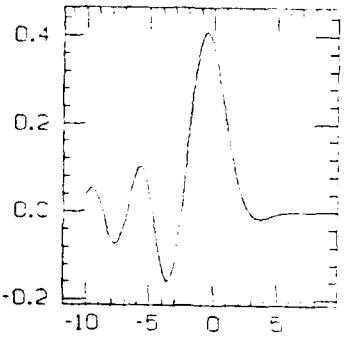

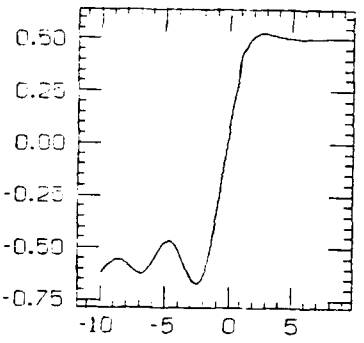

β=.01

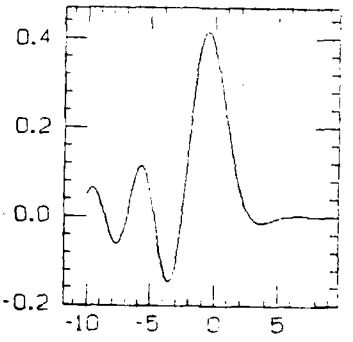

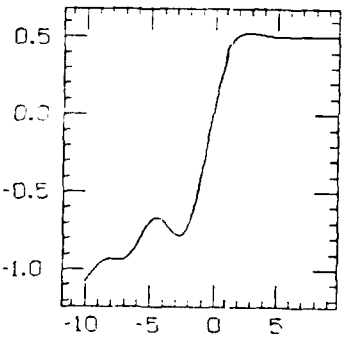

I_0

β=.05

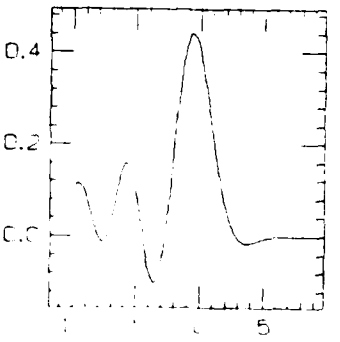

I_1

p=4 q=3

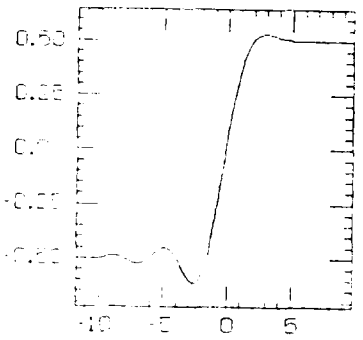

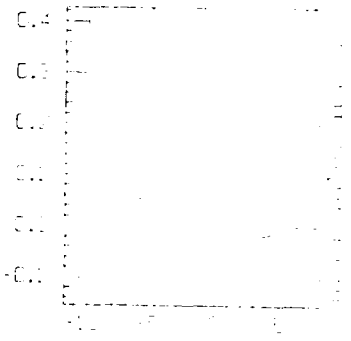

β=0

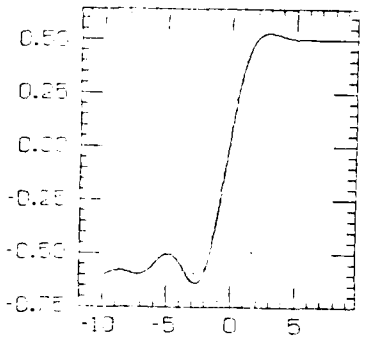

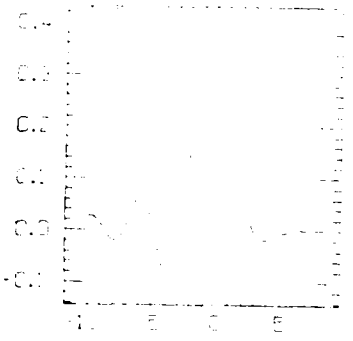

β=.01

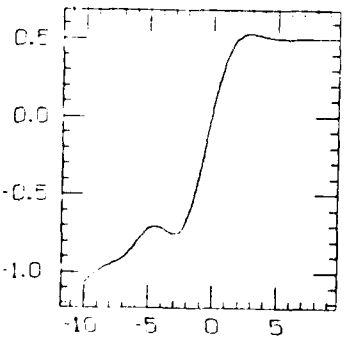

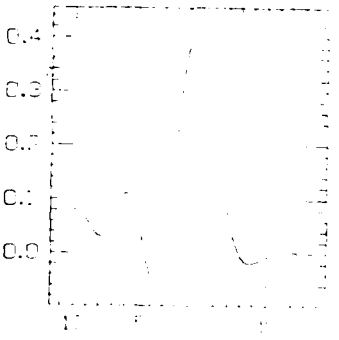

β=.05

I_0

p=4 q=3 α=2.00

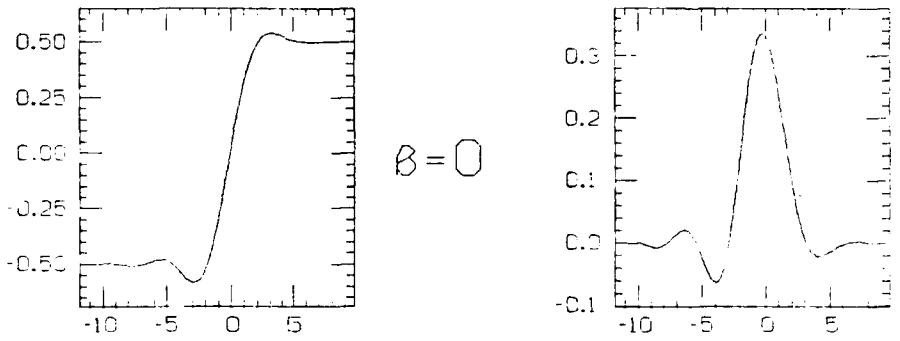

β=0

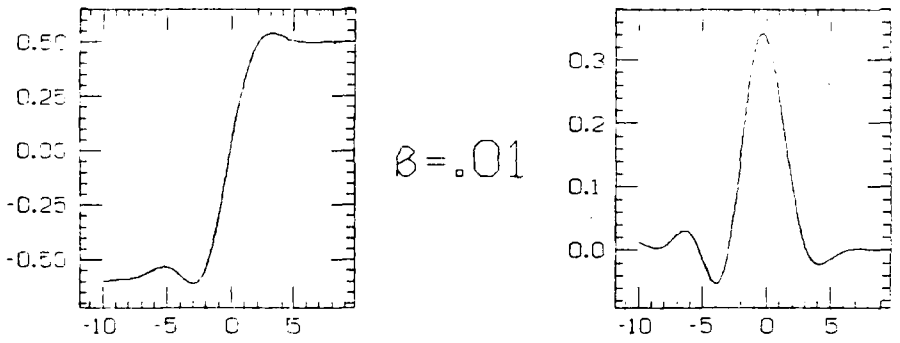

β=.01

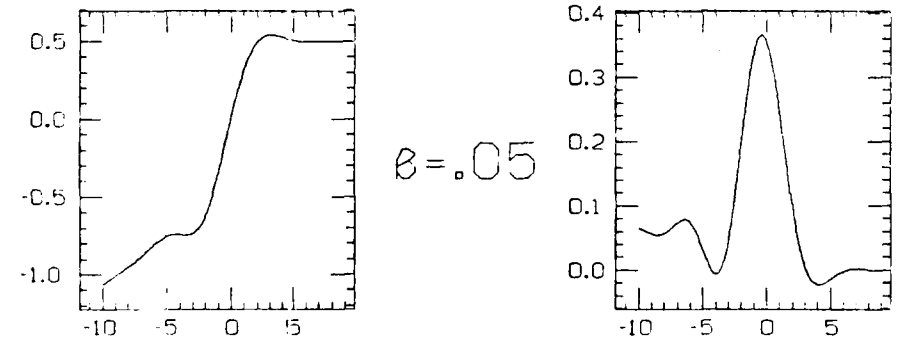

β=.05

I_0 I_1

p=4 q=5 α=0.50

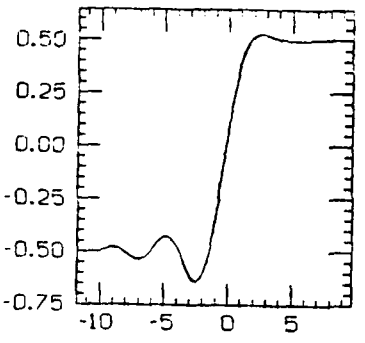

β=0

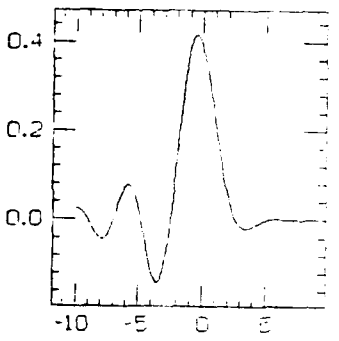

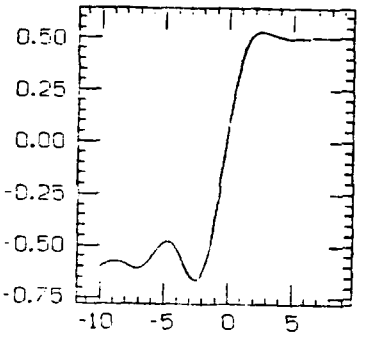

β=.01

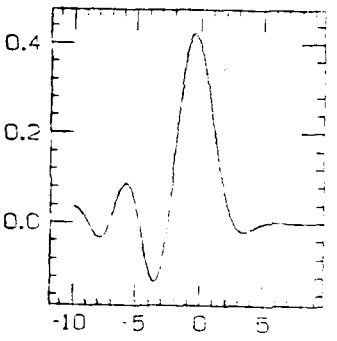

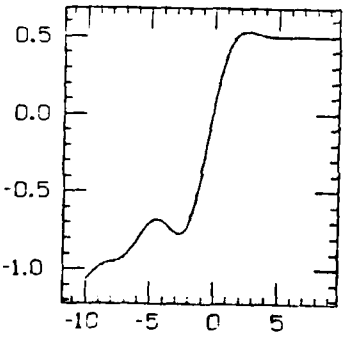

β=.05

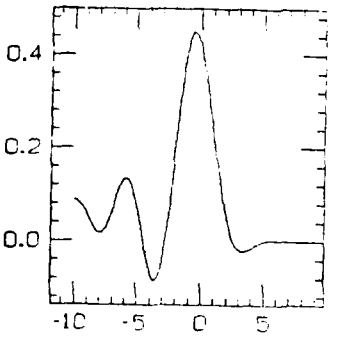

I_0 I_1

p=4 q=5 α=1.00

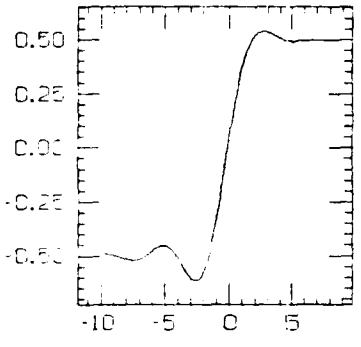

β=0

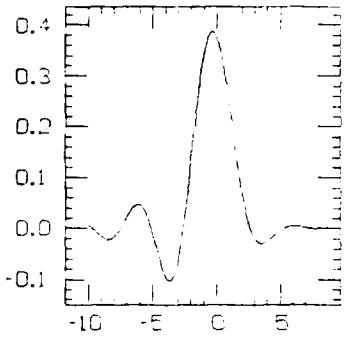

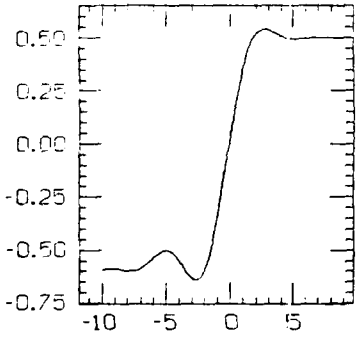

β=.01

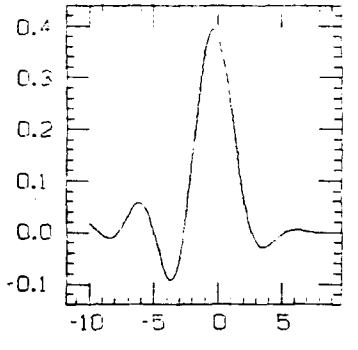

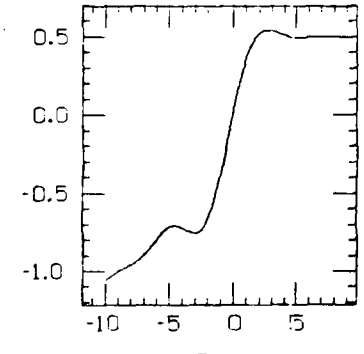

β=.05

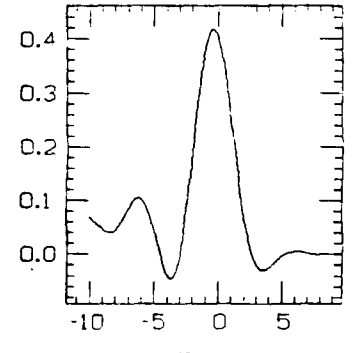

I_0 I_1

p=4 q=5 α=2.00

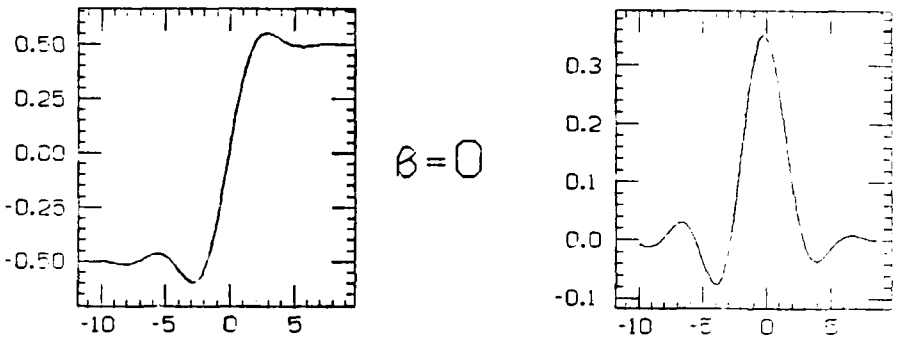

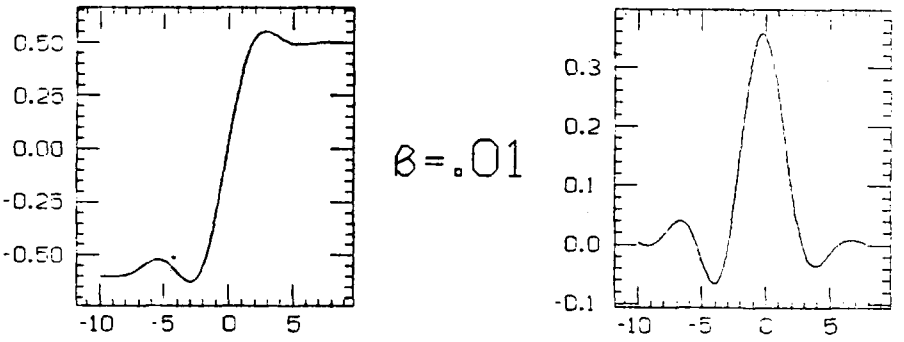

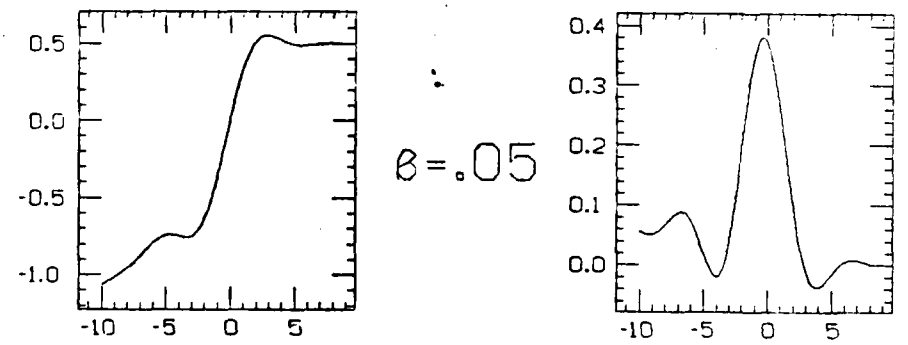

I_0 I_1

p=2 q=0 α=0.0

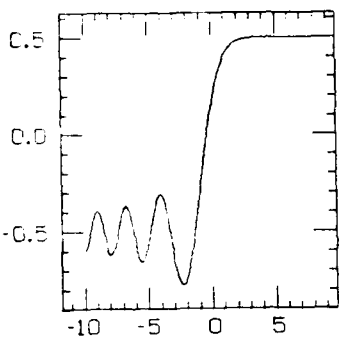

β=0

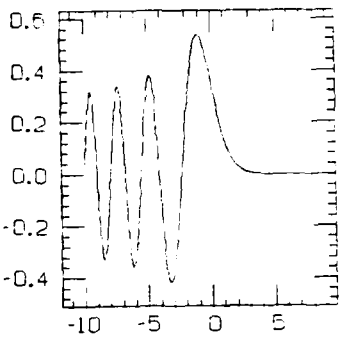

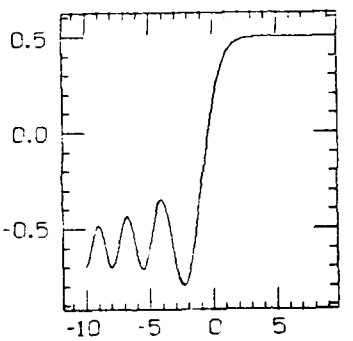

β=.01

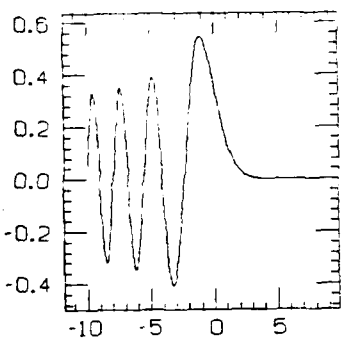

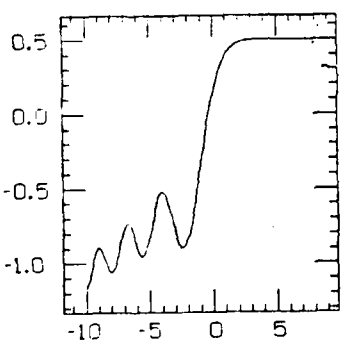

I_0

β=.05

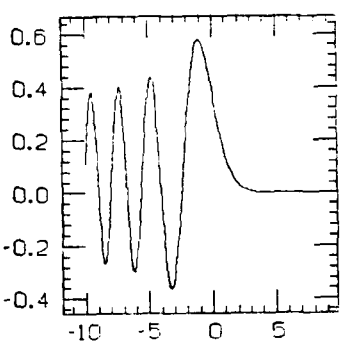

I_1

$p=4 \quad q=0 \quad \alpha=0.0$

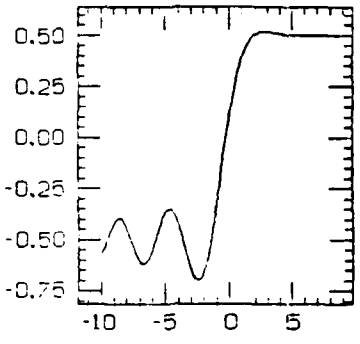

$\beta=0$

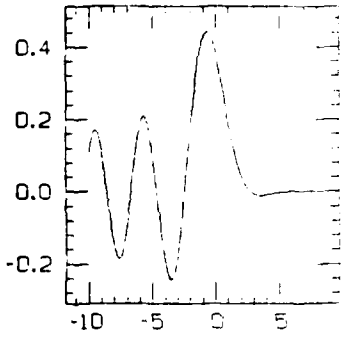

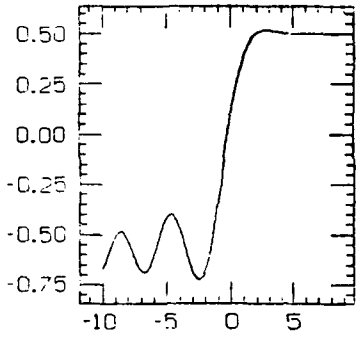

$\beta=.01$

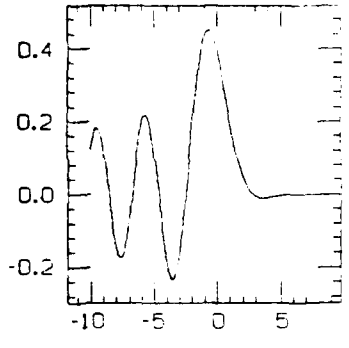

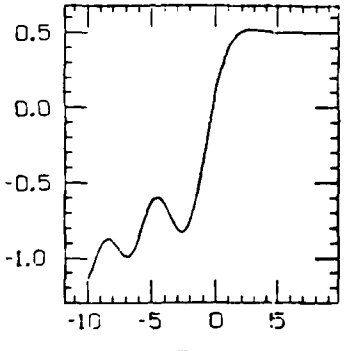

$\beta=.05$

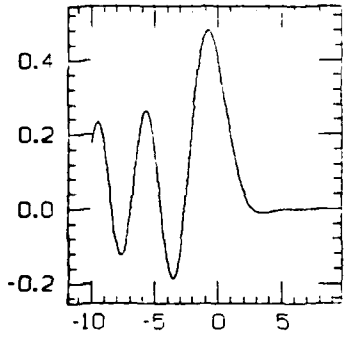

I_0 I_1

p missing q=1 α=1.0

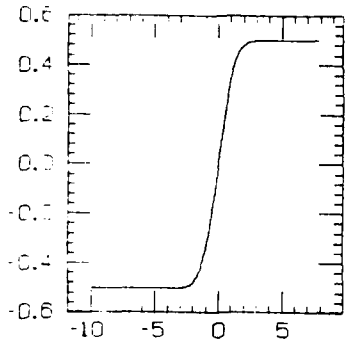

β=0

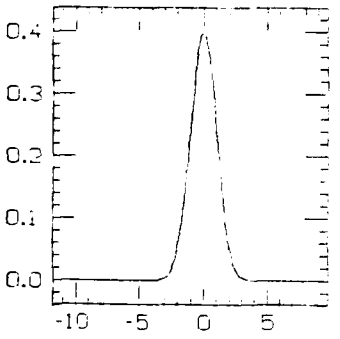

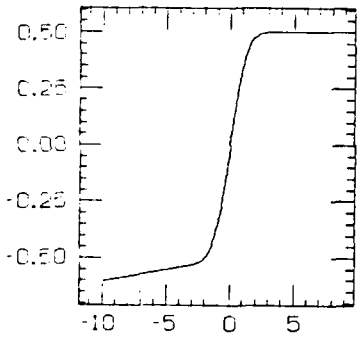

β=.01

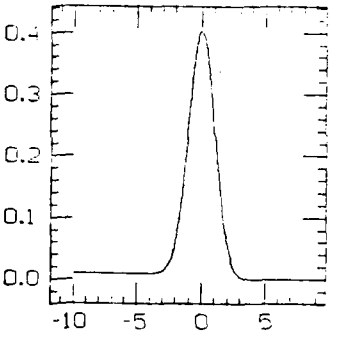

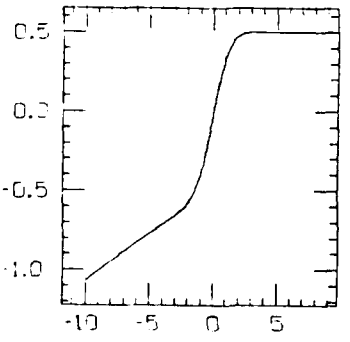

I_0

β=.05

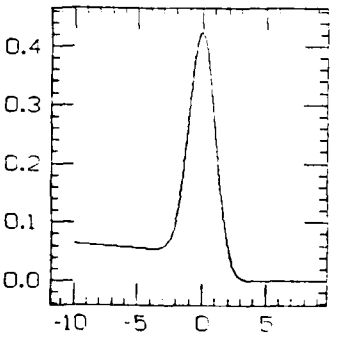

I_1

p missing q=3 α=1.1

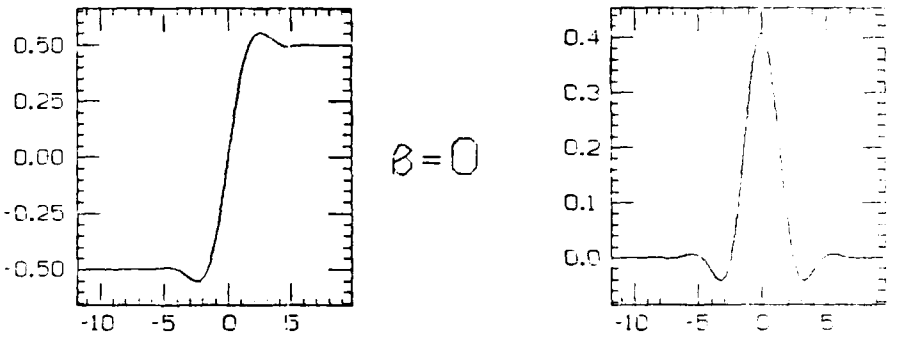

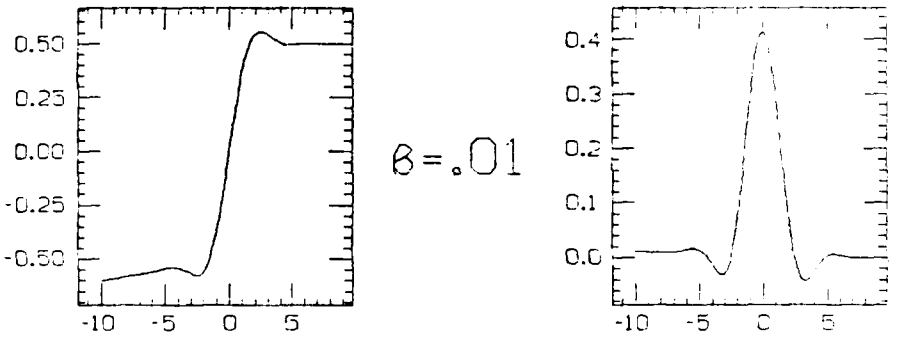

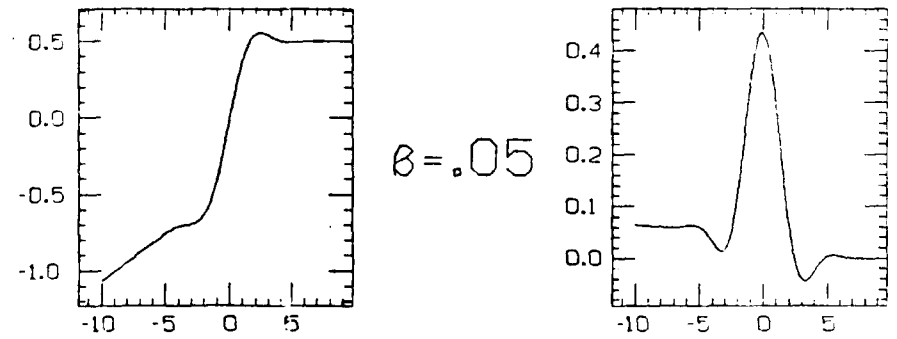

I_0 I_1

Explanation and Use of the Graphs

These graphs show the qualitative similarity of the behavior of difference approximations to the scalar wave equation (represented by $\beta = 0$) and the telegrapher's equation ($\beta \neq 0$) near a discontinuity.

The first thing to notice from these graphs is the qualitative similiarity for graphs that differ only in β. The only noticeable change in the graphs as β increases from 0 is, for l_0, a change in slope on the left of the jump and, for l_1, a change in the zero level of the oscillations on the left of the jump. From this we can conclude that near the discontinuity, oscillations in the approximate solution to (1.1) are qualitatively similiar to those of the wave equation ($\beta = 0$).

We may also compare these graphs to the calculations of actual methods presented above. For example, the graph for $p = 2$, $q = 3$, $\alpha = 1/2$, and $\beta = 0.05$ and the Lax-Wendroff solution are very similiar. The graph for $p = 2$, $\alpha = 0$, and $\beta = 0.05$ shows the long trail of oscillations which we see in both Leapfrog and the second order centered difference approximation. The graph for $p = 4$, $\alpha = 0$, and $\beta = 0.05$ for nondissipative fourth order methods shows both the long trail of oscillations and the small dip ahead of the front which we observed in the graph of the solution by the fourth order method.

As an illustration of the use of these tables, we can see that because the similiarity in the behavior of the approximate solutions is so strong, the same artificial viscosities should work for the telegrapher's equation as for the scalar wave equation (in terms of improving the solution near the discontinuity).

Application to Mesh Refinement

We present here an application of the results in section 4. We will apply mesh refinement to the example used by Majda and Osher [1977]. Their problem was

$$\begin{aligned} &\frac{\partial}{\partial t}\begin{pmatrix} u_1 \\ u_2 \end{pmatrix} = \begin{pmatrix} 1 & 0 \\ 0 & -1 \end{pmatrix}\frac{\partial}{\partial x}\begin{pmatrix} u_1 \\ u_2 \end{pmatrix} + \begin{pmatrix} 0 & 1 \\ -1 & 0 \end{pmatrix}\begin{pmatrix} u_1 \\ u_2 \end{pmatrix} \\ &u_1(x,0) = \begin{cases} 1, & \text{if } x < 0 \\ 0, & \text{if } x > 0 \end{cases} \\ &u_2(x,0) = 0. \end{aligned} \tag{5.5}$$

We will use a fourth order method recommended by Apelkrans [1969] in the region away from the discontinuities, and the second order Lax-Wendroff method around the discontinuities and at the boundaries.

The form of mesh refinement that we use is described in detail by Berger, Gropp, and Oliger [unpublished]; the mesh refinement program is due to Berger [unpublished]. Basically, this form of mesh refinement places refined grids dynamically over the problem domain. The grids may be refined to an arbitrary degree.

Since we must compute on a finite domain, we must introduce a boundary and a boundary approximation. From the results in Gustafsson [1975], we know that the boundary approximation must be at least third order accurate if we want fourth order accuracy for the computation as a whole. There are two common ways to achieve this: use a third order uncentered scheme such as that recommended in Cliger [1974] for the scalar wave equation, or use a second order method and mesh refinement, as recommended in Oliger [1976]. We have chosen the second approach as it is the easiest to apply in this problem.

Our algorithm for this problem is the following: we apply a fourth order, dissipative scheme on a grid with mesh size h_c except near the boundaries and the discontinuities at $x = \pm t$, and we apply a second order, dissipative method on a grid with mesh size $h_f = h_c^2$ at those places.

The first question which may come to mind is the computational complexity of such an algorithm. We will first estimate the total number of mesh points, both coarse and fine, needed by the algorithm. From that result, we will be able to compute the computational effort required by this algorithm. There are three contributions to the number of mesh points: the coarse grid, the fine grid at the boundaries, and the fine grid around the discontinuities. The coarse grid has $O(1/h_c)$ mesh points. The fine grid at the boundaries has $O(1/h_f) \times 4h_c = O(1/h_c)$ mesh points, since the boundary grid only extends over 4 coarse grid points.

To determine the number of fine grid mesh points around the discontinuity, we must determine the width of the front. We make the two assumptions: the region of refinement is asymptotically of the same size as the width of the front, and the derivative discontinuity at $x = t$ is asymptotically no larger than the discontinuity at $x = -t$. On the fine grid, the results of section 4 show that the width of the front is $O(h_f^{2/3})$. But since $h_f = h_c^2$, the width of the front on the scale of the coarse grid is $O(h_c^{4/3})$. Thus, as $h_c \to 0$, the number of coarse mesh points that the front is spread across tends to zero. Because of the way that the mesh refinement program works, there is a minumum of seven coarse grid points (six cells) which must be refined around the fronts. Thus, the number of fine grids points

around the discontinuities is $O(1/h_f) \times 6h_c = O(1/h_c)$. Combining these gives $O(1/h_c)$ total mesh points.

The computational work is easily derived from the above analysis. To integrate to time T_0 with time step k_c on the coarse grid and time step $k_f = k_c^2$ on the fine grid, we need

$$O(1/h_c) \times \frac{T_0}{k_c} \qquad \text{on the coarse grid}$$

$$O(1/h_c) \times \frac{T_0}{k_f} \qquad \text{on the fine grid}$$

or $O(1/h_c^2) + O(1/h_c^3)$ work (assuming $k_c/h_c =$ constant). Thus we see that the work on the fine grid dominates the work on the coarse grid. These estimates are observed in computations.

These results show that this algorithm is practical in space (it uses no more space than the coarse grid would alone), but less practical in time. The advantage of this method is the ability to compute a more accurate solution for a given coarse grid than is possible without refinement.

For our computational example, we computed the solution to (5.5) at $t = 0.5$ with $h_c = 0.02$ and $h_c = 0.01$. The time step k was taken as $h_c/2$. Computations with and without mesh refinement at the discontinuities were done; their results are presented in the following table. These choices of t and h were made to facilitate comparisions with the results in Majda and Osher [1977].

x	solution u_1	MR: $h = 0.02$	MR: $h = 0.01$	no MR: $h = 0.02$	no MR: $h = 0.01$
-0.8	8.775826E-1	3.9E-7	<1E-7	3.0E-7	<1E-7
-0.7	8.775826E-1	<1E-7	<1E-7	-3.1E-5	<1E-7
-0.6	8.775826E-1	2.5E-6	<1E-7	-3.8E-3	2.1E-5
-0.5	-1.224174E-1	-6.6E-1	-6.6E-1	-5.7E-1	-5.7E-1
-0.4	-9.879886E-2	-3.8E-3	3.5E-5	-4.2E-2	2.7E-2
-0.3	-7.788613E-2	7.9E-5	-7.1E-6	-1.1E-2	1.2E-3
-0.2	-5.956894E-2	8.0E-5	-1.9E-7	-2.4E-3	-6.2E-5
-0.1	-4.377426E-2	-6.6E-7	-2.6E-7	1.9E-4	3.0E-6
0.0	-3.044362E-2	2.8E-6	3.2E-7	9.9E-6	2.0E-6
0.1	-1.953720E-2	-4.9E-7	4.9E-7	7.6E-6	2.0E-6
0.2	-1.103355E-2	-1.5E-6	5.1E-7	8.1E-6	2.0E-6
0.3	-4.929534E-3	-6.0E-7	2.6E-8	8.4E-6	2.0E-6
0.4	-1.234040E-3	-3.1E-9	2.7E-8	8.6E-6	1.5E-6
0.5	0.0	4.1E-7	6.6E-8	1.3E-5	3.9E-6
0.6	0.0	1.0E-11	-5.2E-16	1.5E-7	-1.5E-9
0.7	0.0	8.0E-15	-3.9E-21	4.1E-11	6.0E-15
0.8	0.0	4.3E-18	-3.3E-28	3.2E-13	-1.9E-20

Table 4: Errors in the computed solution at $x = -.8(.1).8$ for the fourth order method, *with and without* mesh refinement. The columns labeled MR are the results of the mesh refinement computations.

It is clear from this table that mesh refinement significantly improves the accuracy of the results. Further, the rate of convergence is higher for the mesh refinement calculation than for the unrefined calculation.

This method is not the most efficient way to solve (5.5). (For this problem, front tracking is more efficient.) It does, however, illustrate the use of mesh refinement, coupled with knowledge of the behavior of the problem, to get a high accuracy solution.

6. Conclusion

Summary of Results

We have shown that the asymptotic width of the front is $h^{p/(p+1)}$, where p is the order of the approximation, for a fairly general class of difference approximations to the telegrapher's equation. This behavior is very similiar to the behavior near the front for the scalar wave equation, and shows that the effects of numerical dispersion and/or dissipation near the discontinuity overwhelm any other numerical artifacts which may be present, such as the effect discovered by Majda and Osher [1977].

The canonical forms that we constructed contain a great deal of information on the detailed behavior of the solution. Given a difference scheme that fits the framework in section 4, we can use the graphs of the canonical forms dislayed in section 5 to get an idea of how the solution to the difference scheme will behave near a discontinuity.

The detailed examination of the non-dissipative second order difference scheme studied in section 3 shows that the canonical forms displayed in section 5 are actually a good approximation to the exact canonical form near the front (see figures 10 and 11). These results also show that the model equation is a good approximation near the front (because $h\xi$ for the saddle points is $o(1)$ near the front). Finally, the canonical form for the approximation in section 3 shows that away from the front, the model equation formulation is not accurate (figure 11).

Another difficulty in determining the solution away from the front is the complicated behavior of the unexponentiated term in the integral for the solution. Even for the exact (continuous) problem, this is difficult to deal with.

In section 4 we also investigated the effect of the coupling term. We showed that the effect of the coupling term is controlled by the cell wave-coupling number, which is equal to the product of the step size and the coupling strength, divided by the speed of propagation (hp/c). As long as R is small, the behavior near the front of approximations to the telegrapher's equation is similar to the behavior of approximations to the scalar wave equation. This result is remarkable because the results of Majda and Osher [1977] show that away from the front, the behavior of approximations to these two equations is very different. The analysis in section 4 showed further that the effect of the coupling term is

noticeable only very near the front (where it affects the U_- or forward moving term) and well away from the front (where the noise generated at the front, moving away from the front, shows up in the U_+ term).

An interesting feature of difference approximations to the telegrapher's problem which we have shown is the different frequency content of the solution of the differential equation as compared to the solution of difference approximations. For the differential equation, we saw in section 2 that the leading terms in the expansion of the inverse Fourier transform were at infinite frequency. Specifically, the saddle points were converging on infinity in the frequency (ξ) plane as the front was approached. In contrast, we saw in sections 3 and 4 that the saddle points for the difference approximations converged on zero in the $h\xi$ plane. It is this fact that makes the model equations analysis in section 4 work, since the model equation is essentially an expansion in $h\xi$.

The computations presented in section 5 support our theory. In every case the asymptotic width of the front matched the $h^{p/(p+1)}$ prediction. The graphs of the canonical forms for various difference schemes matched the qualitative behavior near the front for those difference schemes.

Implications

The results in this thesis show that the effect of numerical dispersion and dissipation near a discontinuity overwhelms the numerical artifact introduced by coupling in the equations. This implies that the effect discovered by Majda and Osher may be neglected if (a) accurate computation of the front is of primary importance and (b) second order accuracy is sufficient in the smooth regions. In this case, mesh refinement guided by the knowledge of the width of the front, can be used to accurately compute the discontinuity. Further, artificial viscosities which are good for the scalar wave equation will be good here since artificial viscosities are designed to reduce certain high frequencies, and our results show that the frequency of the oscillations near the front are nearly the same for the scalar wave equation and the telegrapher's equation.

If an accurate solution is needed everywhere, mesh refinement can be used as above, with the added requirement that the solution near any discontinuity be calculated accurately enough to prevent the contamination of the smooth part of the solution. This was demonstrated in section 5.

AD-A115 989 STANFORD UNIV CA DEPT OF COMPUTER SCIENCE F/G 12/1
NUMERICAL SOLUTION OF TRANSPORT EQUATIONS.(U)
DEC 81 W D GROPP N00014-75-C-1132
UNCLASSIFIED STAN-CS-81-886 NL

END
DATE FILMED
DTIC

Topics for Further Study

The study of even such a narrow topic as this is never complete; below are a number of questions that arose during the research into this problem.

Multiple time scales — Many transport equations that arise in practice involve two radically different materials. For example, astrophysical transport problems often involve the interaction of electromagnetic radiation with gas. The scale of time during which the radiation moves is orders of magnitute different from the scale of time on which the gas moves. A current approach to these problems is to solve seperate equations for the gas and the radiation, then coupling them together at long (for the radiation intervals). Another approach to these problems is to use stiff-integrators to integrate the equations in time. Questions that arise here are (a) how accurate is this? (b) how do these algorithms behave in the presence of discontinuities? (c) are there better ways?

Asymptotic solution away from the front — For the general problem we were unable to find an asymptotic representation for the solution except near the discontinuity. The model equation approach does not seem powerful enough to ever provide a way to represent the solution away from the front. Is there a general technique? (Specific methods can be studied, as we did in section 3, and some specific problems can be studied as in Majda and Osher [1977].)

Initial Boundary Value Problem — What is the effect of coupling through boundary conditions? The methods used in this thesis, with Fourier transforms replaced by Laplace transforms, would give an answer.

Appendix A: Two Integral Identities

We prove in this appendix two integral identities that we used in section 2. We first show that

$$\int_{-\infty}^{+\infty} g(\xi)\exp(\phi(\xi)t)\,d\xi = 0 \tag{A.1}$$

where

$$g(\xi) = \frac{1 + i\sqrt{4\xi^2 - 1} - 2i\xi}{4\xi\sqrt{4\xi^2 - 1}}$$

and

$$\phi(\xi) = \frac{i}{2}\sqrt{4\xi^2 - 1} + i\omega\xi.$$

As always, the integral is the Cauchy principle value, and we pass above the branch cut $[-1/2, 1/2]$. To make the proof somewhat clearer, we will assume that $t = 1$. It will be clear that the proof will hold for any $t > 0$.

The proof is a simple exercise in using the Cauchy integral theorem. We close the contour in the upper half plane with a semicircle of radius R. The proof consists of showing that as $R \to \infty$, the contribution to the integral over the closed contour from the semicircle tends to zero. Finally, it is demonstrated that, despite appearances, $g(\xi)$ is regular at the origin and only of the order of $(\xi \pm \frac{1}{2})^{-1/2}$ at $\frac{1}{2}$ and $-\frac{1}{2}$.

Along the semicircle, we have $\xi = Re^{i\theta}$. We will make this substitution in the integral as we go along in the proof.

We start by finding a bound on $\Re(\frac{i}{2}\sqrt{4\xi^2 - 1})$. This gives us the magnitude of the exponential in the integral. First, we see that

$$\Re\left(\frac{i}{2}\sqrt{4\xi^2 - 1}\right) = -R\Im\left(e^{i\theta}\sqrt{1 - \frac{e^{-2i\theta}}{4R^2}}\right)$$

where $\Re(z)$ is the real part of z and $\Im(z)$ is the imaginary part of z. This is equal to

$$-R\sin\theta\,\Re\left(\sqrt{1 - \frac{e^{-2i\theta}}{4R^2}}\right) - R\cos\theta\,\Im\left(\sqrt{1 - \frac{e^{-2i\theta}}{4R^2}}\right).$$

Now, a quick look at Ahlfors [1979] shows us that

$$\Re\left(\sqrt{1-\frac{e^{-2i\theta}}{4R^2}}\right)=\sqrt{\frac{1-\frac{\cos 2\theta}{4R^2}+\sqrt{1+\frac{1}{16R^4}-\frac{\cos 2\theta}{2R^2}}}{2}}$$

$$\Im\left(\sqrt{1-\frac{e^{-2i\theta}}{4R^2}}\right)=-\sqrt{\frac{\frac{\cos 2\theta}{4R^2}-1+\sqrt{1+\frac{1}{16R^4}-\frac{\cos 2\theta}{2R^2}}}{2}}.$$

We bound $\Re\left(\sqrt{1-\frac{e^{-2i\theta}}{4R^2}}\right)$ from below. The argument of the inner square root satisfies

$$\left(1+\frac{1}{4R^2}\right)^2 \geq 1+\frac{1}{16R^4}-\frac{\cos 2\theta}{2R^2} \geq \left(1-\frac{1}{4R^2}\right)^2$$

so that

$$\Re\left(\sqrt{1-\frac{e^{-2i\theta}}{4R^2}}\right) \geq \sqrt{\frac{1-\frac{\cos 2\theta}{4R^2}+1-\frac{1}{4R^2}}{2}} \geq \sqrt{1-\frac{1}{2R^2}} \geq \frac{1}{2} \qquad \text{(A.2)}$$

for $R \geq 1$. Similiarly, we get a bound on the imaginary part

$$0 \geq \Im\left(\sqrt{1-\frac{e^{-2i\theta}}{4R^2}}\right) \geq -\sqrt{\frac{\frac{1}{4R^2}-1+1+\frac{1}{4R^2}}{2}} = -\frac{1}{2R}$$

for $R \geq \frac{1}{2}$. Thus,

$$|\exp(\phi(\xi))| \leq \exp\left(-R\sin\theta+\frac{|\cos\theta|}{2}\right)|\exp(i\omega\xi)| < 2\exp\left(-\frac{R}{2}(\frac{1}{2}+\omega)\sin\theta\right). \qquad \text{(A.3)}$$

We also need a bound on $|g(\xi)|$.

$$|g(Re^{i\theta})| \leq \frac{1+|\sqrt{4\xi^2-1}|+2R}{4R|\sqrt{4\xi^2-1}|}.$$

We can bound $|\sqrt{4\xi^2-1}| = \sqrt{|4R^2e^{2i\theta}-1|} = |16R^4-8R^2\cos 2\theta+1|^{\frac{1}{4}}$ by

$$3R \geq \sqrt{|4R^2e^{2i\theta}-1|} \geq R$$

for $R \geq 1$. Thus,

$$|g(Re^{i\theta})| \leq \frac{1+3R+2R}{4R^2} \leq \frac{2}{R}. \qquad \text{(A.4)}$$

for $R \geq 1$.

Now, using (A.3) and (A.4), we can bound the contribution to the integral over the semicircle by

$$8\int_0^{\frac{\pi}{2}} e^{-R(\frac{1}{2}+\omega)\sin\theta}\,d\theta \qquad \text{(A.5)}$$

We can bound this integral by dividing it into two parts. The first part is $0 \le \theta \le \epsilon/16$. The part of the integral over this range of θ is no greater than $\epsilon/2$ for $R \ge 1$. The second part is for $\epsilon/16 \le \theta \le \pi/2$. In this range of θ, we can pick R to satisfy

$$R > \max\left(\frac{\ln \frac{8\pi}{\epsilon}}{(\frac{1}{2}+\omega)\sin\frac{\epsilon}{16}}, 1\right).$$

Then the integrand is less than $\epsilon/8\pi$, and the contribution to the integral is less than $\epsilon/2$. Thus, by choosing R large enough, we can make the integral (A.5) as small as we want (for $\omega > -1/2$).

Next, we must treat the singularities of $g(\xi)$. By inspection, it is clear that there are at most three points of singularity in $g(\xi)$. We can investigate these by using MACSYMA (Mathlab Group [1975]) to expand $g(\xi)$ about the points 1, $\frac{1}{2}$, and $-\frac{1}{2}$. We have

$$g(\xi) = -\frac{1}{2} - \frac{i\xi}{2} - \xi^2 + \cdots \qquad \text{for } \xi \approx 0$$

$$g(\xi) = \pm\frac{i-1}{4\sqrt{\xi \pm \frac{1}{2}}} \mp \frac{i}{2} \pm \frac{(5-i)\sqrt{\xi \pm \frac{1}{2}}}{8} + \cdots \qquad \text{for } \xi \approx \mp\tfrac{1}{2}$$

Thus there is *no* contribution to the Cauchy principle value of (A.1) from any of these, as they are weaker than simple poles. The relation (A.1) is now proved.

A stronger result can be proved from (A.3) and (A.2) by noticing that the $\frac{1}{2}$ in $(\frac{1}{2}+\omega)$ is really the $(1 - 1/(2R^2))^{1/2}$ in (A.2). Therefore, as $R \to \infty$, the bound on (A.3) is asymptotically

$$|\exp(\phi(\xi))| \lesssim 2\exp(-R(1+\omega)\sin\theta)$$

for $\omega > -1$. This matches what we would expect to get from an asymptotic expansion of ϕ, since $\phi(\xi) \sim i(1+\omega)\xi$ for $|\xi|$ large.

We next prove that

$$\int_{-\infty}^{+\infty} x^{\nu-1} e^{-\gamma x - \beta/x}\, dx = 2\pi i(-1)^{\nu}\left(\frac{\beta}{\gamma}\right)^{\nu/2} I_{\nu}(2\sqrt{\beta\gamma}) \tag{A.6}$$

for integer $\nu \ge 0$ and and β and γ pure imaginary. Of course, we show this in the generalized sense of Gel'fand and Shilov [1964].

We start by assuming

$$\int_{-\infty}^{+\infty} x^{-1} e^{-\gamma x - \beta/x}\, dx = 2\pi i I_0(2\sqrt{\beta\gamma}). \tag{A.7}$$

We proceed to show that we can get (A.6) from this by formally differentiating each side of this with respect to γ, passing the derivative through the integral.

First, we note that

$$\begin{aligned}\int_{-\infty}^{+\infty} x^{\nu-1}e^{-\gamma x-\beta/x}\,dx &=(-1)^{\nu}\int_{-\infty}^{+\infty} x^{-1}\frac{d^{\nu}}{d\gamma^{\nu}}e^{-\gamma x-\beta/x}\,dx\\ &=(-1)^{\nu}\frac{d^{\nu}}{d\gamma^{\nu}}\int_{-\infty}^{+\infty} x^{-1}e^{-\gamma x-\beta/x}\,dx\\ &=(-1)^{\nu}2\pi i\frac{d^{\nu}}{d\gamma^{\nu}}I_0(2\sqrt{\beta\gamma}).\end{aligned}$$

We can evaluate the derivative by an induction argument.

From Abramowitz and Stegun [1972], we have the formula

$$\left(\frac{1}{z}\frac{d}{dz}\right)\left(\frac{1}{z^{\nu}}I_{\nu}(z)\right)=\frac{1}{z^{\nu+1}}I_{\nu+1}(z)$$

or

$$-\frac{\nu}{z^{\nu+2}}I_{\nu}(z)+\frac{1}{z^{\nu+1}}\frac{d}{dz}I_{\nu}(z)=\frac{1}{z^{\nu+1}}I_{\nu+1}(z).$$

Now, let $z=2\sqrt{\beta\gamma}$, and multiply the above by $(2\beta)^{\nu+1}$. This leaves us with

$$-\frac{\nu}{2\sqrt{\beta\gamma}}\left(\frac{\beta}{\gamma}\right)^{\frac{\nu+1}{2}}I_{\nu}(2\sqrt{\beta\gamma})+\left(\frac{\beta}{\gamma}\right)^{\frac{\nu+1}{2}}\frac{d}{dz}I_{\nu}(z)\Big|_{z=2\sqrt{\beta\gamma}}=\left(\frac{\beta}{\gamma}\right)^{\frac{\nu+1}{2}}I_{\nu+1}(2\sqrt{\beta\gamma}). \qquad \text{(A.8)}$$

Now, we start with the induction proof. The first term, $\nu=1$, we can get from the fact that $I_0'=I_1$. This gives us

$$\frac{d}{d\gamma}I_0(2\sqrt{\beta\gamma})=\left(\frac{\beta}{\gamma}\right)^{\frac{1}{2}}\frac{d}{dz}I_0(z)\Big|_{z=2\sqrt{\beta\gamma}}=\left(\frac{\beta}{\gamma}\right)I_1(2\sqrt{\beta\gamma})$$

which is the first term in the induction. For the n^{th} term in the induction, we need to show

$$\frac{d}{d\gamma}\left(\frac{\beta}{\gamma}\right)^{\frac{n-1}{2}}I_{n-1}(2\sqrt{\beta\gamma})=\left(\frac{\beta}{\gamma}\right)^{\frac{n}{2}}I_n(2\sqrt{\beta\gamma}).$$

We do this by performing the indicated differentiation and then applying (A.8).

$$\begin{aligned}\frac{d}{d\gamma}\left(\frac{\beta}{\gamma}\right)^{\frac{n-1}{2}}I_{n-1}(2\sqrt{\beta\gamma}) &=-\frac{n-1}{2\gamma}\left(\frac{\beta}{\gamma}\right)^{\frac{n-1}{2}}I_{n-1}+\left(\frac{\beta}{\gamma}\right)^{\frac{n}{2}}\frac{d}{dz}I_{n-1}(z)\Big|_{z=2\sqrt{\beta\gamma}}\\ &=\left(\frac{\beta}{\gamma}\right)^{\frac{n}{2}}I_n(2\sqrt{\beta\gamma}).\end{aligned}$$

Here we have substituted $n-1$ for ν in (A.8).

We need only prove (A.7) to prove (A.6). We make the change of variable $x = iu$ in (A.7). This gives us

$$\int_{-i\infty}^{+i\infty} u^{-1} e^{-\gamma u/i - \beta i/u}\, du.$$

From page 245 of Erdélyi [1954], this is just an inverse Laplace transform with value $2\pi i I_0(2\sqrt{\beta\gamma})$. Note that for β and $\gamma = 0$, a singular functional which coincides with zero for β and $\gamma \not\equiv 0$ must be added to (A.6). This completes our proof of (A.6).

Appendix B: Computing the Exact Solution

This appendix discusses the method used to compute the exact solution to the continous model problem in section 2. From section 2, we know that we need to evaluate the integral

$$u_- = \frac{1}{2\pi}\int_{-\infty}^{+\infty} \alpha_-(1+\lambda_-)e^{\phi-t}\,d\xi$$
$$= \frac{1}{2\pi}\int_{-\infty}^{+\infty} \frac{1-2i\xi-i\sqrt{4\xi^2-1}}{4\xi\sqrt{4\xi^2-1}}e^{\phi-t}\,d\xi + \frac{1}{4}.$$

We need to perform this integration numerically. First, we will deform the path of integration to a path "close" to the path of steepest descent. The figures below show the qualitative behavior of the path of steepest descent; we will use these to guide us in our choice of path.

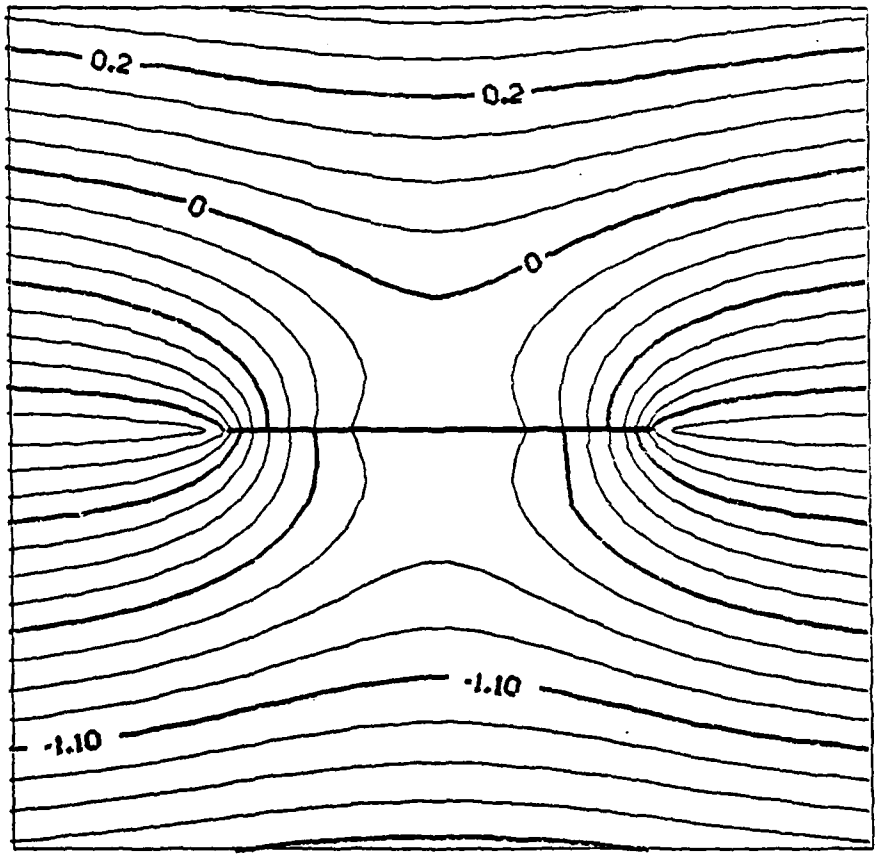

Figure 13: $\Re(\phi_-)$ for $\omega = 0.3$.

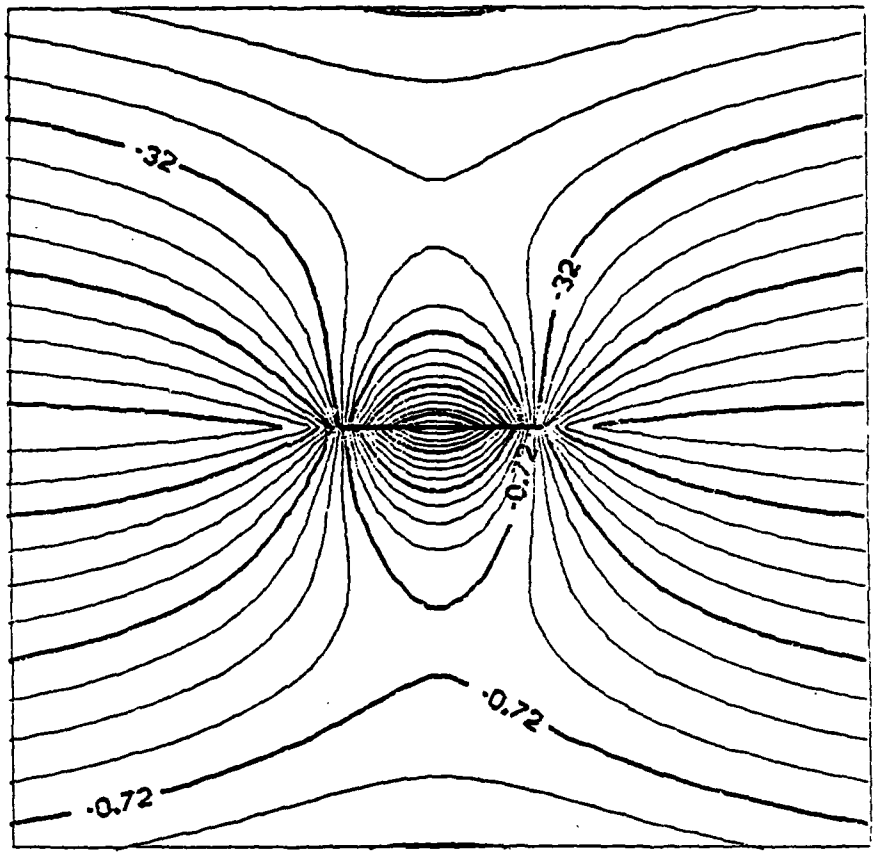

Figure 14: $\Re(\phi_-)$ for $\omega = 0.9$.

From these figures it is clear that the path to take is a circle about the origin. In deforming the path to this circle, we will pick up $-\frac{1}{4}$ from the pole at the origin. We can show by techniques similiar to those in Appendix A that there is no contribution from closing the contour in the lower half plane.

The resulting integral is

$$\frac{i}{2\pi}\int_0^{2\pi} \frac{1-2i\xi-i\sqrt{4\xi^2-1}}{4\sqrt{4\xi^2-1}} e^{\phi-t}\,d\theta \tag{B.1}$$

where $\xi = re^{i\theta}$ and r has been chosen as $\max(\omega/2\sqrt{1-\omega^2}, \frac{1}{2}+\epsilon)$, ϵ some small positive number. This choice of r makes the path pass through the saddle points unless the path would pass within ϵ of the branch cut $[-\frac{1}{2}, \frac{1}{2}]$, in which case the path is expanded.

This integral has a special form. The integrand is periodic analytic in a strip around the region of integration. It is well known that the trapezoidal rule converges very quickly for periodic functions (Davis and Rabinowitz [1975]); in particular, for periodic analytic

functions which satisfy certain technical assumptions, the convergence is exponential (see Rabinowitz [1968] and Lyness and Delves [1967]). Using this fact, the integral (B.1) was integrated with the trapezoidal rule.

We would like to point out a few features. Along the steepest descent path, the imaginary part of ϕ_- is constant. This means that the integrand should not have serious oscillations along the path of integration. Secondly, since most of the effect is concentrated at the saddle points, we would expect an automatic quadrature routine which places points adaptively not to be that much less efficient than the trapezoidal rule. Experimentally this is the case. The routine QAGS (de Doncker [1978]) was roughly as fast as a simple trapezoidal sum. Finally, the choice of ϵ, the minimum distance from the singularities, can have a big effect. Since there are singularities at $\xi = \pm\frac{1}{2}$, we should keep the path well away from these points. A choice of $\frac{1}{4}$ for ϵ seems to work well.

Bibliography

M. Abramowitz and I. Stegun, *Handbook of Mathematical Functions,* Dover, New York, 1972.

L. Ahlfors, *Complex Analysis,* 3rd ed., McGraw-Hill, New York, 1979.

M. Apelkrans, "On Difference Schemes for Hyperbolic Equations with Discontinuous Initial Values," *Math. Comp.,* **22** (1968) 525–539.

M. Apelkrans, "Some Properties of Difference Schemes for Hyperbolic Equations with Discontinuities and a New Method with Almost Quadratic Convergence," Report 15A, Uppsala University, Department of Computer Science (1969).

G. Bell and S. Glasstone, *Nuclear Reactor Theory,* Van Nostrand Reinhold Co., New York, 1970.

M. Berger, Ph.D. Thesis, in preparation.

M. Berger, W. Gropp, and J. Oliger, "Adaptive Mesh Refinement," in preparation.

G. Birkhoff and R. Lynch, "Numerical Soultion of the Telegraph and Related Equations," in *Numerical Solution of Partial Differential Equations,* ed. by J. Bramble, Academic Press, 1966.

N. Bleistein, "Uniform Asymptotic Expansions of Integrals with Stationary Point Near Algebraic Singularity," *Comm. Pure Appl. Math.,* **19** (1966) 353–370.

N. Bleistein and R. Handelsman, *Asymptotic Expansions of Integrals,* Holt, Rinehart, and Winston, New York, 1975.

P. Brenner and V. Thomée, "Stability and Convergence Rates in L_p for Certain Difference Schemes," *Math. Scand.,* **27** (1970) 5–23.

P. Brenner and V. Thomée, "Estimates near Discontinuities for some Difference Schemes," *Math. Scand.,* **28** (1971) 329–340.

R. Chin, "Notes on the Article 'Local Error of Difference Approximations to Hyperbolic Equations'," *J. Comp. Phys.,* **16** (1974) 311-313.

R. Chin, "Dispersion and Gibbs Phenomenon Associated with Difference Approximations to Initial Boundary-Value Problems for Hyperbolic Equations," *J. Comp. Phys.*, **18** (1975) 233–247.

R. Chin and G. Hedstrom, "A Dispersion Analysis for Difference Schemes: Tables of Generalized Airy Functions," *Math. Comp.*, **32** (1978) 1163–1170.

R. Chin and G. Hedstrom, "A Survey of Results on the Modified Equation," to appear in *J. Comp. Phys.*

W. Coughran, Jr., "On the Approximate Solution of Hyperbolic Initial Boundary Value Problems," Stanford Univ. Comp. Sci. Report STAN-CS-80-806 (1980).

P. Davis and P. Rabinowitz, *Methods of Numerical Integration,* Academic Press, New York, 1975.

E. de Doncker, "An Adaptive Extrapolation Algorithm for Automatic Integration," *ACM Signum Newsletter,* **13** (1978) 12–18.

A. Erdélyi, *Tables of Integral Transforms,* vol. 1, McGraw-Hill, New York, 1954.

A. Erdélyi, *Asymptotic Expansions,* Dover, New York, 1956.

G. Forsythe, M. Malcolm, and C. Moler, *Computer Methods for Mathematical Computations,* Prentice-Hall, Englewood Cliffs, New Jersey, 1977.

I. Gel'fand and G. Shilov, *Generalized Functions,* vol. 1, Academic Press, New York, 1964.

V. Guillemin and S. Sternberg, *Geometric Asymptotics,* Am. Math. Soc., Providence, Rhode Island, 1977.

B. Gustafsson, "The Convergence Rate for Difference Approximations to Mixed Initial Boundary Value Problems," *Math. Comp.*, **29** (1975) 396–406.

B. Gustafsson, H.-O. Kreiss, and A. Sundström, "Stability Theory of Difference Approximations for Mixed Initial Boundary Value Problems. II," *Math. Comp.*, **26** (1972) 649–686.

G. Hedstrom, "Models of Difference Schemes for $u_t + u_x = 0$ by Partial Differential Equations," *Math. Comp.*, **29** (1975) 969–977.

G. Hedstrom, private communication, 1979.

G. Hedstrom and A. Osterheld, "The Effect of Cell Reynolds Number on the Computation of a Boundary Layer," *J. Comp. Phys.*, **37** (1980) 399–421.

F. John, *Partial Differential Equations*, Springer-Verlag, New York, 1978.

H.-O. Kreiss and E. Lundqvist, "On Difference Approximations with Wrong Boundary Values," *Math. Comp.*, **22** (1968) 1–12.

P. Lax, "On the Stability of Difference Approximations to Solutions of Hyperbolic Differential Equations," *Comm. Pure Appl. Math.*, **14** (1961) 497–520.

J. N. Lyness and L. M. Delves, "On Numerical Contour Integration Round a Closed Contour," *Math. Comp.*, **21** (1967) 561–577.

A. Majda and S. Osher, "Propagation of Error into Regions of Smoothness for Accurate Difference Approximations to Hyperbolic Equations," *Comm. Pure Appl. Math.*, 30 (1977) 671–705.

Mathlab Group, *MACSYMA Reference Manual, Version 8*, Massachusetts Institute of Technology, Cambridge, Mass., 1975.

P. Morse and H. Feshbach, *Methods of Theoretical Physics*, Vol. 1, McGraw-Hill, New York, 1953.

J. Oliger, "Fourth Order Difference Methods for the Initial Boundary-Value Problem for Hyperbolic Equations," *Math. Comp.*, **28** (1974) 15–25.

J. Oliger, "Hybrid Difference Methods for the Initial Boundary-Value Problem for Hyperbolic Equations," *Math. Comp.*, **30** (1976) 724–738.

F. Olver, *Asymptotics and Special Functions*, Academic Press, New York, 1974.

S. Orszag and L. Jayne, "Local Errors of Difference Approximations to Hyperbolic Equations," *J. Comp. Phys.*, **14** (1974) 1–11.

C. Pearson, "Asymptotic Behavior of Solutions to the Finite-Difference Wave Equation," *Math. Comp.*, **23** (1969) 711–715.

P. Rabinowitz, "Practical Error Coefficients in the Integration of Periodic Analytic Functions by the Trapezoidal Rule," *Comm. ACM*, **11** (1968) 764–765.

R. Richtmyer and K. Morton, *Difference Methods for Initial-Value Problems*, Interscience, New York, 1967.

S. Serdjukova, "The Oscillations which Arise in the Numerical Computation of the Discontinuous Solutions of Differential Equations," *USSR Comp. Math. and Math. Phys.*, **11**, no. 2 (1971) 140–154.

L. Shampine, H. Watts, and S. Davenport, "Solving Nonstiff Ordinary Differential Equations—The State of the Art," *SIAM Rev.*, **18** (1976) 376–411.

V. Thomée, "Stability Theory for Partial Difference Operators," *SIAM Rev.*, **11** (1969) 152–195.

B. van der Waerden, "On the Method of Saddle Points," *Appl. Sci. Res. Ser. B*, **2** (1951) 33–45.

R. Warming and B. Hyett, "The Modified Equation Approach to the Stability and Accuracy of Finite-Difference Methods," *J. Comp. Phys.*, **14** (1974) 159–179.

R. Wong, "Error Bounds for Asymptotic Expanssions of Integrals," *SIAM Rev.*, **22** (1980) 401–435.


DATE
FILMED
7
8